ANALYSIS OF CARBON DIOXIDE ABSORPTION IN SOLUTIONS OF POTASSIUM SALTS OF GLYCINE AND SARCOSINE

A thesis submitted

by

Yi Gu

In partial fulfillment of the requirements

for the degree of

Master of Science

in

Chemical Engineering

TUFTS UNIVERSITY

February, 2012

ADVISOR:

Prof. Jerry H. Meldon

“L’espoir sera être réfracté pourvu que le cœur reste transparent.”

ABSTRACT

CO_2 absorption in aqueous solutions of amino acid salts (AAS) involves simultaneous mass transfer with multiple reversible chemical reactions. The process is mathematically modeled by a set of nonlinear ordinary differential equations (ODEs) which cannot be solved analytically. However, near-exact solutions may be derived using the "Thick Film" linearization technique developed by K. A. Smith for application to the analysis of carrier-facilitated membrane transport [1, 2]. This technique is a variant of singular perturbation methods and is computationally efficient.

In this thesis, the Thick Film analysis is applied, in the context of the Film Model of mass transfer, to calculate rates of absorption of CO_2 in solutions of potassium glycinate (PG) and potassium sarcosinate (PS). Calculated enhancement factors, E, by which reaction multiplies absorption rates are in excellent agreement with values obtained via more computation-intensive numerical methods.

ACKNOWLEDGEMENTS

I gratefully acknowledge Prof. Jerry H. Meldon for providing intellectual guidance, for making things possible that otherwise would have been impossible, and for his trust in my abilities. I have been learning a lot and appreciating the beauty of mathematical modeling.

I am grateful for the partial tuition scholarship granted by the Department of Chemical and Biological Engineering at Tufts University during my second year as a graduate student.

Many thanks to Prof. Nakho Sung and Prof. Christoph Borgers for being on my thesis committee.

I would like to thank my professors and friends who share the same technical language since the early undergraduate days.

Last, I am very much indebted to all of my family who has supported me in everything.

TABLE OF CONTENTS

LIST OF FIGURES

LIST OF TABLES

LIST OF SCHEMES

1. INTRODUCTION

Anthropogenic emissions of the greenhouse gas, carbon dioxide, are responsible for some 60% global warming effects [3]. The total amount of carbon on earth, and in the atmosphere and lithosphere, was relatively constant before industrialization. However, the atmospheric CO_2 concentration increased dramatically from an estimated 282 ppmv in the year 1800 to 377 ppmv in the year 2004 [4]. Combustion of fossil fuels for electrical power generation is the primary source of CO_2 emissions.

Reducing these emissions (to stabilize atmospheric CO_2 levels) will require [5] a combination of more efficient use of energy, switching to using non-fossil fuels, and development of technologies to capture and sequester CO_2.

Conventional CO_2 capture techniques fall into essentially the three categories shown in Figure 1.1: post-combustion capture, pre-combustion capture and fuel combustion with oxygen-enriched air followed by capture of CO_2. CO_2 may be captured after combustion through a variety of separation processes including absorption, adsorption and membrane permeation [6, 7]. However, post-combustion exhaust gases typically contain low concentrations of CO_2 (4-14% v/v) [8, 9], which requires chemically reactive scrubbing solutions to capture it.

In pre-combustion capture, fuel is partially oxidized with oxygen (separated from air) and/or steam, to form a mixture of H_2 and CO_2. The CO_2 is separated from H_2, which is burned in the power plant. The higher CO_2 concentrations and pressures, compared to

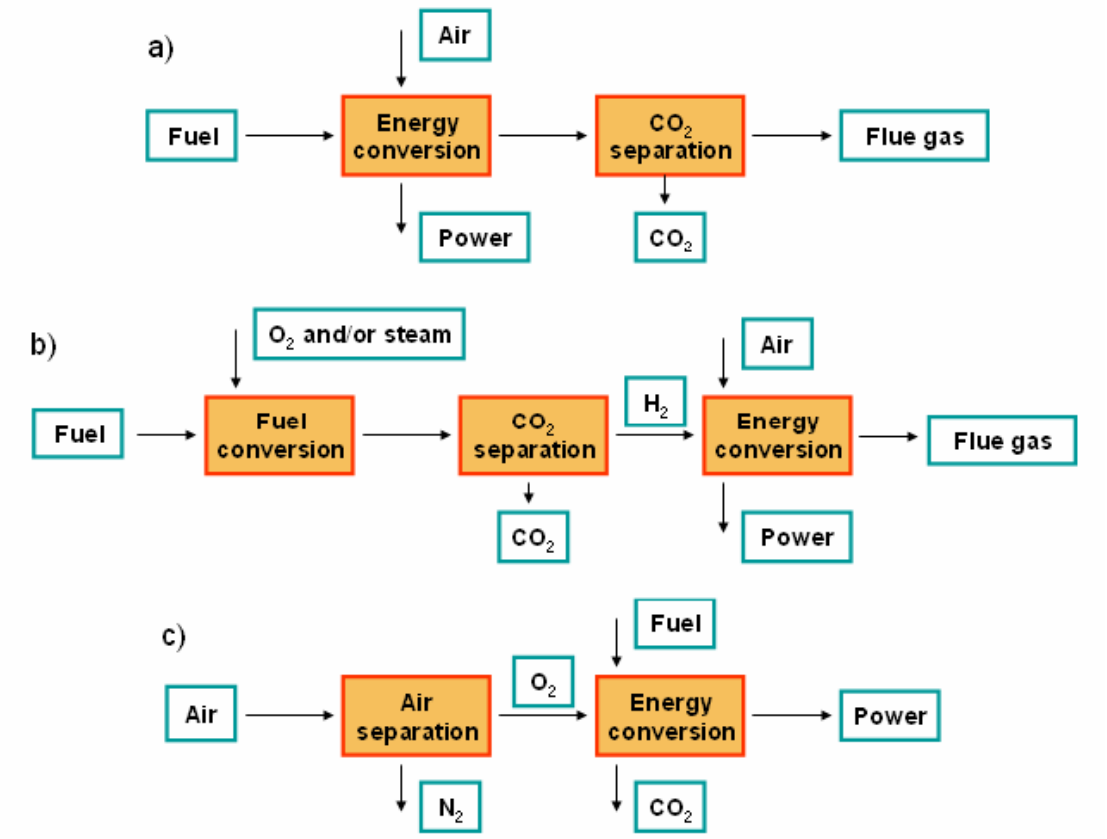

Figure 1.1 CO_2 capture schemes for fossil-fueled power plants [10]: (a) post-combustion system; (b) pre-combustion system; (c) oxy-fuel capture system.

post-combustion capture, reduce CO_2 capture operating costs, at the expenses of higher capital costs.[9]. Oxy-fuel combustion (i.e., with pure oxygen) produces CO_2 and H_2O at elevated temperatures and with negligible NO_x production at high temperature, because of the absence of N_2. The steam is separated by condensation [8, 11]. The advantages related to oxy-fuel capture are the high concentration of CO_2 in the output stream (above 80% v/v), and NOx is not formed, while the main cost associated with oxy-fuel capture is the separation of O_2 from air.

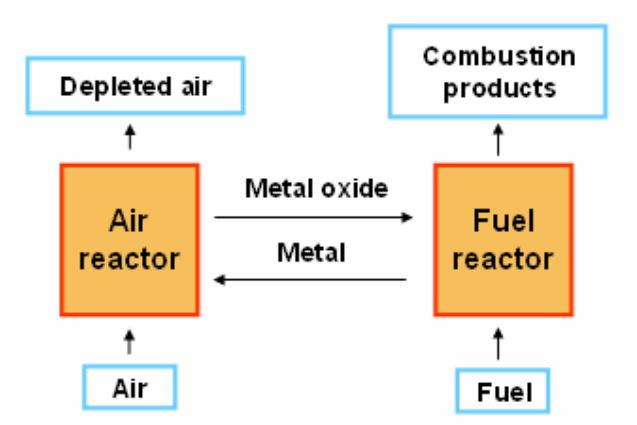

Figure 1.2 Chemical-looping combustion [12].

The novel chemical-looping combustion (CLC) process shown in Figure 1.2 includes internal CO_2 capture. Small particles of a metal oxide such as Fe_2O_3, NiO, CuO or Mn_2O_3 carry oxygen between two separate reactors fed with air and fuel, respectively. This avoids the direct air/fuel contact. In one reactor, the oxygen-depleted carrier is oxidized by air. In the other reactor, the carrier is reduced by the fuel. The advantages of CLC are that the exhaust gas from oxidation reactor is mainly harmless N_2; and negligible NOx is formed at moderate temperatures in the absence of a flame. The exhaust gas from the reduction reactor consists mainly of CO_2 and H_2O, which is separated by condensation.

Regardless of the source of CO_2, the technologies for its capture include both physical and chemical processes, and combinations thereof. The focus here is on absorption.

2. REVIEW OF LITERATURE

2.1 CO_2 absorption technology

The flue gas CO_2 capture systems of greatest current interest involve absorption and desorption (stripping) using solvents containing alkanolamines, amino acid salts, ammonia and ionic liquids, as well as carbonation/calcination cycles [13-42].

Most scrubbing solutions contain alkanolamines – e.g., monoethanolamine (MEA), diethanolamine (DEA), di-isopropanolamine (DIPA) and methyldiethanolamine (MDEA). MEA is particularly well-suited to remove CO_2 from flue gases [13]. In the regenerative process, MEA reacts in solution with CO_2 to form MEA carbamate; the CO_2-rich MEA solution is fed to a stripper where concentrated CO_2 is released by contact with steam; the regenerated (stripped) MEA solution is sent to the absorber [14].

This process is capital and energy-intensive [15-17]. The steam supplied to the stripper, which operates at 110 ~ 130 ^oC, is responsible for up to 70% of the operating costs of CO_2 capture [18]. Reactions of the amine with flue gas SO_2, NO_2, HCl, HF and oxygen forms corrosive degradation products, which requires construction with stainless steel. Other drawbacks of MEA-based processes are relatively low CO_2 loading capacity and amine volatility.

Figure 2.1 shows the reaction pathways between CO_2 and primary or secondary amines. Most of the CO_2 absorbed at relatively low temperature (*ca*. 40 ^oC) forms carbamate and protonated alkanolamine. It can be calculated from the reaction scheme

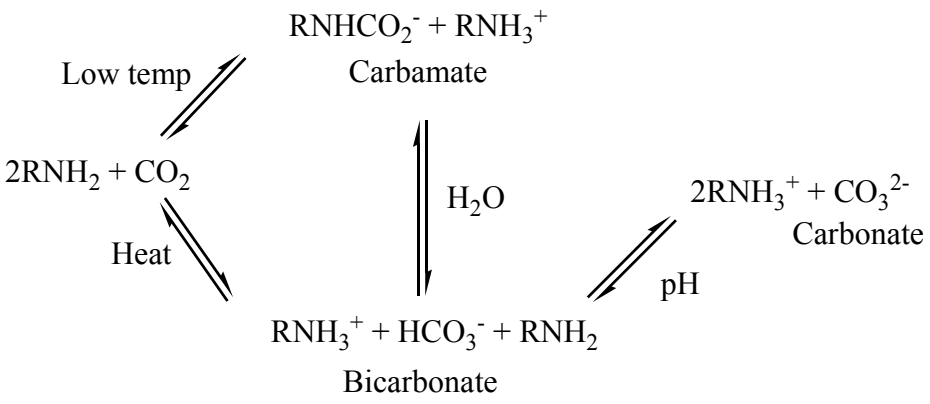

Figure 2.1 Proposed mechanism of reactions between CO_2 and primary or secondary amines [19].

that, there is a theoretical maximum CO_2 loading of 0.5 mol CO_2/mol amine in the absence of hydrolysis of the carbamate [19]. The reaction between amine and CO_2 is very fast in comparison to the carbamate hydrolysis reaction [20]; the correspondingly high heat of carbamate formation results in high solvent regeneration costs. Depending on the residence time of the liquid in the gas-liquid contactor, some degree of carbamate hydrolysis may occur, which results in maximum CO_2 loading values larger than 0.5. Also depending on the temperature and pH value of the reaction system, product proportion of bicarbonate and carbonate vary with the amine, temperature and pH.

Unlike primary and secondary amines, tertiary amines have no hydrogen atom attached to the nitrogen atom and, therefore, form no carbamate. However, tertiary amines facilitate CO_2 hydrolysis, forming bicarbonate via a base-catalyzed hydration [21]:

$$RN_3 + H_2O + CO_2 \rightarrow R_3N^+H + HCO_3^- \qquad (2.1.1)$$

The reaction heat released in bicarbonate formation is lower than that of carbamate

formation, thus reducing solvent regeneration costs. As can be seen from equation 2.1.1, tertiary amines have a high CO_2 loading capacity of 1 mol CO_2/mol amine. In addition, rates of CO_2 absorption in solutions of tertiary amines can be enhanced by the addition of small amounts of primary or secondary amines [22].

Mixed amines can combine the desirable qualities of the individual amines. Mixtures of tertiary amines with primary amines or secondary amines offer the CO_2 reactivity of primary or secondary amines *and* higher CO_2 capacities – therefore lower required solvent circulation rates and regeneration costs similar to those of tertiary amines [18].

Not long ago, a new class of amines - *sterically hindered amines* - with regeneration costs lower than those of conventional primary and secondary amines, received considerable attention. A sterically hindered amine is a primary amine whose amino group is attached to a tertiary carbon atom, or a secondary amine whose amino group is attached to a secondary or tertiary carbon atom [23].With a large group attached to the nitrogen atom, these amines form unstable carbamates that hydrolyze to form bicarbonate, thus resulting in a CO_2 capacity of 1 mol CO_2/mol amine [24-26].

Because of the use of alkanolamines for CO_2 absorption is capital and operating expense intensive, development of more efficient solvents is essential for reducing the cost of CO_2 capture. Amino acid salts (AAS), due to their physical and chemical properties, are promising, albeit more expensive, alternatives to alkanolamines. An AAS is formed by neutralizing a weak organic nonvolatile amino acid with an equinormal

amount of strong inorganic base. For example, potassium glycinate (aminoacetic acid, denoted as PG) is the neutral product of glycine and potassium hydroxide.

AAS's are less subject to degradation (less production of toxic degradation products) when exposed to flue gases [27]. Their ionic nature results in negligible volatility and increased surface tension [28]. Additionally, many amino acids are naturally occurring so that they have less environmental or toxicity issues. Their CO_2 absorption capabilities are comparable to those of alkanolamines [29]. Under certain operating conditions, solid precipitates composed of amino acids and more complex, CO_2-containing species have been observed.

Furthermore, amino acids can be neutralized, not only by strong inorganic bases, but also by organic bases including amines. The latter mixtures are called amine amino acid salts (AAAS). Neutralization is only partial because of the weak reaction between weak acid and weak base. AAAS's show higher CO_2 loading, higher cyclic capacity and absorb larger amount of CO_2 than AAS's at the same concentration. The explanation is not entirely clear; it may be related to a lower equilibrium temperature sensitivity of AAAS's [30]. It was also observed that AAAS showed no foaming, discoloration or precipitation under atmospheric conditions up to 80 ^{o}C [30], demonstrating good signs of stability.

Ammonia is yet another alternative that avoid the drawbacks of MEA [16, 17]. Aqueous ammonia absorbs CO_2 to form ammonium bicarbonate and ammonium carbonate. Before reacting with aqueous ammonia in a wet scrubber at low temperature

(0 ~ 20 ^{o}C), flue gas needs to be pretreated by oxidizing SO_2 and NO to SO_3 and NO_2. In this temperature range, ammonium carbonate and bicarbonate precipitate in the absorber. The ammonia is regenerated simply by thermal decomposition of the products at high temperatures (100 ~ 200 ^{o}C) [31]. Due to the lower heat of desorption of CO_2, this process reportedly requires 60% less energy input than a process based on MEA. Major byproducts are common fertilizers.

Although this process potentially allows the burning of cheap and sulfer abundant coals, it also produces SO_3 and NO_2 in oxidizing flue gas pretreatment. Another problem is that the absorber off-gas phase contains ammonia, the emission of which must be avoided.

The dual-alkali approach employs ammonia as the primary alkali to promote reaction of CO_2 with NaCl to produce sodium bicarbonate and ammonium chloride. The ammonia is recovered using the second alkali, lime. Thus, the process involves the use of a calcium base that is less expensive and offers higher CO_2 reactivity, and less scaling problems (because the sorbent is a solid). However, there are some obvious drawbacks: Limestone serves as the source of lime which renders the process ineffective, and considerable energy is consumed in calcination. In addition, as indicated below, for every two moles of CO_2 captured, one mole of CO_2 is released by calcination.

$$CO_2 + NaCl + NH_3 + H_2O \rightarrow NaHCO_3 \downarrow + NH_4Cl \quad (2.1.2)$$

$$2NH_4Cl + Ca(OH)_2 \rightarrow 2NH_3 + CaCl_2 + 2H_2O \quad (2.1.3)$$

$$CaCO_3 \rightarrow CaO + CO_2 \quad (2.1.4)$$

The overall reaction is:

$$2NaCl + 2CO_2 + CaO + H_2O \rightarrow 2NaHCO_3 + CaCl_2 \quad (2.1.5)$$

A proposed modified dual-alkali approach is to use methylaminoethanol (MAE) as the primary alkali in the following reaction [32]:

$$CO_2 + NaCl + HOCH_2CH_2(CH_3)NH + H_2O \rightleftarrows NaHCO_3 \downarrow + HOCH_2CH_2(CH_3)NH \cdot HCl \quad (2.1.6)$$

However, a suitable secondary alkali to regenerate the primary alkali, MAE, remains to be identified.

Carbonation/calcination cycles involve two fluidized bed reactors, one an adsorber, the other a regenerator, operating at atmospheric pressure. In the adsorber, CaO is carbonated to $CaCO_3$ at 600-700 ^oC. In the regenerator, which operates above 900 ^oC, $CaCO_3$ is calcinated to release concentrated CO_2. The high percentage of CO_2 captured (greater than 80%) makes this economically competitive technology [33-36]. The major drawback is the decay of absorbent activity; however, it maintains a higher CO_2 uptake rate than many other sorbents, even when fully degraded.

Ionic liquids are known to exhibit unique physiochemical properties that make them attractive for gas separations [37-42]: i.e., extremely low vapor pressure, wide liquid temperature range, high thermal and chemical stability, and ability to dissolve a variety of chemical compounds. In combination with amines, ionic liquids have been shown to offer such advantages as lower heat capacities, lower water contents and energy

savings [37]. Uptake of CO_2 per mole of ionic liquid can approach 0.5, using an ionic liquid consisting of an imidazolium cation with a primary amine moiety and tetrafluoroborate anion, which makes it effective for CO_2 absorption [38]. However, engineering scale-up of CO_2 capture via ionic liquid-based technology has been limited due to high costs and relatively high viscosities [37, 39]. Furthermore, the toxicology of most ionic liquids remains to be evaluated [40-42].

2.2 Kinetics study of CO_2 reactions with amino acid salts

Because the reactive functional groups of amino acids are similar to those of alkanolamines, the reactions mechanism can be expected to be similar. The salts of amino acids have the additional advantage of being an ionic solution, which minimizes volatility, which is especially important at stripper conditions (lowered pressure and elevated temperature). The salt functionality of AAS's increases their surface tension, which makes them promising for gas-liquid membrane applications. In contrast with MEA, which can only be used in combination with expensive membranes due to wetting problems, AAS can be employed in conjunction with cheaper and commercially available membranes such as polypropene, economically improving the process [43]. Therefore, a review of reaction kinetics of CO_2 with AAS is important for design of gas-liquid contactors.

Among various kinds of AAS's, two potassium salts stand out: the potassium salt of glycine (PG) presents several interesting properties such as very good thermal stability and fast reaction rate towards CO_2. Additionally it is commercially available and relatively cheap. For these merits, it is commonly used for characterization as a CO_2 absorbent. Another potassium amino acid salt, potassium sarcosinate (PS) is also a promising candidate sorbent because of its relatively high CO_2 loading capacity and reactivity, and its relative large window of operation without precipitation during CO_2 absorption [28].

During the absorption of CO_2 in aqueous potassium salt of amino acid, the

following reactions can occur (R' = -H for PG, and R' = -CH_3 for PS):

$$CO_2 + 2\ {}^{-}OOCCH_2NHR' \rightleftharpoons {}^{-}OOCCH_2NR'COO^{-} + {}^{-}OOCCH_2NH_2^{+}R' \qquad (2.2.1)$$

$$CO_2 + OH^{-} \rightleftharpoons HCO_3^{-} \qquad (2.2.2)$$

$$CO_2 + H_2O \rightleftharpoons HCO_3^{-} + H^{+} \qquad (2.2.3)$$

Reaction 2.2.1 is the key reaction in the absorption system, and its forward reaction rate needs to be determined accurately. The forward rate constants and the equilibrium constants of the reactions 2.2.1 and 2.2.2 are available in the literature [44-48]. The reaction between CO_2 and OH^- (equation 2.2.2) is fast; however, due to the trace amounts of OH^-, this reaction is often negligible [47]. The total rate of CO_2 absorption in an aqueous AAS solution is given by the sum of the reaction rates given by equations 2.2.1-3.

A detailed knowledge of the CO_2 reaction mechanism for alkanolamines is essential for a fundamental understanding of the reaction systems. Generally, the reaction kinetics can be described by either the two-step zwitterion mechanism (proposed originally by Caplow [49] and later reintroduced by Danckwerts [24]) or by the single-step termolecular mechanism (proposed originally by Crooks and Donellan [50] and recently revisited by da Silva and Svendsen [51]). Both mechanisms are extendable to aqueous AAS solution.

The principle difference in applying the zwitterion mechanism to aqueous alkanolamines and AAS is the additional ionic charge associated with the reactant,

product and intermediate species. This may significantly influence the stability and deprotonation rate of the zwitterion, and thereby the overall order of the reaction in aqueous AAS solutions. In this mechanism, the initial step in the reaction of CO_2 with amino acid anion is the formation of the protonated di-carbamate (the key short-lived intermediate) which can then be deprotonated by any base, B_j, in a competitive way, to form the di-carbamate anion according to the following reactions:

$$CO_2 + {}^{-}OOCCH_2NHR' \underset{k_{-1}}{\overset{k_1}{\rightleftharpoons}} {}^{-}OOCCH_2N^{+}HR'COO^{-} \tag{2.2.4}$$

$${}^{-}OOCCH_2N^{+}HR'COO^{-} + B_j \underset{k_{-B_j}}{\overset{k_{B_j}}{\rightleftharpoons}} {}^{-}OOCCH_2NR'COO^{-} + B_jH^{+} \tag{2.2.5}$$

The base can be the amino acid anion, water, or a hydroxyl ion [52]. Note that if deprotonation is carried out by the amino acid anion, it forms a zwitterion (protonated carbamate, which can exist at relatively large amount in the solution [53]).

Assuming a quasi-steady-state condition for the protonated di-carbamate concentration, and first order behavior of CO_2 (this is achieved by considering the second proton transfer step to be irreversible, as is the case in the kinetic constant measurement experiments carried out in the pseudo-first-order reaction regime [28]), the overall forward rate of the reaction is given by

$$r_{CO_2} = \frac{k_1 C_{AAS} C_{CO_2}}{1 + \dfrac{k_{-1}}{\Sigma k_{Bj} C_{Bj}}} \tag{2.2.6}$$

where $\Sigma k_{Bj} C_{Bj}$ is the contribution of all the bases present in the solution for the removal of proton. Because the hydroxyl concentration is typically low, its contribution to the

deprotonation of the protonated di-carbamate ion is generally assumed to be negligible [52, 54, 55]. However, in some concentrated AAS solutions, the pH can be quite high, in which case the hydroxyl ion contribution to the deprotonation may not be negligible.

Under certain limiting conditions, reaction 2.2.6 may be simplified as follows.

1. $k_{-1}/(\Sigma k_{Bj}C_{Bj}) << 1$: this results in a simple second order kinetics, which implies that the protonated di-carbamate ion is deprotonated relatively fast in comparison to the reversion rate to CO_2 and the amino acid anion. The overall reaction order is two:

$$r_{CO_2} = k_1 C_{CO_2} C_{AAS} \tag{2.2.7}$$

2. $k_{-1}/(\Sigma k_{Bj}C_{Bj}) >> 1$: This results in a more complex kinetic rate expression.

$$r_{CO_2} = k_1 C_{CO_2} C_{AAS} (\Sigma \frac{k_{Bj}}{k_{-1}} C_{Bj}) \tag{2.2.8}$$

Depending on the relative contribution of various bases present in the aqueous solution to the deprotonation of the protonated di-carbamate ion, the above expression can explain any reaction order. It can also describe the shifting reaction orders with respect to AAS concentration. For very low AAS concentration, equation 2.2.8 will reduce to the following form and the partial reaction order in AAS is one.

$$r_{CO_2} = k_1 C_{CO_2} C_{AAS} (\frac{k_{H_2O}}{k_{-1}} C_{H_2O}) \tag{2.2.9}$$

At moderately high AAS concentrations, the contribution of amino acid anion and water to the protonated di-carbamate anion deprotonation are equally significant, hence equation 2.2.8 must be used in its complete form to describe the experimental

kinetic data.

3. When CO_2 absorbs in a non-aqueous (e.g., alcohol) solution of an AAS, deprotonation of the protonated di-carbamate ion is solely due to amino acid anion. In this case, reaction 2.2.6 reduces to

$$r_{CO_2} = \frac{k_1 C_{AAS} C_{CO_2}}{1 + \frac{k_{-1}}{k_{AAS} C_{AAS}}} \qquad (2.2.10)$$

At low concentrations of AAS, the second term in the denominator becomes significant and the partial order in AAS is higher than one and this reduces to one at very high AAS concentrations.

For accurate determination of zwitterion rate constants, experimental measurements need to be undertaken with very low to very high concentrations of AAS. From equation 2.2.9, when AAS concentration is very low, k_{H_2O} / k_{-1} can be estimated accurately, whereas when AAS is at a very high concentration (equation 2.2.7), k_1 can be obtained independently of other kinetic constants.

For aqueous AAS solutions, there seems to be a significant difference in the kinetic behavior as well as in the magnitude of the rate constants for the formation of di-carbamate anion, compared with the behavior with aqueous alkanolamines. Firstly, contrary to primary aqueous alkanolamines, the partial reaction order in AAS containing the primary amino group changes with the molar salt concentration. This is apparently

because the deprotonation step in the zwitterion mechanism is not much faster than the protonated di-carbamate ion formation step, a behavior similar to that of secondary aqueous alkanolamines. In addition, it indicates that the protonated di-carbamate ion of AAS is inherently less stable compared to the zwitterion of primary alkanolamine, due to the multiple charges associated with the protonated di-carbamate ion. Other charged species may also have a negative influence on its stability.

Secondly, the ratio of the AAS deprotonation rate constant to the reverse rate constant of protonated di-carbamate formation, k_{AAS}/k_{-1}, is lower than that for aqueous secondary alkanolamines; while that of k_{H_2O}/k_{-1} is higher by almost an order of magnitude. (Note that the steric hindrance of secondary alkanolamine has a negative influence on the deprotonation of the zwitterion by a base as compared to primary alkanolamines.) It is apparently relatively easy for the uncharged water molecule to form a hydrogen bond with the protonated di-carbamate ion (which is charged at both ends) as compared to the charged amino acid anion. This indicates that water contributes significantly to the deprotonation even at moderately high AAS concentrations.

Thirdly, precipitation is a problem uniquely associated with the absorption of CO_2 in aqueous AAS solutions that may influence kinetic measurements. Precipitation occurs at high salt concentrations (> 2 mol/L), depending on temperature and the nature of the AAS [27, 56]. Notably, absorption of CO_2 in aqueous PG and PS solutions is not accompanied by, precipitation, even at high CO_2 loading [27, 47].

Crooks and Donnellan [50] questioned the validity of the zwitterion mechanism,

arguing that the number of fitting parameters required to describe the experimental data is too high and the numerical values of the parameters (especially the deprotonation rate constants) in some cases seem to be physically unrealistic. They proposed a single-step, termolecular mechanism (see scheme 2.2) to describe their experimental kinetic data. This mechanism was used by Kumar et al. [57] to describe CO_2 reaction kinetics with aqueous solutions of potassium taurinate (PT) and PG, assuming that the AAS's react simultaneously with one molecule of CO_2 and one molecule of a base. The reaction is said to proceed in a single step with a loosely bound encounter complex as the intermediate, rather than a zwitterion. The complex dissociates primarily to form CO_2 and salt (i.e., the reactant molecules); a small fraction reacts with a base molecule to give carbamate.

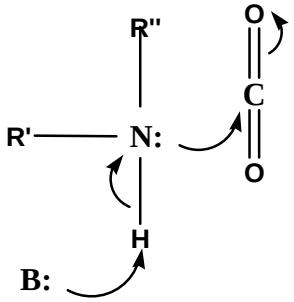

Scheme 2.2 Termolecular mechanism (B is any base, i.e. H_2O, OH^- or amino acid anion in the solution) [50]

$$CO_2 + R'R''NH + B \underset{k_{-1}}{\overset{k_1}{\rightleftharpoons}} [\text{Encounter Complex}] \xrightarrow{k_e} R'R''NCOO^- + BH^+ \quad (2.2.11)$$

Assuming a quasi-steady-state for the encounter complex, the reaction rate for this mechanism (shown by scheme 2.2 and equation 2.2.11) is given by equation 2.2.12,

which, in fact, is analogous to one of the limiting cases ($k_{-1}/(\Sigma k_{Bj}C_{Bj}) >> 1$) of the zwitterion mechanism.

$$r = (k_{R'R"NH}C_{R'R"NH} + k_{OH^-}C_{OH^-} + k_{H_2O}C_{H_2O})C_{R'R"NH}C_{CO_2} \quad (2.2.12)$$

(Not that $k_{R'R"NH} = \frac{k_e}{k_{-1}+k_e}k_{1,R'R"NH}$, $k_{OH^-} = \frac{k_e}{k_{-1}+k_e}k_{1,OH^-}$, and $k_{H_2O} = \frac{k_e}{k_{-1}+k_e}k_{1,H_2O}$)

Equation 2.2.12 suggests that all bases in solution influence the reaction in parallel. Because hydroxyl ion concentrations are typically low, their contribution is generally assumed to be negligible [52, 54, 55]. When water is the dominant base and the contributions of amino acid anion and OH^- to carbamate formation are negligible, the reaction is first order with respect to the salt, i.e.:

$$r = k_{H_2O}C_{H_2O}C_{R'R"NH}C_{CO_2} \quad (2.2.13)$$

When amino acid anion is the dominant base, the reaction is second order with respect to the salt, and the rate is given by

$$r = k_{R'R"NH}C_{R'R"NH}{}^2C_{CO_2} \quad (2.2.14)$$

It is clear from equation 2.2.12 that the number of fitting parameters in the termolecular mechanism is fewer by one than that in the zwitterion mechanism. Although the termolecular mechanism can describe fractional and higher order kinetics for aqueous alkanolamine solutions [58], it fails to explain the changing reaction orders with respect to amine concentration in nonaqueous solutions of alkanolamines [59, 60].

For most practical purposes (which involve aqueous solutions), equation 2.2.12 and its limiting cases formulations provide a workable engineering model to a wide range

of amine kinetic behavior.

Both the zwitterion mechanism and the termolecular mechanism are commonly used in literature to fit the experimental kinetic data.

2.3 Linearization techniques

From the preceding review of the kinetic study of CO_2 with amines/AAS, it can be seen a set of reversible reactions mediate mass transfer of CO_2. The reaction rate expressions enter into differential species mass balances, which form a set of nonlinear differential equations (see chapter 3). Consequently, mathematical modeling of CO_2 absorption in AAS solutions in packed towers is a computation-intensive task with multiple dimensions of trial-and-error. The most robust algorithms developed for the latter purpose implement numerical methods of analysis [61, 62].

Closed-form approximations based on linearization techniques provide less computation-intensive alternatives and are very useful for preliminary calculations [63-66]. However, they are valid over limited ranges of operating conditions or, with the exception of Onda et al.'s work [65, 66], are applicable only to systems involving uncoupled reactions,

Two other linearization techniques, namely "Thin Film Theory" and "Thick Film Theory", were developed by K. A. Smith for application to the analysis of carrier-facilitated membrane transport [1, 2]. The former deploys regular perturbation methods to account for reaction-induced departures from purely mass diffusion, while the latter uses singular perturbation methods to calculate diffusion-induced departures from local reaction equilibrium.

"Thick Film Theory" has been applied - within the framework of the steady-state Two-Film Theory of interphase mass transfer [67, 68] - to the analysis of absorption with

a single reversible reaction, whose mathematical description differs from that of carrier-facilitated transport only in the conditions at one boundary [69]. A simple trial-and-error search solves the residual algebra, resulting in enhancement factors, E (by which reaction multiplies absorption rates), that essentially overlap with those obtained via either numerical methods or the venerable linearization scheme developed by Van Krevelen and Hoftijzer [70]. Recently, "Thick Film Theory" was applied to the analysis of CO_2 absorption in and desorption from solutions of monoethanolamine (MEA), a more challenging mathematical problem involving multiple reversible reactions with widely disparate time scales [71].

More-realistic non-steady-state models, such as "Penetration Theory" [72] and "Surface Renewal Theory" [73], involve partial differential equations accounting for the dependence of local concentrations on position as well as time. It is notable that the steady-state and non-steady-state models give identical absorption rates when diffusivities are equal. Moreover, absorption rates based on the "Film Theory" approach those based on "Surface Renewal Theory" when diffusivity ratios are replaced in the analysis by their square roots [74, 75].

2.4 Summary

The mathematical analysis adopted here originated with Smith's singular perturbation method [1, 2], and is a direct derivative of the recent work by Meldon [69, 71]. Mathematical analysis of the CO_2-AAS system is very similar to that of the CO_2-MEA system developed by Meldon and Morales-Cabrera [71]. A Film Model is set up with appropriate boundary conditions; differential mass balances are solved via linearizing approximations; yielding a set of algebraic relations that is solved by trial-and-error.

Unlike the reaction kinetics of CO_2 and MEA, where carbamate zwitterion formation is rate-determining (i.e. deprotonation of the zwitterion is fast), the reaction kinetics is more complex. Accordingly, the analysis of CO_2 absorption in solutions of potassium salts of glycine and sarcosine is more complex than that developed for MEA, and is more generally applicable. Deprotonation of the protonated di-carbamate by both the amino acid anion and water are taken into account in the CO_2-AAS system, whereas the contribution of water is neglected in the CO_2-MEA system. Accordingly, the denominator of the di-carbamate consumption rate expression (equation 3.1.9) is algebraically more complex in the CO_2-AAS analysis, whereas in the case of MEA, the algebraic term denominator is negligible. Another major difference is the intrinsically ionic nature of potassium salts, which influences physiochemical properties as well as reaction kinetics.

3. DEVELOPMENT OF THE MATHEMATICAL MODEL

3.1 Reactions

The following shorthand notation for species is adopted here:

$A \equiv CO_2$, $B^- \equiv HCO_3^-$, $W \equiv H_2O$, $C^{2-} \equiv CO_3^{2-}$,

$R \equiv^- OOCCH_2N^+H_2R'$, $R^- \equiv^- OOCCH_2NHR'$, $R^{2-} \equiv^- OOCCH_2NR'COO^-$,

$R^z \equiv^- OOCCH_2N^+HR'COO^-$

Note that for PG, $R' = -H$; while for PS, $R' = -CH_3$.

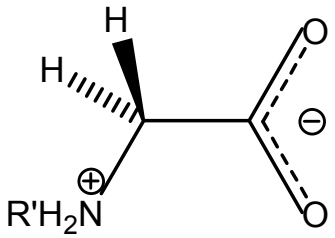

Figure 3.1.1 Zwitterionic structure of glycine (R' = -H) or sarcosine (R' = -CH_3)

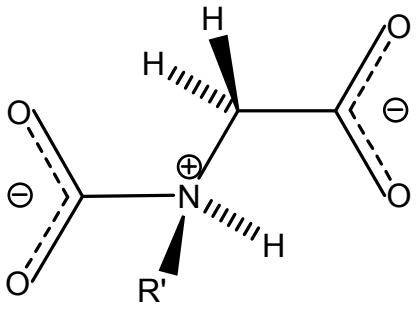

Figure 3.1.2 Structure of protonated di-carbamate ion (R^z) of glycine (R' = -H) or sarcosine (R' = -CH_3)

Potassium amino acid salts are completely ionized in water as potassium cations, and amino acid anions (R^-) with a deprotonated amino group that reacts with CO_2 to form a di-carbamate (R^{2-}). The zwitterionic structure of amino acids in the solid state has been

confirmed by neutron diffraction measurements [76]. As such, the zwitterion (R) formed by protonation of the amino acid anion, may assume the structure shown in Figure 3.1.1. The protonated di-carbamate ion (R^z) is a short-lived intermediate with charge at three locations; its possible structure is shown in Figure 3.1.2.

It is assumed that di-carbamate formation follows the two-step "zwitterion mechanism" [24, 49, 57]:

i) formation of the protonated di-carbamate ion, R^z:

$$A + R^- \underset{k_{-1a}}{\overset{k_{1a}}{\rightleftharpoons}} R^z \quad \text{(protonated di-carbamate ion)} \tag{3.1.1a}$$

$$r_{1a} = k_{1a}[A][R^-] - k_{-1a}[R^z]$$

$$K_{1a} = \frac{k_{1a}}{k_{-1a}} = \left(\frac{[R^z]}{[A][R^-]} \right)^{eq}$$

Here, "eq" denotes a condition of reaction equilibrium.

ii) deprotonation of protonated di-carbamate ion:

The protonated di-carbamate ion undergoes deprotonation by any base in solution, B_j, in a competitive way, resulting in a di-carbamate.

$$R^z + B_j \underset{k_{-B_j}}{\overset{k_{B_j}}{\rightleftharpoons}} R^{2-} + B_jH^+ \tag{3.1.1b}$$

$B_j = W,\ R^-$ (the OH^- is usually at negligible concentration)

$$r_{1b_j} = k_{B_j}[R^z][B_j] - k_{-B_j}[R^{2-}][B_jH^+]$$

$$K_{1b_j} = \frac{k_{B_j}}{k_{-B_j}} = \left(\frac{[R^{2-}][B_jH^+]}{[R^z][B_j]} \right)^{eq} = \left(\frac{[R^{2-}][H^+]}{[R^z]} \cdot \frac{[B_jH^+]}{[B_j][H^+]} \right)^{eq}$$

$$= K_{Acid_j}\left(\frac{[R^{2-}][H^+]}{[R^z]}\right)^{eq} = K_{Acid_j}\left(\frac{[A][R^-]}{[R^z]}\right)^{eq}\left(\frac{[R^{2-}][H^+]}{[A][R^-]}\right)^{eq} = \frac{K_{Acid_j}K_{Carb}}{K_{1a}}$$

where $K_{Acid_j} \equiv \left(\frac{[B_jH^+]}{[B_j][H^+]}\right)^{eq}$, $K_{Carb} \equiv \left(\frac{[R^{2-}][H^+]}{[A][R^-]}\right)^{eq}$

Overall reaction j (the sum of 3.1.1a and 3.1.1b):

$$A + R^- + B_j \rightleftarrows R^{2-} + B_jH^+ \qquad (3.1.1)$$

$$K_{1j} = K_{1a}K_{1bj} = \left(\frac{[R^{2-}]}{[A][R^-]}\right)^{eq}\left(\frac{[B_jH^+]}{[B_j]}\right)^{eq} = \left(\frac{[R^{2-}][H^+]}{[A][R^-]}\right)^{eq}\left(\frac{[B_jH^+]}{[B_j][H^+]}\right)^{eq} \equiv K_{Carb}K_{Acid_j}$$

Other reactions in solution are:

CO_2 hydration: $A + W \underset{k_{-2}}{\overset{k_2}{\rightleftarrows}} B^- + H^+$ $\qquad r_2 = k_2[A] - k_{-2}[B^-][H^+]$ (3.1.2)

Bicarbonate formation: $A + OH^- \underset{k_{-3}}{\overset{k_3}{\rightleftarrows}} B^-$ $\qquad r_3 = k_3[A][OH^-] - k_{-3}[B^-]$ (3.1.3)

Carbonate formation: $B^- \underset{k_{-4}}{\overset{k_4}{\rightleftarrows}} C^{2-} + H^+$ $\qquad K_4 = \frac{[C^{2-}][H^+]}{[B^-]}$ (3.1.4)

Water ionization: $W \underset{k_{-5}}{\overset{k_5}{\rightleftarrows}} H^+ + OH^-$ $\qquad K_5 = [H^+][OH^-] = \frac{K_2}{K_3}$ (3.1.5)

Carbamate zwitterion deprotonation: $R \underset{k_{-6}}{\overset{k_6}{\rightleftarrows}} R^- + H^+$ $\qquad K_6 = \frac{[R^-][H^+]}{[R]}$ (3.1.6)

Reaction 3.1.4-6 are effectively instantaneous. Reaction 3.1.2 combines the slow formation and rapid dissociation of carbonic acid. The concentration of water is implicitly incorporated into k_2 and K_5.

The quasi-steady-state assumption is applied to the protonated di-carbamate ion:

$$\frac{d[R^z]}{dt} = r_{1a} - \Sigma r_{1b} = 0 = k_{1a}[A][R^-] - k_{-1a}[R^z] - \Sigma k_{B_j}[B_j][R^z] + \Sigma k_{-B_j}[R^{2-}][B_jH^+] \qquad (3.1.7)$$

The protonated di-carbamate ion concentration then becomes:

$$[R^z] = \frac{k_{1a}[A][R^-] + [R^{2-}]\Sigma k_{-B_j}[B_jH^+]}{k_{-1a} + \Sigma k_{B_j}[B_j]} \tag{3.1.8}$$

Therefore,

$$r_{1a} = \frac{k_{1a}[A][R^-]\Sigma k_{B_j}[B_j] - k_{-1a}[R^{2-}]\Sigma k_{-B_j}[B_jH^+]}{k_{-1a} + \Sigma k_{B_j}[B_j]}$$

$$= \frac{k_{1a}[A][R^-]\Sigma\left(k_{B_j}[B_j]\left(1 - \frac{[R^{2-}][B_jH^+]}{K_{1a}K_{1b_j}[B_j][A][R^-]}\right)\right)}{k_{-1a} + \Sigma k_{B_j}[B_j]}$$

$$= \frac{\Sigma\left[\left(k_{1a}k_{B_j}[B_j][A][R^-]\right)\left(1 - \frac{[R^{2-}][B_jH^+]}{K_{Carb}K_{Acid_j}[B_j][A][R^-]}\right)\right]}{k_{-1a} + \Sigma k_{B_j}[B_j]} \tag{3.1.9}$$

3.2 Mass transfer model

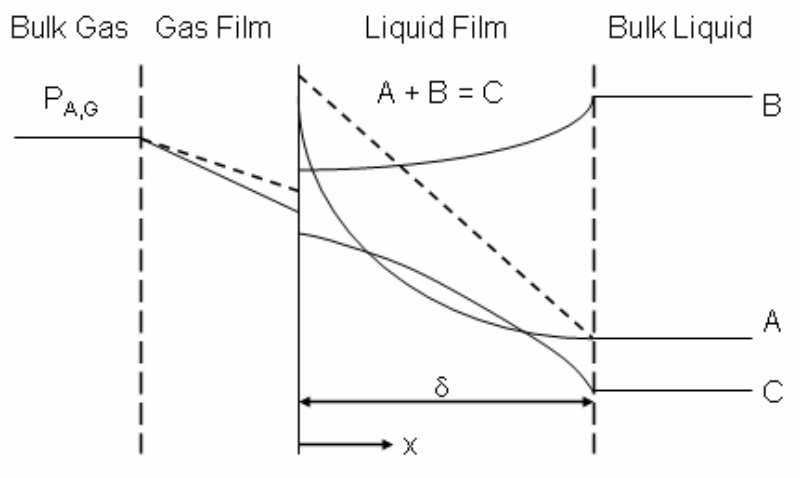

Figure 3.2 Concentration profiles in the steady-state "Film Theory" model (for A + B = C reaction); (dotted lines: physical absorption; solid lines: absorption with reversible reaction)

The analysis is based on simple steady-state Film Theory [67, 68] (Figure 3.2) in which interphase mass transfer is controlled by diffusion and reaction in gas and liquid films that separate well-mixed bulk fluids. Given the compositions of the latter, calculation of purely physical mass transfer rates is straightforward; while calculation of reaction-enhanced mass transfer rates requires the solution of nonlinear ordinary differential equations.

3.3 Differential mass balance

The key equations are species mass balances:

$$D_i \frac{d^2 C_i}{dx^2} = \rho_i \qquad (0 \le x \le \delta) \tag{3.3}$$

ρ_i is the local rate of consumption and D_i the diffusion coefficient of component i; δ is the liquid film thickness, calculated as D_{CO_2}/k_L^o, where k_L^o is CO_2's liquid phase mass transfer coefficient. Gas phase mass transfer resistance is neglected, and electrical effects due to differences in diffusivities of ionic species are also neglected. For simplicity, ionic species are assumed to have the same diffusion coefficient, D*. Analysis of electrical effects indicates that the above assumption introduces little error when applied to the system considered here [2, 64].

3.4 Boundary conditions

$$\text{At } x = 0: \quad [A] = \alpha p_{A,G}, \quad \frac{d[i]}{dx} = 0 \quad (i \ne A) \tag{3.4.1}$$

$$\text{At } x = \delta: \quad [i] = [i]^{eq} \tag{3.4.2}$$

The assumption of overall reaction equilibrium at $x = \delta$ implies sufficiently long residence times in bulk liquid, i.e. sufficient liquid hold-up.

3.5 Preliminary analysis

Electroneutrality, which effectively prevails locally within the liquid film, is expressed as follows (neglecting the contributions of short-lived protonated di-carbamate ions, H^+ and OH^-):

$$[K^+] = [B^-] + [R^-] + 2[R^{2-}] + 2[C^{2-}] \quad \left([K^+] \text{ is a constant}\right) \tag{3.5.1}$$

"CO_2 loading", L, is defined as follows (again neglecting the contributions of the short-lived protonated di-carbamate ions):

$$L \cdot [R]_{total} = [A] + [R^{2-}] + [B^-] + [C^{2-}] = \alpha p_{A,G} + [R^{2-}] + [B^-] + [C^{2-}] \tag{3.5.2}$$

i.e. L is total moles of reversibly absorbed CO_2 per mole of amine or amino acid.

The reaction terms in equation 3.3 may be expanded as follows:

$$\rho_A = r_{1a} + r_2 + r_3, \quad \rho_{B^-} = -r_2 - r_3 + r_4, \quad \rho_{R^-} = r_{1a} + r_{1b,R^-} - r_6, \quad \rho_{R^{2-}} = -\Sigma r_{1b} = -r_{1a},$$

$$\rho_R = -r_{1b,R^-} + r_6, \quad \rho_{C^{2-}} = -r_4$$

We neglect the contribution of OH^- to protonated di-carbamate deprotonation due to its negligible concentration in the solution, i.e. the significant bases are amino acid anion and water (k_W and k_{R^-} denote rate constants for protonated di-carbamate deprotonation by water and amino acid anion, respectively). Equations 3.1.5 and 3.1.6 are used to eliminate H^+ and OH^-. Thus, equation 3.3, applied to CO_2, becomes:

$$D_A \frac{d^2[A]}{dx^2} = \frac{\Sigma\left[\left(k_{1a}k_{B_j}[B_j][A][R^-]\right)\left(1 - \frac{[R^{2-}][B_jH^+]}{K_{Carb}K_{Acid_j}[B_j][A][R^-]}\right)\right]}{k_{-1a} + \Sigma k_{B_j}[B_j]}$$

$$+ k_2[A] - k_{-2}[B^-][H^+] + k_3[A][OH^-] - k_{-3}[B^-]$$

$$= \frac{\left[\begin{array}{l} k_{1a}k_{R^-}[A][R^-]^2\left(1-\frac{[R^{2-}][R]}{K_{Carb}K_{Acid,R^-}[A][R^-]^2}\right)+ \\ k_{1a}k_W[W][A][R^-]\left(1-\frac{[R^{2-}][H^+]}{K_{Carb}K_{Acid,W}[W][A][R^-]}\right) \end{array} \right]}{k_{-1a}+k_{R^-}[R^-]+k_W[W]}$$

$$+k_2[A]-\frac{k_{-2}K_6[B^-][R]}{[R^-]}+\frac{k_3K_2[A][R^-]}{K_3K_6[R]}-k_{-3}[B^-]$$

Note that $K_{Acid,R^-}=\frac{1}{K_6}$ and $K_{Acid,W}=\frac{1}{[W]}$, and the above equation becomes:

$$= \frac{k_{1a}k_{R^-}[A][R^-]^2\left(1-\frac{K_6[R^{2-}][R]}{K_{Carb}[A][R^-]^2}\right)+k_{1a}k_W[W][A][R^-]\left(1-\frac{[W][R^{2-}][H^+]}{K_{Carb}[W][A][R^-]}\right)}{k_{-1a}+k_{R^-}[R^-]+k_W[W]}$$

$$+k_2[A]-\frac{k_{-2}K_6[B^-][R]}{[R^-]}+\frac{k_3K_2[A][R^-]}{K_3K_6[R]}-k_{-3}[B^-]$$

$$= \frac{k_{1a}k_{R^-}[A][R^-]^2\left(1-\frac{K_6[R^{2-}][R]}{K_{Carb}[A][R^-]^2}\right)+k_{1a}k_W[W][A][R^-]\left(1-\frac{K_6[R^{2-}][R]}{K_{Carb}[A][R^-]^2}\right)}{k_{-1a}+k_{R^-}[R^-]+k_W[W]}$$

$$+k_2[A]-\frac{k_{-2}K_6[B^-][R]}{[R^-]}+\frac{k_3K_2[A][R^-]}{K_3K_6[R]}-k_{-3}[B^-]$$

$$= \frac{k_{1a}[A][R^-]\left(k_{R^-}[R^-]+k_W[W]\right)\left(1-\frac{K_6[R^{2-}][R]}{K_{Carb}[A][R^-]^2}\right)}{k_{-1a}+k_{R^-}[R^-]+k_W[W]}$$

$$+k_2[A]-\frac{k_{-2}K_6[B^-][R]}{[R^-]}+\frac{k_3K_2[A][R^-]}{K_3K_6[R]}-k_{-3}[B^-] \qquad (3.5.3)$$

Application of equation 3.3 to the three amino acid species and summation of the results gives:

$$D*\frac{d^2}{dx^2}\left([R^-]+[R^{2-}]+[R]\right)=0 \qquad (3.5.4)$$

Successive integrations of equation 3.5.4, and application of zero-flux boundary

conditions and the specified total amine concentration in bulk liquid, yields the following relationship, which is applicable throughout the liquid film:

$$[R^-]+[R^{2-}]+[R]=[R]_{total} \tag{3.5.5}$$

Likewise, application of equation 3.3 to CO_2, bicarbonate, carbonate and di-carbamate, followed by summation, yields:

$$D_A\frac{d^2[A]}{dx^2}+D^*\frac{d^2}{dx^2}\left([B^-]+[R^{2-}]+[C^{2-}]\right)=0 \tag{3.5.6}$$

Integration gives:

$$D_A\frac{d[A]}{dx}+D^*\frac{d}{dx}\left([B^-]+[R^{2-}]+[C^{2-}]\right)=-\Phi_1 \tag{3.5.7}$$

Φ_1 may be identified as the CO_2 absorption rate expressed as a flux.

A second integration of equation 3.5.7, gives:

$$D_A[A]+D^*\left([B^-]+[R^{2-}]+[C^{2-}]\right)=-\Phi_1 x+\Phi_2 \tag{3.5.8}$$

Application of equation 3.5.8 at x = 0, gives:

$$\Phi_2=D_A[A]_{x=0}+D^*\left([B^-]_{x=0}+[R^{2-}]_{x=0}+[C^{2-}]_{x=0}\right) \tag{3.5.9a}$$

Application of equation 3.5.8 at x = δ, gives:

$$\Phi_2=\Phi_1\delta+D_A[A]_{x=\delta}+D^*\left([B^-]_{x=\delta}+[R^{2-}]_{x=\delta}+[C^{2-}]_{x=\delta}\right) \tag{3.5.9b}$$

Subtraction of equation 3.5.9a from 3.5.9b and rearrangement yields the following expression for the absorption rate:

$$\Phi_1=\frac{D_A\left([A]_{x=0}-[A]_{x=\delta}\right)+D^*\left([B^-]_{x=0}-[B^-]_{x=\delta}+[R^{2-}]_{x=0}-[R^{2-}]_{x=\delta}+[C^{2-}]_{x=0}-[C^{2-}]_{x=\delta}\right)}{\delta} \tag{3.5.10}$$

Note that $[B^-]_{x=0}$, $[R^{2-}]_{x=0}$ and $[C^{2-}]_{x=0}$ are unknowns.

Reaction effects are typically expressed in terms of the "enhancement factor", E,

defined as the ratio of absorption rates with and without reaction:

$$E = 1 + \beta\left(\frac{[B^-]_{x=0} - [B^-]_{x=\delta} + [R^{2-}]_{x=0} - [R^{2-}]_{x=\delta} + [C^{2-}]_{x=0} - [C^{2-}]_{x=\delta}}{[A]_{x=0} - [A]_{x=\delta}}\right)\left(\beta \equiv \sqrt{\frac{D^*}{D_A}}\right) \quad (3.5.11)$$

Replacement of the ratio of diffusivities, β, with the ratio of their square roots, brings mass transfer rates calculated on the basis of the Film Model closer to those based on non-steady-state Surface Renewal Theory. The latter, more physically realistic mass transfer model, accounts for periodic replacement of surface liquid with liquid from the bulk. The two models yield identical absorption rates when diffusivities are all equal [74, 75].

3.6 Limiting cases

When δ is small in the sense that reaction times far exceed diffusion times, the extents of reaction 3.1.1-4 are negligible except in bulk liquid. Concentrations of species in the liquid film other than CO_2 are then essentially uniform. The enhancement factor approaches 1, and the absorption rate simplifies to:

$$\Phi_1^{\,o} = k_L^{o}\left([A]_{x=0} - [A]_{x=\delta}\right) \tag{3.6.1}$$

where $k_L^{\,o}$ is CO_2's liquid phase mass transfer coefficient.

Correspondingly, when δ is large enough, all reactions approach local equilibrium effectively instantaneously, and the absorption rate and enhancement factor become:

$$\Phi_1^{eq} = \frac{D_A\left([A]_{x=0} - A_{x=\delta}\right) + D^*\left([B^-]_{x=0}^{eq} - [B^-]_{x=\delta} + [R^{2-}]_{x=0}^{eq} - [R^{2-}]_{x=\delta} + [C^{2-}]_{x=0}^{eq} - [C^{2-}]_{x=\delta}\right)}{\delta} \tag{3.6.2}$$

$$E^{eq} = 1 + \beta\left(\frac{[B^-]_{x=0}^{eq} - [B^-]_{x=\delta} + [R^{2-}]_{x=0}^{eq} - [R^{2-}]_{x=\delta} + [C^{2-}]_{x=0}^{eq} - [C^{2-}]_{x=\delta}}{[A]_{x=0} - [A]_{x=\delta}}\right) \tag{3.6.3}$$

where $[B^-]_{x=0}^{eq}$, $[C^{2-}]_{x=0}^{eq}$ and $[R^{2-}]_{x=0}^{eq}$ follow from equations 3.1.4, 3.1.6, 3.5.1, 3.5.5 and:

$$\left(\frac{[R^{2-}][H^+]}{[A][R^-]}\right)^{eq} = K_{Carb} \tag{3.6.4}$$

$$\left(\frac{[B^-][H^+]}{[A]}\right)^{eq} = K_2 \tag{3.6.5}$$

3.7 General case

Equation 3.3, when applied to R^{2-}, gives:

$$D^{*}\frac{d^{2}[R^{2-}]}{dx^{2}} = -\frac{k_{1a}[A][R^{-}]\left(k_{R^{-}}[R^{-}] + k_{W}[W]\right)\left(1 - \frac{K_{6}[R^{2-}][R]}{K_{Carb}[A][R^{-}]^{2}}\right)}{k_{-1a} + k_{R^{-}}[R^{-}] + k_{W}[W]} \tag{3.7.1}$$

The "Thick Film" linearization technique [1, 2] is suggested by the asymptotic approach to local reaction equilibrium in thick films. Reaction rates may then be safely approximated by retaining only first order terms in their Taylor series expansions (see equation 3.7.2).

$$r \approx \sum_{i} \Delta[i]\left(\frac{\partial r}{\partial \underline{[i]}}\right)_{j \neq i} \tag{3.7.2}$$

$$\Delta[i] \equiv [i] - \underline{[i]} \tag{3.7.3}$$

$\Delta[i]$ is the departure from reaction equilibrium; local pseudo-equilibrium concentrations, $\underline{[i]}$, are defined to satisfy equations 3.5.1, 3.5.5, 3.5.8 and all reaction equilibria, i.e.:

$$\underline{[R^{-}]} + \underline{[R]} + \underline{[R^{2-}]} = [R]_{total} \tag{3.7.4}$$

$$[K^{+}] = \underline{[B^{-}]} + \underline{[R^{-}]} + 2\underline{[R^{2-}]} + 2\underline{[C^{2-}]} \tag{3.7.5}$$

$$D_{A}\underline{[A]} + D^{*}(\underline{[B^{-}]} + \underline{[R^{2-}]} + \underline{[C^{2-}]}) = -\Phi_{1}x + \Phi_{2} \tag{3.7.6}$$

$$\frac{\underline{[R^{2-}]}\underline{[R]}}{\underline{[A]}\underline{[R^{-}]}^{2}} = \frac{K_{Carb}}{K_{6}} \tag{3.7.7}$$

$$\frac{\underline{[B^{-}]}\underline{[R]}}{\underline{[A]}\underline{[R^{-}]}} = \frac{K_{2}}{K_{6}} \tag{3.7.8}$$

Together with equation 3.7.3, paired equations 3.5.1 and 3.7.4, 3.5.5 and 3.7.5, and 3.5.8 and 3.7.6, imply that:

$$\Delta[R^-]+\Delta[R]+\Delta[R^{2-}]=0 \tag{3.7.9}$$

$$\Delta[B^-]+\Delta[R^-]+2\Delta[R^{2-}]+2\Delta[C^{2-}]=0 \tag{3.7.10}$$

$$D_A\Delta[A]+D^*(\Delta[B^-]+\Delta[R^{2-}]+\Delta[C^{2-}])=0 \tag{3.7.11}$$

From the reaction equilibrium $\frac{[H^+][R^-]}{[R]}=K_6$, i.e. $[H^+]=\frac{K_6[R]}{[R^-]}$, substituting this into $\frac{[C^{2-}][H^+]}{[B^-]}=K_4$ gives:

$$\frac{[C^{2-}][R]}{[R^-][B^-]}=\frac{\underline{[C^{2-}][R]}}{\underline{[R^-][B^-]}}=\frac{K_4}{K_6} \tag{3.7.12}$$

$$\Rightarrow\begin{cases}[C^{2-}]=\dfrac{K_4[R^-][B^-]}{K_6[R]} & (3.7.13)\\[2ex] \underline{[C^{2-}]}=\dfrac{K_4\underline{[R^-][B^-]}}{K_6\underline{[R]}} & (3.7.14)\end{cases}$$

Subtraction of equation 3.7.14 from 3.7.13 gives:

$$\Delta[C^{2-}]=\frac{K_4}{K_6}\left(\frac{(\underline{[R^-]}+\Delta[R^-])(\underline{[B^-]}+\Delta[B^-])}{\underline{[R]}+\Delta[R]}-\frac{\underline{[R^-][B^-]}}{\underline{[R]}}\right)$$

$$=\frac{K_4}{K_6}\left(\frac{(\underline{[R^-]}+\Delta[R^-])(\underline{[B^-]}+\Delta[B^-])(\underline{[R]}-\Delta[R])}{\underline{[R]}^2}-\frac{\underline{[R^-][B^-]}}{\underline{[R]}}\right)$$

$$=\frac{K_4}{K_6}\left(\frac{\underline{[R][R^-][B^-]}+\underline{[R][B^-]}\Delta[R^-]+\underline{[R][R^-]}\Delta[B^-]-\underline{[R^-][B^-]}\Delta[R]}{\underline{[R]}^2}-\frac{\underline{[R^-][B^-]}}{\underline{[R]}}\right)$$

$$=\frac{K_4}{K_6}\left(\frac{\underline{[R][B^-]}\Delta[R^-]+\underline{[R][R^-]}\Delta[B^-]-\underline{[R^-][B^-]}\Delta[R]}{\underline{[R]}^2}\right)$$

$$=\frac{K_4\underline{[B^-]}}{K_6\underline{[R]}}\Delta[R^-]+\frac{K_4\underline{[R^-]}}{K_6\underline{[R]}}\Delta[B^-]-\frac{K_4\underline{[R^-][B^-]}}{K_6\underline{[R]}^2}\Delta[R] \tag{3.7.15}$$

Using equations 3.7.9-11 and 3.7.15, $\Delta[B^-]$, $\Delta[R]$, and $\Delta[R^-]$ may be expressed in terms of $\Delta[A]$ and $\Delta[R^{2-}]$:

$$\begin{pmatrix} 0 & 1 & 1 \\ 1+\frac{2K_4[R^-]}{K_6[R]} & -\frac{2K_4[R^-][B^-]}{K_6[R]^2} & 1+\frac{2K_4[B^-]}{K_6[R]} \\ 1+\frac{K_4[R^-]}{K_6[R]} & -\frac{K_4[R^-][B^-]}{K_6[R]^2} & \frac{K_4[B^-]}{K_6[R]} \end{pmatrix} \cdot \begin{pmatrix} \Delta[B^-] \\ \Delta[R] \\ \Delta[R^-] \end{pmatrix} = \begin{pmatrix} -1 & 0 \\ -2 & 0 \\ -1 & -\frac{D_A}{D^*} \end{pmatrix} \cdot \begin{pmatrix} \Delta[R^{2-}] \\ \\ \Delta[A] \end{pmatrix}$$

$$\begin{pmatrix} \Delta[B^-] \\ \Delta[R] \\ \Delta[R^-] \end{pmatrix} = \begin{pmatrix} 0 & 1 & 1 \\ 1+\frac{2K_4[R^-]}{K_6[R]} & -\frac{2K_4[R^-][B^-]}{K_6[R]^2} & 1+\frac{2K_4[B^-]}{K_6[R]} \\ 1+\frac{K_4[R^-]}{K_6[R]} & -\frac{K_4[R^-][B^-]}{K_6[R]^2} & \frac{K_4[B^-]}{K_6[R]} \end{pmatrix}^{-1} \cdot \begin{pmatrix} -1 & 0 \\ -2 & 0 \\ -1 & -\frac{D_A}{D^*} \end{pmatrix} \cdot \begin{pmatrix} \Delta[R^{2-}] \\ \\ \Delta[A] \end{pmatrix}$$

$$\Rightarrow \begin{pmatrix} \Delta[B^-] \\ \Delta[R] \\ \Delta[R^-] \end{pmatrix} \equiv \text{DeltaMatrix}_{3\times 2} \cdot \begin{pmatrix} \Delta[R^{2-}] \\ \\ \Delta[A] \end{pmatrix}$$

Thus,

$$\Delta[B^-] = \omega_1 \Delta[R^{2-}] + \omega_2 \Delta[A] \tag{3.7.16}$$

$$\Delta[R] = \omega_3 \Delta[R^{2-}] + \omega_4 \Delta[A] \tag{3.7.17}$$

$$\Delta[R^-] = \omega_5 \Delta[R^{2-}] + \omega_6 \Delta[A] \tag{3.7.18}$$

$$\begin{pmatrix} \omega_1 = \text{DeltaMatrix}(1,1) & \omega_2 = \text{DeltaMatrix}(1,2) \\ \omega_3 = \text{DeltaMatrix}(2,1) & \omega_4 = \text{DeltaMatrix}(2,2) \\ \omega_5 = \text{DeltaMatrix}(3,1) & \omega_6 = \text{DeltaMatrix}(3,2) \end{pmatrix}$$

Assuming,further,that $\frac{d^2[\underline{i}]}{dx^2} << \frac{d^2\Delta[i]}{dx^2}$, and inserting the linearizating approximations,

equation 3.7.3, for species concentrations, the righthand side of equation 3.7.1 becomes:

$$D*\frac{d^2\Delta[R^{2-}]}{dx^2} = -\frac{k_{1a}([\underline{A}]+\Delta[A])([\underline{R^-}]+\Delta[R^-])\left[k_{R^-}([\underline{R^-}]+\Delta[R^-])+k_W[W]\right]}{k_{-1a}+k_{R^-}([\underline{R^-}]+\Delta[R^-])+k_W[W]}$$

$$\cdot\left(1-\frac{K_6([\underline{R^{2-}}]+\Delta[R^{2-}])([\underline{R}]+\Delta[R])}{K_{Carb}([\underline{A}]+\Delta[A])([\underline{R^-}]+\Delta[R^-])^2}\right)$$

What follows makes use of the approximations:

$$\frac{1}{k_{-1a}+k_{R^-}([\underline{R^-}]+\Delta[R^-])+k_W[W]}$$

$$=\frac{k_{-1a}+k_{R^-}[\underline{R^-}]+k_W[W]-k_{R^-}\Delta[R^-]}{\left(k_{-1a}+k_{R^-}[\underline{R^-}]+k_W[W]+k_{R^-}\Delta[R^-]\right)\left(k_{-1a}+k_{R^-}[\underline{R^-}]+k_W[W]-k_{R^-}\Delta[R^-]\right)}$$

$$=\frac{k_{-1a}+k_{R^-}[\underline{R^-}]+k_W[W]-k_{R^-}\Delta[R^-]}{\left[\begin{array}{l}\left(k_{-1a}+k_{R^-}[\underline{R^-}]+k_W[W]\right)^2+k_{R^-}\Delta[R^-]\left(k_{-1a}+k_{R^-}[\underline{R^-}]+k_W[W]\right)\\ -k_{R^-}\Delta[R^-]\left(k_{-1a}+k_{R^-}[\underline{R^-}]+k_W[W]\right)-\left(k_{R^-}\Delta[R^-]\right)^2\end{array}\right]}$$

$$=\frac{k_{-1a}+k_{R^-}[\underline{R^-}]+k_W[W]-k_{R^-}\Delta[R^-]}{\left(k_{-1a}+k_{R^-}[\underline{R^-}]+k_W[W]\right)^2-\left(k_{R^-}\Delta[R^-]\right)^2}$$

$$\approx\frac{k_{-1a}+k_{R^-}[\underline{R^-}]+k_W[W]-k_{R^-}\Delta[R^-]}{\left(k_{-1a}+k_{R^-}[\underline{R^-}]+k_W[W]\right)^2}$$ (by retaining delta quatities to the first power)

$$=\frac{1}{k_{-1a}+k_{R^-}[\underline{R^-}]+k_W[W]}-\frac{k_{R^-}\Delta[R^-]}{\left(k_{-1a}+k_{R^-}[\underline{R^-}]+k_W[W]\right)^2}$$

By the same token, $\frac{1}{[\underline{A}]+\Delta[A]} \approx \frac{[\underline{A}]-\Delta[A]}{[\underline{A}]^2}$ and $\frac{1}{([\underline{R^-}]+\Delta[R^-])^2} \approx \frac{([\underline{R^-}]-\Delta[R^-])^2}{[\underline{R^-}]^4}$;

the righthand side of equation 3.7.1 then becomes:

$$= -k_{1a}\left(\underline{[A][R^-]} + \underline{[R^-]}\Delta[A] + \underline{[A]}\Delta[R^-]\right)\left(k_{R^-}\underline{[R^-]} + k_{R^-}\Delta[R^-] + k_W[W]\right)$$

$$\cdot\left(\frac{1}{k_{-1a} + k_{R^-}\underline{[R^-]} + k_W[W]} - \frac{k_{R^-}\Delta[R^-]}{\left(k_{-1a} + k_{R^-}\underline{[R^-]} + k_W[W]\right)^2}\right)$$

$$\cdot\left(1 - \frac{K_6(\underline{[R^{2-}][R]} + \underline{[R]}\Delta[R^{2-}] + \underline{[R^{2-}]}\Delta[R])([A] - \Delta[A])(\underline{[R^-]} - \Delta[R^-])^2}{K_{Carb}\underline{[A]}^2\underline{[R^-]}^4}\right)$$

The equilibrium expression, equation 3.7.7, may be used to reduce the following expression:

$$\left(1 - \frac{K_6(\underline{[R^{2-}][R]} + \underline{[R]}\Delta[R^{2-}] + \underline{[R^{2-}]}\Delta[R])([A] - \Delta[A])(\underline{[R^-]} - \Delta[R^-])^2}{K_{Carb}\underline{[A]}^2\underline{[R^-]}^4}\right) \text{ to:}$$

$$-\left(\frac{\Delta[R^{2-}]}{\underline{[R^{2-}]}} + \frac{\Delta[R]}{\underline{[R]}} - \frac{\Delta[A]}{\underline{[A]}} - \frac{2\Delta[R^-]}{\underline{[R^-]}}\right).$$

This simplifies the righthand side of equation 3.7.1 to:

$$= k_{1a}\left(\begin{array}{l} k_{R^-}\underline{[A][R^-]}^2 + k_{R^-}\underline{[R^-]}^2\Delta[A] + 2k_{R^-}\underline{[R^-][A]}\Delta[R^-] \\ \\ +k_W[W]\underline{[A][R^-]} + k_W[W]\underline{[R^-]}\Delta[A] + k_W[W]\underline{[A]}\Delta[R^-] \end{array}\right)$$

$$\cdot\left(\frac{1}{k_{-1a} + k_{R^-}\underline{[R^-]} + k_W[W]} - \frac{k_{R^-}\Delta[R^-]}{\left(k_{-1a} + k_{R^-}\underline{[R^-]} + k_W[W]\right)^2}\right)$$

$$\cdot\left(\frac{\Delta[R^{2-}]}{\underline{[R^{2-}]}} + \frac{\Delta[R]}{\underline{[R]}} - \frac{\Delta[A]}{\underline{[A]}} - \frac{2\Delta[R^-]}{\underline{[R^-]}}\right)$$

Finally, by retaining only the first order delta terms, the righthand side of equation 3.7.1 simplifies to:

$$= k_{1a}\left(\frac{k_{R^-}\underline{[A][R^-]}^2 + k_W[W]\underline{[A][R^-]}}{k_{-1a} + k_{R^-}\underline{[R^-]} + k_W[W]}\right)\cdot\left(\frac{\Delta[R^{2-}]}{\underline{[R^{2-}]}} + \frac{\Delta[R]}{\underline{[R]}} - \frac{\Delta[A]}{\underline{[A]}} - \frac{2\Delta[R^-]}{\underline{[R^-]}}\right)$$

If we then insert equations 3.7.16-18, the above equation becomes:

$$= k_{1a}\left(\frac{k_{R^-}\underline{[A][R^-]}^2 + k_W[W]\underline{[A][R^-]}}{k_{-1a} + k_{R^-}\underline{[R^-]} + k_W[W]}\right)$$

$$\cdot\left(\frac{\Delta[R^{2-}]}{\underline{[R^{2-}]}} + \frac{\omega_3\Delta[R^{2-}] + \omega_4\Delta[A]}{\underline{[R]}} - \frac{\Delta[A]}{\underline{[A]}} - \frac{2(\omega_5\Delta[R^{2-}] + \omega_6\Delta[A])}{\underline{[R^-]}}\right)$$

$$= k_{1a}\left(\frac{k_{R^-}\underline{[A][R^-]}^2 + k_W[W]\underline{[A][R^-]}}{k_{-1a} + k_{R^-}\underline{[R^-]} + k_W[W]}\right)$$

$$\cdot\left(\left(\frac{1}{\underline{[R^{2-}]}} + \frac{\omega_3}{\underline{[R]}} - \frac{2\omega_5}{\underline{[R^-]}}\right)\Delta[R^{2-}] + \left(\frac{\omega_4}{\underline{[R]}} - \frac{1}{\underline{[A]}} - \frac{2\omega_6}{\underline{[R^-]}}\right)\Delta[A]\right)$$

or :

$$\frac{d^2\Delta[R^{2-}]}{dx^2} = \eta_1\Delta[R^{2-}] + \eta_2\Delta[A] \qquad (3.7.19)$$

$$\left[\begin{array}{l} \eta_1 \equiv \dfrac{k_{1a}}{D^*}\left(\dfrac{k_{R^-}\underline{[A][R^-]}^2 + k_W[W]\underline{[A][R^-]}}{k_{-1a} + k_{R^-}\underline{[R^-]} + k_W[W]}\right)\cdot\left(\dfrac{1}{\underline{[R^{2-}]}} + \dfrac{\omega_3}{\underline{[R]}} - \dfrac{2\omega_5}{\underline{[R^-]}}\right) \\ \\ \eta_2 \equiv \dfrac{k_{1a}}{D^*}\left(\dfrac{k_{R^-}\underline{[A][R^-]}^2 + k_W[W]\underline{[A][R^-]}}{k_{-1a} + k_{R^-}\underline{[R^-]} + k_W[W]}\right)\cdot\left(\dfrac{\omega_4}{\underline{[R]}} - \dfrac{1}{\underline{[A]}} - \dfrac{2\omega_6}{\underline{[R^-]}}\right) \end{array}\right]$$

In the same fashion, when the above linearization methods are applied to the sum of reaction rates r_2 and r_3, the result is:

$$r_2 + r_3 = k_2[A] - k_{-2}[B^-][H^+] + k_3[A][OH^-] - k_{-3}[B^-]$$

$$= k_2[A] - \frac{k_{-2}K_6[B^-][R]}{[R^-]} + \frac{k_3K_5[A][R^-]}{K_6[R]} - k_{-3}[B^-]$$

$$= k_2(\underline{[A]} + \Delta[A]) - \frac{k_2K_6(\underline{[B^-]} + \Delta[B^-])(\underline{[R]} + \Delta[R])(\underline{[R^-]} - \Delta[R^-])}{K_2\underline{[R^-]}^2}$$

$$+ \frac{k_3K_5(\underline{[A]} + \Delta[A])(\underline{[R^-]} + \Delta[R^-])(\underline{[R]} - \Delta[R])}{K_6\underline{[R]}^2} - \frac{k_3(\underline{[B^-]} + \Delta[B^-])}{K_3}$$

$$= k_2\underline{[A]} + k_2\Delta[A] - \frac{k_3\underline{[B^-]} + k_3\Delta[B^-]}{K_3}$$

$$- \frac{k_2K_6(\underline{[B^-][R][R^-]} + \underline{[R][R^-]}\Delta[B^-] + \underline{[B^-][R^-]}\Delta[R] - \underline{[B^-][R]}\Delta[R^-])}{K_2\underline{[R^-]}^2}$$

$$+ \frac{k_3K_5(\underline{[A][R^-][R]} + \underline{[R^-][R]}\Delta[A] + \underline{[A][R]}\Delta[R^-] - \underline{[A][R^-]}\Delta[R])}{K_6\underline{[R]}^2}$$

$$= k_2\Delta[A] - \frac{k_3\Delta[B^-]}{K_3} - \frac{k_2\underline{[A]}\Delta[B^-]}{\underline{[B^-]}} - \frac{k_2\underline{[A]}\Delta[R]}{\underline{[R]}} + \frac{k_2\underline{[A]}\Delta[R^-]}{\underline{[R^-]}}$$

$$+ \frac{k_3K_5\underline{[R^-]}\Delta[A]}{K_6\underline{[R]}} + \frac{k_3K_5\underline{[A]}\Delta[R^-]}{K_6\underline{[R]}} - \frac{k_3\underline{[B^-]}\Delta[R]}{K_3\underline{[R]}}$$

$$= k_2\Delta[A] - \frac{k_3\left(\omega_1\Delta[R^{2-}] + \omega_2\Delta[A]\right)}{K_3} - \frac{k_2\underline{[A]}\left(\omega_1\Delta[R^{2-}] + \omega_2\Delta[A]\right)}{\underline{[B^-]}}$$

$$- \frac{k_2\underline{[A]}\left(\omega_3\Delta[R^{2-}] + \omega_4\Delta[A]\right)}{\underline{[R]}} + \frac{k_2\underline{[A]}\left(\omega_5\Delta[R^{2-}] + \omega_6\Delta[A]\right)}{\underline{[R^-]}} + \frac{k_3K_5\underline{[R^-]}\Delta[A]}{K_6\underline{[R]}}$$

$$+ \frac{k_3K_5\underline{[A]}\left(\omega_5\Delta[R^{2-}] + \omega_6\Delta[A]\right)}{K_6\underline{[R]}} - \frac{k_3\underline{[B^-]}\left(\omega_3\Delta[R^{2-}] + \omega_4\Delta[A]\right)}{K_3\underline{[R]}}$$

$$= k_2\Delta[A] - \frac{k_3\omega_1\Delta[R^{2-}]}{K_3} - \frac{k_3\omega_2\Delta[A]}{K_3} - \frac{k_2\underline{[A]}\omega_1\Delta[R^{2-}]}{\underline{[B^-]}} - \frac{k_2\underline{[A]}\omega_2\Delta[A]}{\underline{[B^-]}}$$

$$- \frac{k_2\underline{[A]}\omega_3\Delta[R^{2-}]}{\underline{[R]}} - \frac{k_2\underline{[A]}\omega_4\Delta[A]}{\underline{[R]}} + \frac{k_2\underline{[A]}\omega_5\Delta[R^{2-}]}{\underline{[R^-]}} + \frac{k_2\underline{[A]}\omega_6\Delta[A]}{\underline{[R^-]}} + \frac{k_3K_5\underline{[R^-]}\Delta[A]}{K_6\underline{[R]}}$$

$$+ \frac{k_3K_5\underline{[A]}\omega_5\Delta[R^{2-}]}{K_6\underline{[R]}} + \frac{k_3K_5\underline{[A]}\omega_6\Delta[A]}{K_6\underline{[R]}} - \frac{k_3\underline{[B^-]}\omega_3\Delta[R^{2-}]}{K_3\underline{[R]}} - \frac{k_3\underline{[B^-]}\omega_4\Delta[A]}{K_3\underline{[R]}}$$

$$= \left(k_2 - \frac{k_3\omega_2}{K_3} - \frac{k_2\omega_2\underline{[A]}}{\underline{[B^-]}} - \frac{k_2\omega_4\underline{[A]}}{\underline{[R]}} + \frac{k_2\omega_6\underline{[A]}}{\underline{[R^-]}} + \frac{k_3K_5\underline{[R^-]}}{K_6\underline{[R]}} + \frac{k_3K_5\omega_6\underline{[A]}}{K_6\underline{[R]}} - \frac{k_3\omega_4\underline{[B^-]}}{K_3\underline{[R]}} \right)\Delta[A]$$

$$+ \left(\frac{k_2\omega_5\underline{[A]}}{\underline{[R^-]}} - \frac{k_2\omega_3\underline{[A]}}{\underline{[R]}} + \frac{k_3K_5\omega_5\underline{[A]}}{K_6\underline{[R]}} - \frac{k_3\omega_3\underline{[B^-]}}{K_3\underline{[R]}} - \frac{k_3\omega_1}{K_3} - \frac{k_2\omega_1\underline{[A]}}{\underline{[B^-]}} \right)\Delta[R^{2-}]$$

$$= \lambda_1\Delta[R^{2-}] + \lambda_2\Delta[A] \qquad (3.7.20)$$

$$\left[\lambda_1 \equiv \left(\frac{k_2\omega_5\underline{[A]}}{\underline{[R^-]}} - \frac{k_2\omega_3\underline{[A]}}{\underline{[R]}} + \frac{k_3K_5\omega_5\underline{[A]}}{K_6\underline{[R]}} - \frac{k_3\omega_3\underline{[B^-]}}{K_3\underline{[R]}} - \frac{k_3\omega_1}{K_3} - \frac{k_2\omega_1\underline{[A]}}{\underline{[B^-]}} \right) \right.$$

$$\left. \lambda_2 \equiv \left(k_2 - \frac{k_3\omega_2}{K_3} - \frac{k_2\omega_2\underline{[A]}}{\underline{[B^-]}} - \frac{k_2\omega_4\underline{[A]}}{\underline{[R]}} + \frac{k_2\omega_6\underline{[A]}}{\underline{[R^-]}} + \frac{k_3K_5\underline{[R^-]}}{K_6\underline{[R]}} + \frac{k_3K_5\omega_6\underline{[A]}}{K_6\underline{[R]}} - \frac{k_3\omega_4\underline{[B^-]}}{K_3\underline{[R]}} \right) \right]$$

By analogy to the derivation of equations 3.7.19 and 3.7.20, equation 3.5.3 becomes:

$$\Rightarrow \frac{d^2\Delta[A]}{dx^2} = -\frac{D^*}{D_A}\eta_1\Delta[R^{2-}] - \frac{D^*}{D_A}\eta_2\Delta[A] + \frac{\lambda_1}{D_A}\Delta[R^{2-}] + \frac{\lambda_2}{D_A}\Delta[A]$$

$$= \eta_3\Delta[R^{2-}] + \eta_4\Delta[A] \qquad \left(\eta_3 \equiv \frac{\lambda_1}{D_A} - \frac{D^*}{D_A}\eta_1 \quad \eta_4 \equiv \frac{\lambda_2}{D_A} - \frac{D^*}{D_A}\eta_2 \right) \qquad (3.7.21)$$

Equations 3.7.19 and 3.7.21 are, finally, linearized by setting each of the η parameters to their values at x = 0.

The solution to the set of two coupled linear differential equations is then assumed

to be as follows:

$\Delta[R^{2-}] = ae^{mx}$ (3.7.22a), $\Delta[A]=be^{mx}$ (3.7.23a)

Thus:

$$\frac{d\Delta[R^{2-}]}{dx} = mae^{mx} \quad (3.7.22b), \qquad \frac{d\Delta[A]}{dx} = mbe^{mx} \quad (3.7.23b)$$

$$\begin{cases} \dfrac{d^2\Delta[R^{2-}]}{dx^2} = m^2ae^{mx} = \eta_1 ae^{mx} + \eta_2 be^{mx} \\ \dfrac{d^2\Delta[A]}{dx^2} = m^2be^{mx} = \eta_3 ae^{mx} + \eta_4 be^{mx} \end{cases} \quad \text{So:} \begin{cases} (m^2-\eta_1)a - \eta_2 b = 0 \\ \eta_3 a + (\eta_4 - m^2)b = 0 \end{cases}$$

The two linear equations in a and b are satisfied only when:

$$\begin{cases} a = \dfrac{\eta_2}{m^2-\eta_1} b = \dfrac{m^2-\eta_4}{\eta_3} b \equiv \varepsilon b \quad \text{and:} \\ \begin{vmatrix} (m^2-\eta_1) & -\eta_2 \\ \eta_3 & (\eta_4 - m^2) \end{vmatrix} = 0 \end{cases}$$

It follows that $\eta_2\eta_3 - (u-\eta_4)(u-\eta_1) = 0$ where $u \equiv m^2$

or: $u^2 - (\eta_1+\eta_4)u + (\eta_1\eta_4 - \eta_2\eta_3) = 0$

There are two roots, $u_1, u_2 = \dfrac{(\eta_1+\eta_4) \pm \sqrt{(\eta_1+\eta_4)^2 - 4(\eta_1\eta_4 - \eta_2\eta_3)}}{2}$

Accordingly, there are 4 m values: $m_1 = \sqrt{u_1}, m_2 = -m_1, m_3 = \sqrt{u_2}, m_4 = -m_3$

and 4 ε values: $\varepsilon_1 = \varepsilon_2 \equiv E_1 = \dfrac{\eta_2}{u_1 - \eta_1}$; $\varepsilon_3 = \varepsilon_4 \equiv E_2 = \dfrac{\eta_2}{u_2 - \eta_1}$

And it follows that:

$$\begin{cases} \Delta[R^{2-}] = \sum_{j=1}^{4} a_j e^{m_j x} = \sum_{j=1}^{4} \varepsilon_j b_j e^{m_j x} \quad (3.7.22c) \\ \Delta[A] = \sum_{j=1}^{4} b_j e^{m_j x} \quad (3.7.23c) \end{cases}$$

The two first derivatives become:

$$\begin{cases} \frac{d\Delta[R^{2-}]}{dx} = \sum_{j=1}^{4} \varepsilon_j m_j b_j e^{m_j x} \quad (3.7.22d) \\ \frac{d\Delta[A]}{dx} = \sum_{j=1}^{4} m_j b_j e^{m_j x} \quad (3.7.23d) \end{cases}$$

The b's are constants of integration, which are determined by the boundary conditions:

i) $[A]_{x=0} = \underline{[A]}_{x=0} + \Delta[A]_{x=0} = \underline{[A]}_{x=0} + \sum_{j=1}^{4} b_j$

$$\Rightarrow b_1 + b_2 + b_3 + b_4 = [A]_{x=0} - \underline{[A]}_{x=0} \quad (3.7.24)$$

ii) $\left(\frac{d[R^{2-}]}{dx}\right)_{x=0} = 0$

$$\Rightarrow \left(\frac{d\Delta[R^{2-}]}{dx}\right)_{x=0} = E_1 m_1 (b_1 - b_2) + E_2 m_3 (b_3 - b_4) = -\left(\frac{d\underline{[R^{2-}]}}{dx}\right)_{x=0} \quad (3.7.25)$$

$$\left.\begin{array}{l} \text{iii) } \Delta[A]_{x=\delta} = b_1 e^{m_1 \delta} + b_2 e^{-m_1 \delta} + b_3 e^{m_3 \delta} + b_4 e^{-m_3 \delta} = 0 \\ \text{iv) } \Delta[R^{2-}]_{x=\delta} = E_1 \left(b_1 e^{m_1 \delta} + b_2 e^{-m_1 \delta}\right) + E_2 \left(b_3 e^{m_3 \delta} + b_4 e^{-m_3 \delta}\right) = 0 \end{array}\right\}$$

$$\Rightarrow b_1 = -b_2 e^{-2m_1 \delta},\ b_3 = -b_4 e^{-2m_3 \delta} \quad (3.7.26)$$

$$\Rightarrow \Delta[R^{2-}]_{x=0} = E_1 (b_1 + b_2) + E_2 (b_3 + b_4) \quad (3.7.27)$$

Equation 3.7.24 becomes:

$$b_2\left(1-e^{-2m_1\delta}\right)+\ b_4\left(1-e^{-2m_3\delta}\right)=[A]_{x=0}-\underline{[A]}_{x=0}\equiv c_1 \tag{3.7.28}$$

Equation 3.7.25 becomes:

$$E_1m_1b_2\left(1+e^{-2m_1\delta}\right)+E_2m_3b_4\left(1+e^{-2m_3\delta}\right)=\left(\frac{d[\underline{R^{2-}}]}{dx}\right)_{x=0}\equiv c_2 \tag{3.7.29}$$

The 2 c's are constants, which are determined by the underbarred concentrations at the interface. From equations 3.7.28 and 3.7.29 it follows that:

$$b_2=\frac{\begin{vmatrix} c_1 & 1-e^{-2m_3\delta} \\ c_2 & E_2m_3\left(1+e^{-2m_3\delta}\right)\end{vmatrix}}{\begin{vmatrix} 1-e^{-2m_1\delta} & 1-e^{-2m_3\delta} \\ E_1m_1\left(1+e^{-2m_1\delta}\right) & E_2m_3\left(1+e^{-2m_3\delta}\right)\end{vmatrix}}$$

$$=\frac{E_2m_3c_1\left(1+e^{-2m_3\delta}\right)-\left(1-e^{-2m_3\delta}\right)c_2}{E_2m_3\left(1+e^{-2m_3\delta}\right)\left(1-e^{-2m_1\delta}\right)-E_1m_1\left(1+e^{-2m_1\delta}\right)\left(1-e^{-2m_3\delta}\right)} \tag{3.7.30}$$

$$b_4=\frac{\begin{vmatrix} 1-e^{-2m_1\delta} & c_1 \\ E_1m_1\left(1+e^{-2m_1\delta}\right) & c_2\end{vmatrix}}{\begin{vmatrix} 1-e^{-2m_1\delta} & 1-e^{-2m_3\delta} \\ E_1m_1\left(1+e^{-2m_1\delta}\right) & E_2m_3\left(1+e^{-2m_3\delta}\right)\end{vmatrix}}$$

$$=\frac{\left(1-e^{-2m_1\delta}\right)c_2-E_1m_1c_1\left(1+e^{-2m_1\delta}\right)}{E_2m_3\left(1+e^{-2m_3\delta}\right)\left(1-e^{-2m_1\delta}\right)-E_1m_1\left(1+e^{-2m_1\delta}\right)\left(1-e^{-2m_3\delta}\right)} \tag{3.7.31}$$

Therefore:

$$\Delta[A]=\frac{\left[E_2m_3c_1\left(1+e^{-2m_3\delta}\right)-\left(1-e^{-2m_3\delta}\right)c_2\right]\left(e^{-m_1x}-e^{-2m_1\delta}e^{m_1x}\right)}{E_2m_3\left(1+e^{-2m_3\delta}\right)\left(1-e^{-2m_1\delta}\right)-E_1m_1\left(1+e^{-2m_1\delta}\right)\left(1-e^{-2m_3\delta}\right)}$$

$$+\frac{\left[\left(1-e^{-2m_1\delta}\right)c_2-E_1m_1c_1\left(1+e^{-2m_1\delta}\right)\right]\left(e^{-m_3x}-e^{-2m_3\delta}e^{m_3x}\right)}{E_2m_3\left(1+e^{-2m_3\delta}\right)\left(1-e^{-2m_1\delta}\right)-E_1m_1\left(1+e^{-2m_1\delta}\right)\left(1-e^{-2m_3\delta}\right)}$$

$$=\frac{\left[E_2m_3c_1\left(e^{m_3\delta}+e^{-m_3\delta}\right)-c_2\left(e^{m_3\delta}-e^{-m_3\delta}\right)\right]\left[e^{m_1(\delta-x)}-e^{-m_1(\delta-x)}\right]}{E_2m_3\left(e^{m_3\delta}+e^{-m_3\delta}\right)\left(e^{m_1\delta}-e^{-m_1\delta}\right)-E_1m_1\left(e^{m_1\delta}+e^{-m_1\delta}\right)\left(e^{m_3\delta}-e^{-m_3\delta}\right)}$$

$$+\frac{\left[\left(e^{m_1\delta}-e^{-m_1\delta}\right)c_2-E_1m_1c_1\left(e^{m_1\delta}+e^{-m_1\delta}\right)\right]\left[e^{m_3(\delta-x)}-e^{-m_3(\delta-x)}\right]}{E_2m_3\left(e^{m_3\delta}+e^{-m_3\delta}\right)\left(e^{m_1\delta}-e^{-m_1\delta}\right)-E_1m_1\left(e^{m_1\delta}+e^{-m_1\delta}\right)\left(e^{m_3\delta}-e^{-m_3\delta}\right)}$$

$$=\frac{\left[E_2m_3c_1\cosh(m_3\delta)-c_2\sinh(m_3\delta)\right]\sinh\left[m_1(\delta-x)\right]}{E_2m_3\sinh(m_1\delta)\cosh(m_3\delta)-E_1m_1\sinh(m_3\delta)\cosh(m_1\delta)}$$

$$+\frac{\left[c_2\sinh(m_1\delta)-E_1m_1c_1\cosh(m_1\delta)\right]\sinh\left[m_3(\delta-x)\right]}{E_2m_3\sinh(m_1\delta)\cosh(m_3\delta)-E_1m_1\sinh(m_3\delta)\cosh(m_1\delta)}$$

$$=\frac{\left[E_2m_3c_1-c_2\tanh(m_3\delta)\right]\sinh\left[m_1(\delta-x)\right]}{E_2m_3\sinh(m_1\delta)-E_1m_1\tanh(m_3\delta)\cosh(m_1\delta)}$$

$$+\frac{\left[c_2\tanh(m_1\delta)-E_1m_1c_1\right]\sinh\left[m_3(\delta-x)\right]}{E_2m_3\tanh(m_1\delta)\cosh(m_3\delta)-E_1m_1\sinh(m_3\delta)} \qquad (3.7.32)$$

Accordingly:

$$\Delta[A]_{x=0}=\frac{\left[E_2m_3c_1-c_2\tanh(m_3\delta)\right]\sinh(m_1\delta)}{E_2m_3\sinh(m_1\delta)-E_1m_1\tanh(m_3\delta)\cosh(m_1\delta)}$$

$$+\frac{\left[c_2\tanh(m_1\delta)-E_1m_1c_1\right]\sinh(m_3\delta)}{E_2m_3\tanh(m_1\delta)\cosh(m_3\delta)-E_1m_1\sinh(m_3\delta)}$$

$$= \frac{\left[E_2 m_3 c_1 - c_2 \tanh(m_3\delta)\right]\tanh(m_1\delta)}{E_2 m_3 \tanh(m_1\delta) - E_1 m_1 \tanh(m_3\delta)} + \frac{\left[c_2 \tanh(m_1\delta) - E_1 m_1 c_1\right]\tanh(m_3\delta)}{E_2 m_3 \tanh(m_1\delta) - E_1 m_1 \tanh(m_3\delta)}$$

$$= \frac{\left[E_2 m_3 c_1 - c_2 \tanh(m_3\delta)\right]\tanh(m_1\delta) + \left[c_2 \tanh(m_1\delta) - E_1 m_1 c_1\right]\tanh(m_3\delta)}{E_2 m_3 \tanh(m_1\delta) - E_1 m_1 \tanh(m_3\delta)} \quad (3.7.33)$$

$$\frac{d\Delta[A]}{dx} = -\frac{m_1\left[E_2 m_3 c_1 - c_2 \tanh(m_3\delta)\right]\cosh\left[m_1(\delta - x)\right]}{E_2 m_3 \sinh(m_1\delta) - E_1 m_1 \tanh(m_3\delta)\cosh(m_1\delta)}$$

$$-\frac{m_3\left[c_2 \tanh(m_1\delta) - E_1 m_1 c_1\right]\cosh\left[m_3(\delta - x)\right]}{E_2 m_3 \tanh(m_1\delta)\cosh(m_3\delta) - E_1 m_1 \sinh(m_3\delta)} \quad (3.7.34)$$

$$\left(\frac{d\Delta[A]}{dx}\right)_{x=0} = -\frac{m_1\left[E_2 m_3 c_1 - c_2 \tanh(m_3\delta)\right]\cosh(m_1\delta)}{E_2 m_3 \sinh(m_1\delta) - E_1 m_1 \tanh(m_3\delta)\cosh(m_1\delta)}$$

$$-\frac{m_3\left[c_2 \tanh(m_1\delta) - E_1 m_1 c_1\right]\cosh(m_3\delta)}{E_2 m_3 \tanh(m_1\delta)\cosh(m_3\delta) - E_1 m_1 \sinh(m_3\delta)}$$

$$= -\frac{m_1\left[E_2 m_3 c_1 - c_2 \tanh(m_3\delta)\right]}{E_2 m_3 \tanh(m_1\delta) - E_1 m_1 \tanh(m_3\delta)} - \frac{m_3\left[c_2 \tanh(m_1\delta) - E_1 m_1 c_1\right]}{E_2 m_3 \tanh(m_1\delta) - E_1 m_1 \tanh(m_3\delta)}$$

$$= -\frac{m_1\left[E_2 m_3 c_1 - c_2 \tanh(m_3\delta)\right] + m_3\left[c_2 \tanh(m_1\delta) - E_1 m_1 c_1\right]}{E_2 m_3 \tanh(m_1\delta) - E_1 m_1 \tanh(m_3\delta)} \quad (3.7.35)$$

$$\frac{d^2\Delta[A]}{dx^2} = \frac{m_1^{\,2}\left[E_2 m_3 c_1 - c_2 \tanh(m_3\delta)\right]\sinh\left[m_1(\delta - x)\right]}{E_2 m_3 \sinh(m_1\delta) - E_1 m_1 \tanh(m_3\delta)\cosh(m_1\delta)}$$

$$+\frac{m_3^{\,2}\left[c_2 \tanh(m_1\delta) - E_1 m_1 c_1\right]\sinh\left[m_3(\delta - x)\right]}{E_2 m_3 \tanh(m_1\delta)\cosh(m_3\delta) - E_1 m_1 \sinh(m_3\delta)} \quad (3.7.36)$$

Next we proceed to derive the derivatives of the underbarred concentrations:

Differentiation of equations 3.7.4-5, 3.7.7-8 and 3.7.14, and cancel out $d[\underline{C^{2-}}]$, gives:

$$d[\underline{R^-}] + d[\underline{R}] + d[\underline{R^{2-}}] = 0 \quad \Rightarrow d[\underline{R}] = -d[\underline{R^-}] - d[\underline{R^{2-}}] \tag{3.7.37}$$

$$d[\underline{B^-}] + d[\underline{R^-}] + 2d[\underline{R^{2-}}] + 2d[\underline{C^{2-}}] = 0 \tag{3.7.38}$$

$$[\underline{R^{2-}}]d[\underline{R}] + [\underline{R}]d[\underline{R^{2-}}] = \frac{2K_{Carb}[\underline{A}][\underline{R^-}]}{K_6} d[\underline{R^-}] + \frac{K_{Carb}[\underline{R^-}]^2}{K_6} d[\underline{A}] \tag{3.7.39}$$

$$[\underline{B^-}]d[\underline{R}] + [\underline{R}]d[\underline{B^-}] = \frac{K_2[\underline{A}]}{K_6} d[\underline{R^-}] + \frac{K_2[\underline{R^-}]}{K_6} d[\underline{A}] \tag{3.7.40}$$

$$d[\underline{C^{2-}}] = \frac{K_4[\underline{B^-}]}{K_6[\underline{R}]} d[\underline{R^-}] + \frac{K_4[\underline{R^-}]}{K_6[\underline{R}]} d[\underline{B^-}] - \frac{K_4[\underline{R^-}][\underline{B^-}]}{K_6[\underline{R}]^2} d[\underline{R}] \tag{3.7.41}$$

$$\Rightarrow \begin{cases} \left(1 + \dfrac{2K_4[\underline{R^-}]}{K_6[\underline{R}]}\right) d[\underline{B^-}] + \left(1 + \dfrac{2K_4[\underline{B^-}]}{K_6[\underline{R}]} + \dfrac{2K_4[\underline{R^-}][\underline{B^-}]}{K_6[\underline{R}]^2}\right) d[\underline{R^-}] \\ \qquad + \left(2 + \dfrac{2K_4[\underline{R^-}][\underline{B^-}]}{K_6[\underline{R}]^2}\right) d[\underline{R^{2-}}] = 0 \\ \left([\underline{R^{2-}}] + \dfrac{2K_{Carb}[\underline{A}][\underline{R^-}]}{K_6}\right) d[\underline{R^-}] + \left([\underline{R^{2-}}] - [\underline{R}]\right) d[\underline{R^{2-}}] = -\dfrac{K_{Carb}[\underline{R^-}]^2}{K_6} d[\underline{A}] \\ -[\underline{R}]d[\underline{B^-}] + \left([\underline{B^-}] + \dfrac{K_2[\underline{A}]}{K_6}\right) d[\underline{R^-}] + [\underline{B^-}]d[\underline{R^{2-}}] = -\dfrac{K_2[\underline{R^-}]}{K_6} d[\underline{A}] \end{cases}$$

$$\Rightarrow \begin{cases} d[\underline{B^-}] = \dfrac{\theta_2}{\theta_1} d[\underline{A}] & (3.7.42) \\ d[\underline{R^-}] = \dfrac{\theta_3}{\theta_1} d[\underline{A}] & (3.7.43) \\ d[\underline{R^{2-}}] = \dfrac{\theta_4}{\theta_1} d[\underline{A}] & (3.7.44) \\ d[\underline{R}] = -\dfrac{\theta_3 + \theta_4}{\theta_1} d[\underline{A}] & (3.7.45) \\ d[\underline{C^{2-}}] = \dfrac{\theta_5}{\theta_1} d[\underline{A}] & (3.7.46) \end{cases}$$

where $\theta_1 \equiv \begin{vmatrix} \left(1 + \dfrac{2K_4[\underline{R^-}]}{K_6[\underline{R}]}\right) & \left(1 + \dfrac{2K_4[\underline{B^-}]}{K_6[\underline{R}]} + \dfrac{2K_4[\underline{R^-}][\underline{B^-}]}{K_6[\underline{R}]^2}\right) & \left(2 + \dfrac{2K_4[\underline{R^-}][\underline{B^-}]}{K_6[\underline{R}]^2}\right) \\ 0 & \left([\underline{R^{2-}}] + \dfrac{2K_{Carb}[\underline{A}][\underline{R^-}]}{K_6}\right) & \left([\underline{R^{2-}}] - [\underline{R}]\right) \\ -[\underline{R}] & \left([\underline{B^-}] + \dfrac{K_2[\underline{A}]}{K_6}\right) & [\underline{B^-}] \end{vmatrix}$

$\theta_2 \equiv \begin{vmatrix} 0 & \left(1 + \dfrac{2K_4[\underline{B^-}]}{K_6[\underline{R}]} + \dfrac{2K_4[\underline{R^-}][\underline{B^-}]}{K_6[\underline{R}]^2}\right) & \left(2 + \dfrac{2K_4[\underline{R^-}][\underline{B^-}]}{K_6[\underline{R}]^2}\right) \\ \left(-\dfrac{K_{carb}[\underline{R^-}]^2}{K_6}\right) & \left([\underline{R^{2-}}] + \dfrac{2K_{Carb}[\underline{A}][\underline{R^-}]}{K_6}\right) & \left([\underline{R^{2-}}] - [\underline{R}]\right) \\ \left(-\dfrac{K_2[\underline{R^-}]}{K_6}\right) & \left([\underline{B^-}] + \dfrac{K_2[\underline{A}]}{K_6}\right) & [\underline{B^-}] \end{vmatrix}$

$$\theta_3 \equiv \begin{vmatrix} \left(1+\frac{2K_4[R^-]}{K_6[R]}\right) & 0 & \left(2+\frac{2K_4[R^-][B^-]}{K_6[R]^2}\right) \\ 0 & \left(-\frac{K_{carb}[R^-]^2}{K_6}\right) & \left([R^{2-}]-[R]\right) \\ -[R] & \left(-\frac{K_2[R^-]}{K_6}\right) & [B^-] \end{vmatrix}$$

$$\theta_4 \equiv \begin{vmatrix} \left(1+\frac{2K_4[R^-]}{K_6[R]}\right) & \left(1+\frac{2K_4[B^-]}{K_6[R]}+\frac{2K_4[R^-][B^-]}{K_6[R]^2}\right) & 0 \\ 0 & \left([R^{2-}]+\frac{2K_{Carb}[A][R^-]}{K_6}\right) & \left(-\frac{K_{carb}[R^-]^2}{K_6}\right) \\ -[R] & \left([B^-]+\frac{K_2[A]}{K_6}\right) & \left(-\frac{K_2[R^-]}{K_6}\right) \end{vmatrix}$$

$$\theta_5 \equiv \frac{K_4[B^-]}{K_6[R]}\theta_3 + \frac{K_4[R^-]}{K_6[R]}\theta_2 + \frac{K_4[R^-][B^-]}{K_6[R]^2}\left(\theta_3+\theta_4\right)$$

Differentiation of equation 3.7.6 and insertion of equations 3.7.42, 3.7.44 and 3.7.46 gives:

$$D_A d[A] + D^*\left(\frac{\theta_2+\theta_4+\theta_5}{\theta_1}\right) d[A] = -\Phi_1 dx$$

or :

$$\frac{d[A]}{dx} = -\frac{\theta_1\Phi_1}{\theta_1 D_A + D^*\left(\theta_2+\theta_4+\theta_5\right)} \qquad (3.7.47)$$

It follows that:

$$\frac{d[R^{2-}]}{dx} = -\frac{\theta_4\Phi_1}{\theta_1 D_A + D^*\left(\theta_2+\theta_4+\theta_5\right)} \qquad (3.7.48)$$

The solution is implemented as a search for $\underline{[A]}_{x=0}$:

1) a guess of $\underline{[A]}_{x=0}$ is made;

2) all other underbar quantities at x = 0 are calculated from equations 3.7.4-5, 3.7.7-8, and 3.7.14;

3) Φ_1 follows from equation 3.7.6 and the boundary conditions:

$$\Phi_1 = \frac{D_A\left(\underline{[A]}_{x=0} - [A]_{x=\delta}\right) + D^*\left(\underline{[B^-]}_{x=0} - [B^-]_{x=\delta} + \underline{[R^{2-}]}_{x=0} - [R^{2-}]_{x=\delta} + \underline{[C^{2-}]}_{x=0} - [C^{2-}]_{x=\delta}\right)}{\delta} \quad (3.7.49);$$

4) values of θ_1-θ_5, ω_1-ω_6, λ_1, λ_2, η_1-η_4, u_1, u_2, m_1-m_4, E_1, and E_2 at x = 0 are calculated;

5) $\Delta[A]_{x=0} = \alpha p_{A,G} - \underline{[A]}_{x=0}$, from which c_1 follows;

6) $\left(\frac{d\underline{[A]}}{dx}\right)_{x=0}$ and $\left(\frac{d\underline{[R^{2-}]}}{dx}\right)_{x=0}$ are calculated from equations 3.7.47- 48, from which c_2 follows;

7) $\left(\frac{d\Delta[A]}{dx}\right)_{x=0}$ is calculated from equation 3.7.35;

8) $\Phi_1 = -D_A\left[\left(\frac{d\underline{[A]}}{dx}\right)_{x=0} + \left(\frac{d\Delta[A]}{dx}\right)_{x=0}\right]$ is compared with the value calculated in step 3).

3.8 Numerical validation

An exact numerical solution to the same differential equations provides a test of the above analysis. The two second order differential equations will be transformed into a set of first order differential equations and solved as an initial value problem.

As a first step, $[B^-]$, $[R]$, $[R^-]$ and $[C^{2-}]$ are expressed as functions of $[A]$, $[R^{2-}]$, y and Φ_1 :

$$D_A[A] + D^*\left([B^-] + [R^{2-}] + [C^{2-}]\right) = \Phi_1\delta(1-y) + \xi \quad \left(x \equiv \delta y, y = [0,1]\right)$$

$$\left(\xi \equiv D_A[A]_{x=\delta} + D^*([B^-]_{x=\delta} + [R^{2-}]_{x=\delta} + [C^{2-}]_{x=\delta})\right)$$

Thus :

$$[B^-] + [R^{2-}] + [C^{2-}] = \frac{\Phi_1\delta(1-y) + \xi - D_A[A]}{D^*} \equiv Q \tag{3.8.1}$$

$$\begin{cases} [R] + [R^-] + [R^{2-}] = [K^+] \\ [B^-] + [R^-] + 2[R^{2-}] + 2[C^{2-}] = [K^+] \\ [B^-] + [R^{2-}] + [C^{2-}] = Q \\ \dfrac{[C^{2-}][R]}{[B^-][R^-]} = \dfrac{K_4}{K_6} \end{cases} \quad \text{Thus :} \quad \begin{cases} [C^{2-}] = Q - [R^{2-}] - [B^-] & (3.8.2) \\ [R^-] = [K^+] - 2Q + [B^-] & (3.8.3) \\ [R] = 2Q - [B^-] - [R^{2-}] & (3.8.4) \end{cases}$$

It follows from the last three equations that:

$$\left(Q - [R^{2-}] - [B^-]\right)\left(2Q - [B^-] - [R^{2-}]\right) = \frac{K_4}{K_6}[B^-]\left([K^+] - 2Q + [B^-]\right)$$

$$\left(2Q^2 - 3Q[R^{2-}] + [R^{2-}]^2\right) + \left(2[R^{2-}] - 3Q\right)[B^-] + [B^-]^2 = \frac{K_4\left([K^+] - 2Q\right)}{K_6}[B^-] + \frac{K_4}{K_6}[B^-]^2$$

$$\left(1 - \frac{K_4}{K_6}\right)[B^-]^2 + \left(2[R^{2-}] - 3Q - \frac{K_4\left([K^+] - 2Q\right)}{K_6}\right)[B^-] + \left(2Q^2 - 3Q[R^{2-}] + [R^{2-}]^2\right) = 0$$

Thus,

$$\left(1-\frac{K_4}{K_6}\right)[B^-]^2+G[B^-]+J=0 \tag{3.8.5}$$

where:

$$G\equiv 2[R^{2-}]-3Q-\frac{K_4\left([K^+]-2Q\right)}{K_6}$$

$$J\equiv 2Q^2-3Q[R^{2-}]+[R^{2-}]^2$$

Therefore:

$$[B^-]=\frac{-G-\sqrt{G^2-4\left(1-\frac{K_4}{K_6}\right)J}}{2\left(1-\frac{K_4}{K_6}\right)} \tag{3.8.6}$$

Note that the other root for $[B^-]$, $\dfrac{-G+\sqrt{G^2-4\left(1-\frac{K_4}{K_6}\right)J}}{2\left(1-\frac{K_4}{K_6}\right)}$, turns out to be physically impossible.

Now we return to the differential equations:

$$\frac{d^2[A]}{dy^2}=\frac{\delta^2 k_{1a}[A][R^-]\left(\frac{k_{R^-}}{k_{-1a}}[R^-]+\frac{k_W}{k_{-1a}}[W]\right)\left(1-\frac{K_6[R^{2-}][R]}{K_{Carb}[A][R^-]^2}\right)}{D_A\left(1+\frac{k_{R^-}}{k_{-1a}}[R^-]+\frac{k_W}{k_{-1a}}[W]\right)}$$

$$+\frac{\delta^2 k_2[A]}{D_A}-\frac{\delta^2 k_2 K_6[B^-][R]}{D_A K_2[R^-]}+\frac{\delta^2 k_3 K_5[A][R^-]}{D_A K_6[R]}-\frac{\delta^2 k_3[B^-]}{D_A K_3} \tag{3.5.3}$$

$$\frac{d^2[R^{2-}]}{dy^2}=-\frac{\delta^2 k_{1a}[A][R^-]\left(\frac{k_{R^-}}{k_{-1a}}[R^-]+\frac{k_W}{k_{-1a}}[W]\right)\left(1-\frac{K_6[R^{2-}][R]}{K_{Carb}[A][R^-]^2}\right)}{D^*\left(1+\frac{k_{R^-}}{k_{-1a}}[R^-]+\frac{k_W}{k_{-1a}}[W]\right)} \tag{3.7.1}$$

Both $\frac{d^2[A]}{dy^2}$ and $\frac{d^2[R^{2-}]}{dy^2}$ are now expressible as functions of [A], $[R^{2-}]$, y and Φ_1.

We next make the following definitions:

$$x_1 = [A] \tag{3.8.7}$$

$$x_2 = \frac{d[A]}{dy} \tag{3.8.8}$$

$$x_3 = [R^{2-}] \tag{3.8.9}$$

$$x_4 = \frac{d[R^{2-}]}{dy} \tag{3.8.10}$$

It follows that:

$$\frac{dx_1}{dy} = x_2$$

$$\frac{dx_2}{dy} = \frac{\delta^2 k_{1a} x_1 [R^-]\left(\frac{k_{R^-}}{k_{-1a}}[R^-] + \frac{k_W}{k_{-1a}}[W]\right)\left(1 - \frac{K_6 x_3 [R]}{K_{Carb} x_1 [R^-]^2}\right)}{D_A\left(1 + \frac{k_{R^-}}{k_{-1a}}[R^-] + \frac{k_W}{k_{-1a}}[W]\right)} + \frac{\delta^2 k_2 x_1}{D_A} - \frac{\delta^2 k_2 K_6 [B^-][R]}{D_A K_2 [R^-]} + \frac{\delta^2 k_3 K_5 x_1 [R^-]}{D_A K_6 [R]} - \frac{\delta^2 k_3 [B^-]}{D_A K_3}$$

$$\frac{dx_3}{dy} = x_4$$

$$\frac{dx_4}{dy} = -\frac{\delta^2 k_{1a} x_1 [R^-]\left(\frac{k_{R^-}}{k_{-1a}}[R^-] + \frac{k_W}{k_{-1a}}[W]\right)\left(1 - \frac{K_6 x_3 [R]}{K_{Carb} x_1 [R^-]^2}\right)}{D^*\left(1 + \frac{k_{R^-}}{k_{-1a}}[R^-] + \frac{k_W}{k_{-1a}}[W]\right)}$$

The boundary conditions are:

$$x_1(0) = \alpha p_{A,G} \qquad x_1(\delta) = [A]_{x=\delta}$$

$$x_2(0) = -\frac{\Phi_1 \delta}{D_A} \qquad x_3(\delta) = [R^{2-}]_{x=\delta}$$

$$x_4(0) = 0$$

Since the boundary conditions refer to two different positions, a solution must be obtained by trial and error:

Guess Φ_1 and $[R^{2-}]_{x=0}$, then solve the above four first-order ODE's numerically. If $x_1(\delta) = [A]_{x=\delta}$ and $x_3(\delta) = [R^{2-}]_{x=\delta}$, the initial guess is correct. Once $[R^{2-}]_{x=0}$ and Φ_1 are known, all the rest concentrations can be calculated.

4. RESULTS FOR CO_2-PG SYSTEM

4.1 Physiochemical parameters

The temperature and concentration dependence of solubility, density, and diffusivity, as well as equilibrium and kinetic parameters is discussed below.

4.1.1 Solubility data

Since the partial pressures of CO_2 considered are generally less than 1 atm, the vapor phase may be considered ideal and vapor-liquid equilibrium may be described by the Henry law:

$$p_{A,G} \equiv \frac{1}{\alpha}[A] = H_{CO_2}[A] \qquad (4.1.1.1)$$

where $p_{A,G}$ is CO_2 partial pressure and H_{CO_2} is the Henry's law coefficient of CO_2 in the PG solution given by Portugal, Versteeg and van Swaaij [77, 78]:

$$\log\left(\frac{H_{CO_2}}{H_{CO_2,w}}\right) = K[PG]_o \qquad (4.1.1.2)$$

$$\text{where } K = \frac{62.183098}{T} - 0.111175 \quad (\text{mol}^{-1}\ \text{dm}^3)$$

$$H_{CO_2,w} = \frac{\exp(-2044/T)}{3.54\times10^{-7}} \quad (\text{Pa mol}^{-1}\ \text{m}^3)$$

4.1.2 Density data

Densities of PG solutions were measured by Portugal et al. [77], and are tabulated in Table 4.1.2.

Table 4.1.2 Densities of PG solutions [77]

T (K)	ρ (kg m^{-3})			
	293	298	303	313
[PG] (M)				
0	998.29	997.13	995.71	992.25
0.102	1004.37	1003.06	1001.59	997.28
0.296	1015.97	1014.56	1013.00	1001.77
0.594	1033.28	1031.69	1030.02	1025.15
1.003	1056.57	1054.81	1052.98	1047.94
1.992	1112.29	1110.13	1108.01	1102.34
2.984	1163.85	1161.44	1159.07	1150.37

4.1.3 Diffusivity data

Diffusivities of CO_2 and ionic species in aqueous PG solutions are as follows [77-79]:

$$D_A = [2.35\times10^{-6}\exp(-2119/T)](1+0.2109[PG]+0.05124[PG]^2)^{-0.48}\ (m^2\ s^{-1}) \quad (4.1.3.1)$$

$$D^* = D_{PG} = (-2.412 - 9.403\times10^{-3}T + 7.110\times10^{-5}T^2 - 0.2177[PG] - 5.447\times10^{-2}[PG]^2 + 1.296\times10^{-3}T[PG])\times10^{-9}\ (m^2\ s^{-1}) \quad (4.1.3.2)$$

4.1.4 Reaction equilibrium data

Benamor and Aroua [80] provide the following data:

For CO_2 hydration, equation 3.1.2:

$$K_2 = \left(\frac{[B^-][H^+]}{[A]} \right)_{eq} = \exp(-\frac{12092.1}{T} - 36.7816 \ln T + 235.482) \quad (\text{mol dm}^{-3}) \qquad (4.1.4.1)$$

For carbonate formation, equation 3.1.4:

$$K_4 = \frac{[C^{2-}][H^+]}{[B^-]} = \exp(-\frac{12431.7}{T} - 35.4819 \ln T + 220.067) \quad (\text{mol dm}^{-3}) \qquad (4.1.4.2)$$

For water's ionization, equation 3.1.5, the constant $K_5 \left(= \frac{K_2}{K_3} \right)$ varies as follows:

$$K_5 = [OH^-][H^+] = \exp(-\frac{13445.9}{T} - 22.4773 \ln T + 140.932) \quad (\text{mol dm}^{-3})^2 \qquad (4.1.4.3)$$

For carbamate zwitterion deprotonation, equation 3.1.6, K_6 is given by Perrin [81]:

$$K_6 = \frac{[R^-][H^+]}{[R]} = \exp(-0.000237956T^2 + 0.202203T - 61.6499) \quad (\text{mol dm}^{-3}) \qquad (4.1.4.4)$$

The di-carbamate hydrolysis reaction is not treated as an independent reaction in the analysis here, since it is a linear combination of the di-carbamate and carbonate formation reactions. Its equilibrium constant is given by Jensen [82] as:

$$K_{carbhydrolysis} = \left(\frac{[R^-][B^-]}{[R^{2-}]} \right)_{eq} = \exp(\frac{-2767.18}{T} + 6.10312) \quad (\text{mol dm}^{-3}) \qquad (4.1.4.5)$$

It follows from the definition, $K_{Acid_j} \equiv \left(\frac{[B_jH^+]}{[B_j][H^+]} \right)^{eq}$, that:

$$K_{Acid,R^-} = \frac{1}{K_6} \qquad (4.1.4.6)$$

and:

$$K_{Acid,W} = \frac{1}{[W]} \qquad (4.1.4.7)$$

From the definition, $K_{Carb} \equiv \left(\frac{[R^{2-}][H^+]}{[A][R^-]} \right)^{eq}$, it follows that:

$$K_{Carb} = \frac{K_2}{K_{carbhydrolysis}} \qquad (4.1.4.8)$$

4.1.5 Kinetic data

The zwitterion mechanism rate constants are given as follows by Portugal et al. [77], but do not account for ionic strength:

$$k_{1a} = 2.81 \times 10^{10} \exp(-5800/T) \quad (m^3\ mol^{-1}\ s^{-1}) \qquad (4.1.5.1)$$

$$k_W / k_{-1a} = 1.05 \times 10^{-4} \exp(-1265/T) \quad (m^3\ mol^{-1}) \qquad (4.1.5.2)$$

$$k_{R^-} / k_{-1a} = 4.89 \times 10^{3} \exp(-5307/T) \quad (m^3\ mol^{-1}) \qquad (4.1.5.3)$$

The forward rate constant of carbonic acid formation (at zero ionic strength) is given by Danckwerts and Sharma [20] as:

$$\log k_2 = 329.850 - 110.541 \log T - 17265.4/T \qquad (k_2\ [=]\ s^{-1}) \qquad (4.1.5.4)$$

The forward rate constant of bicarbonate formation (at zero ionic strength), is given by Danckwerts and Sharma [20] as:

$$\log k_3 = 13.635 - 2895/T \qquad (k_3\ [=]\ dm^3\ mol^{-1}\ s^{-1}) \qquad (4.1.5.5)$$

4.2 Results and discussion

4.2.1 Speciation profiles

Figures 4.2.1.1-4 depict equilibrium speciation profiles in 1 M and 3 M PG at 293 K and 313 K, respectively, calculated from equations 3.1.4, 3.1.6, 3.4.1, 3.5.1, 3.5.5 and 3.6.4 at equilibrium.

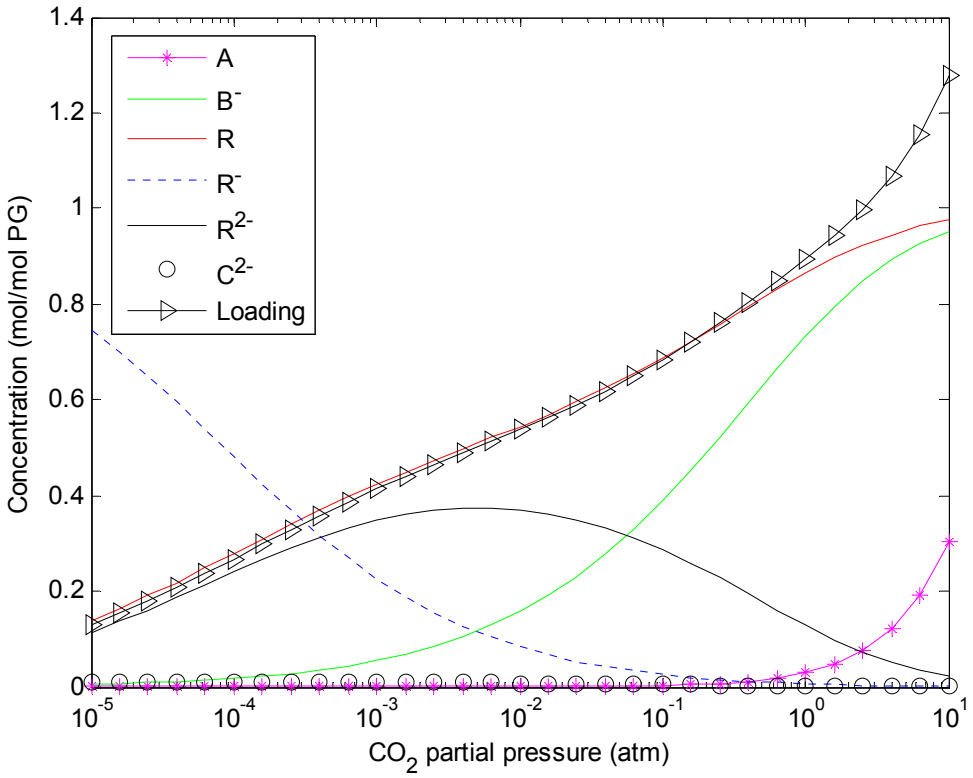

Figure 4.2.1.1 Speciation and CO_2 loading *vs*. CO_2 partial pressure (1 M PG, 293 K).

At CO_2 partial pressures less than 10^{-4} atm, dissolved CO_2 combines primarily with R^- to form equal proportions of R and R^{2-}. At higher partial pressures, CO_2 forms mainly bicarbonate ions via CO_2 hydration reactions. Until it is exhausted, R^- buffers hydrogen ions co-produced with bicarbonate ions, forming the carbamate zwitterions R. Therefore,

at higher CO_2 partial pressures, the dominant overall reaction is:

$$A + W + R^- \rightleftharpoons R + B^- \qquad (4.2.1.1)$$

After the free glycinate anion is depleted, the hydrogen ions combine with di-carbamate ions in reverse reaction 3.1.1, which explains the peak in R^{2-}. The overall reaction becomes:

$$A + 2W + R^{2-} \rightleftharpoons R + 2B^- \qquad (4.2.1.2)$$

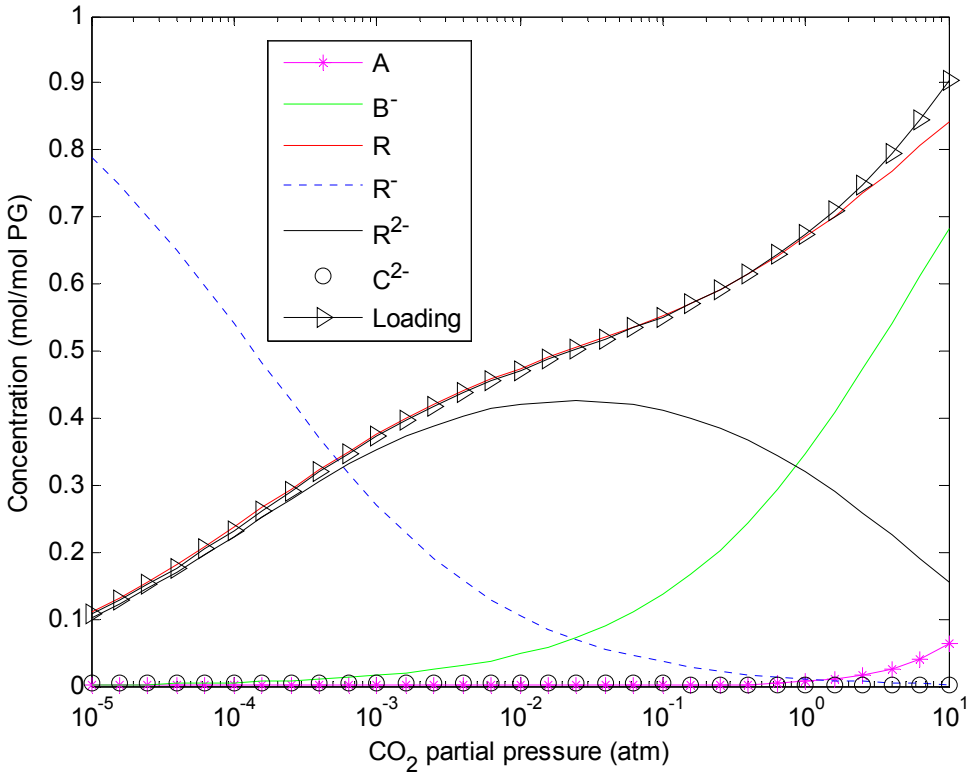

Figure 4.2.1.2 Speciation and CO_2 loading *vs*. CO_2 partial pressure (3 M PG, 293 K).

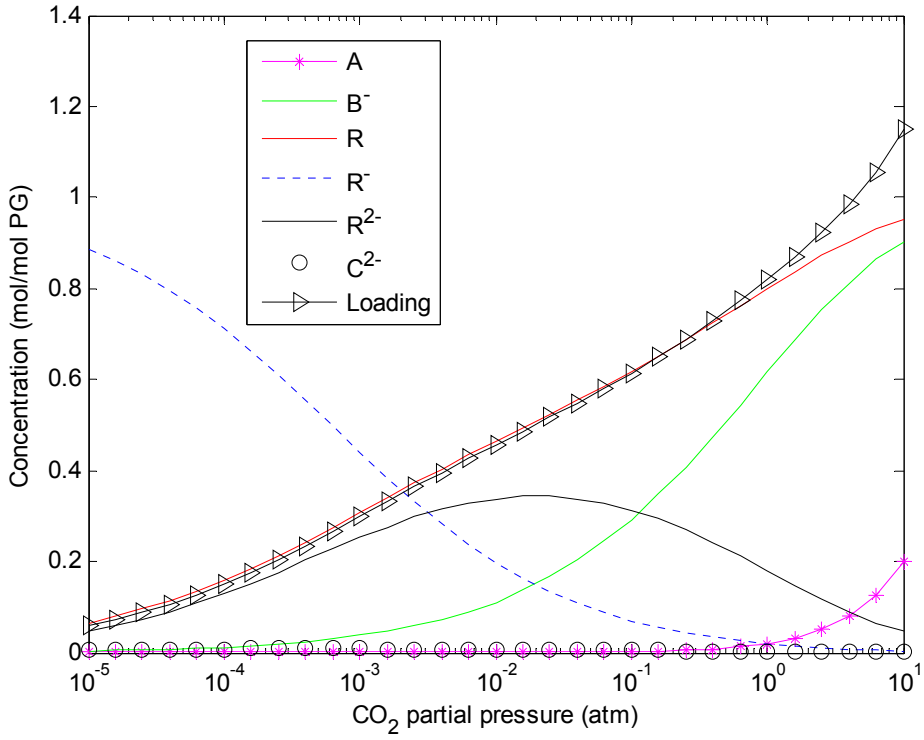

Figure 4.2.1.3 Speciation and CO_2 loading *vs*. CO_2 partial pressure (1 M PG, 313 K).

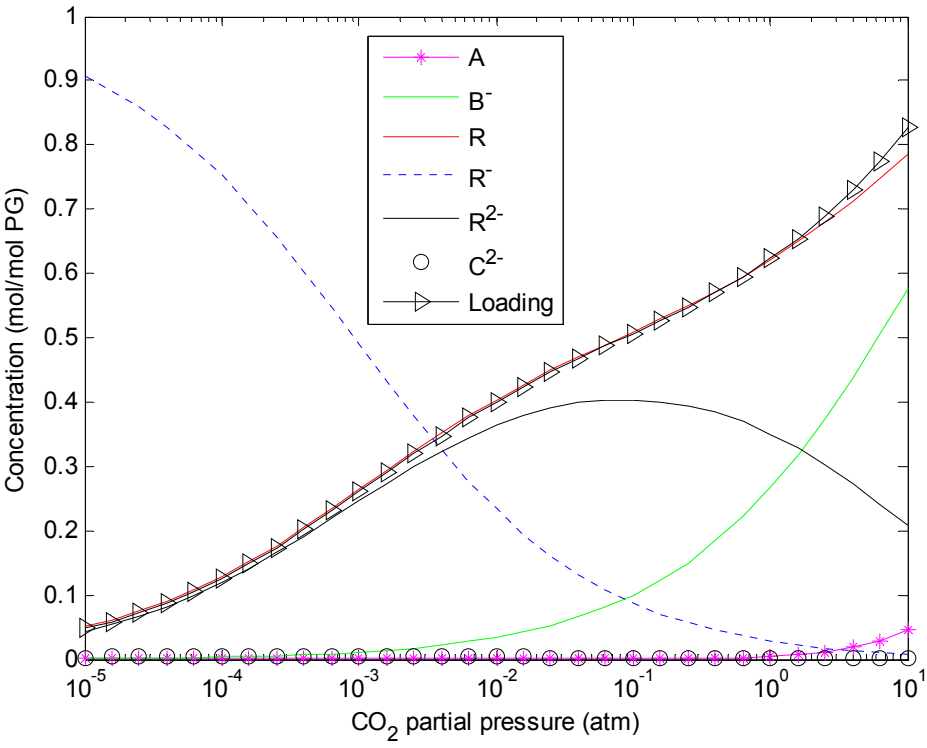

Figure 4.2.1.4 Speciation and CO_2 loading *vs*. CO_2 partial pressure (3 M PG, 313 K).

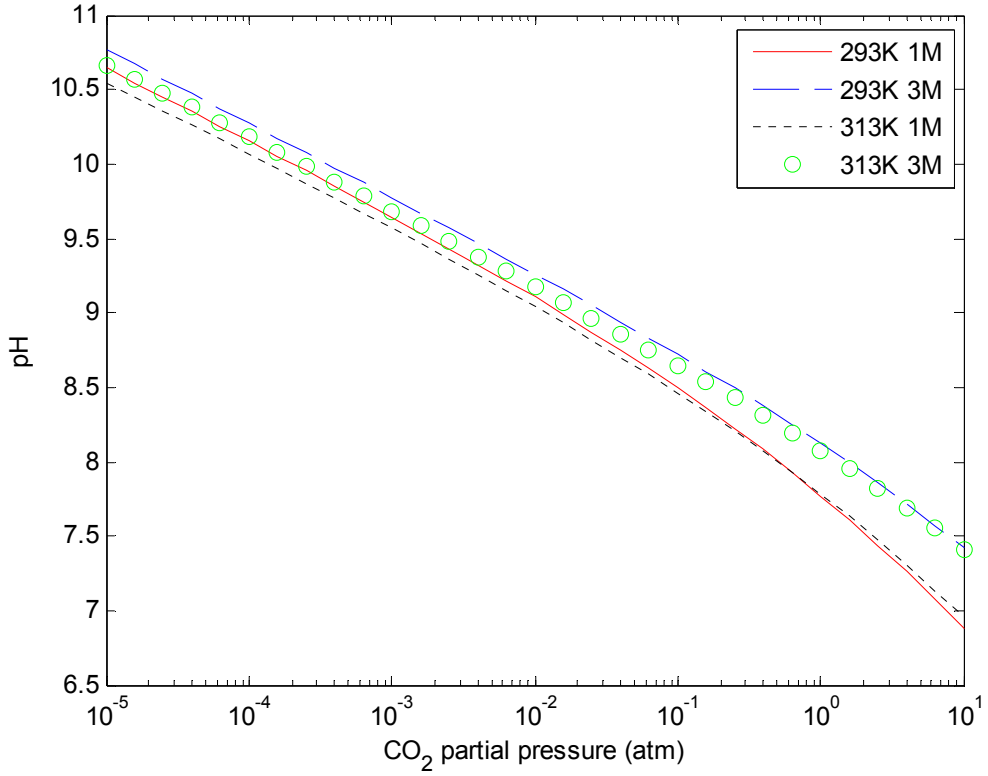

Figure 4.2.1.5 pH *vs.* CO_2 partial pressure.

Figure 4.2.1.5 depicts the dependence of pH on CO_2 partial pressure. The pH decreases steadily from around 10.6 at 10^{-5} atm to under 7.5 at 10 atm, with more sensitivity to PG concentration than to temperature. At CO_2 partial pressures typical of coal-fired power plant flue gases (0.10-0.15 atm), the solution is slightly basic (pH ≈ 8.5).

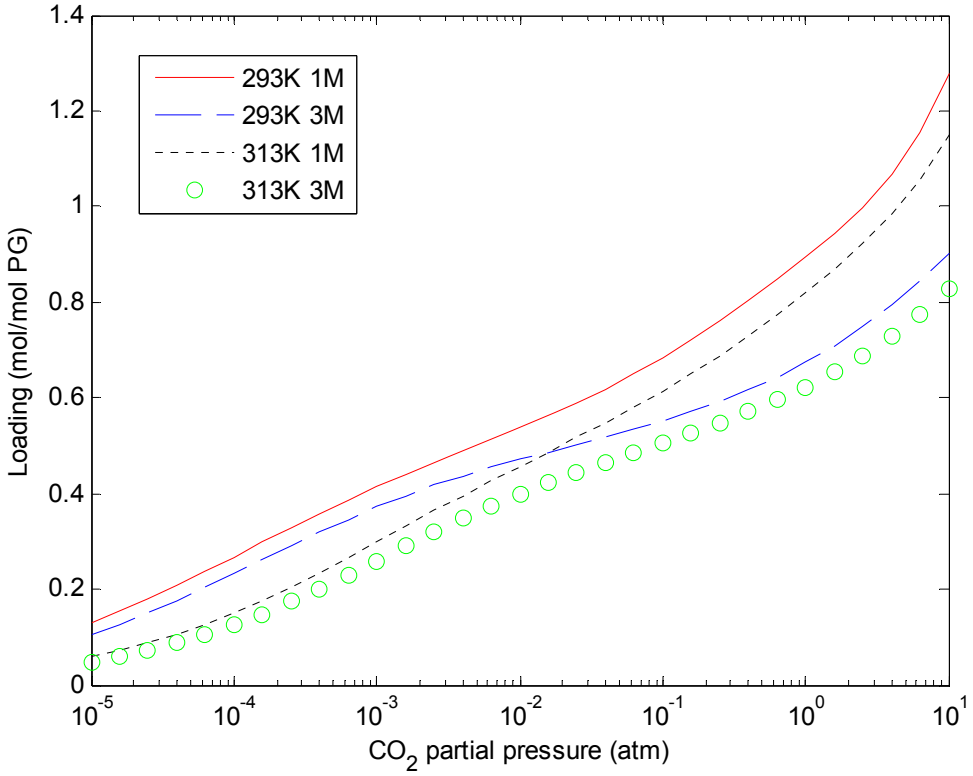

Figure 4.2.1.6 Loading *vs*. CO_2 partial pressure.

Figure 4.2.1.6 shows the CO_2 partial pressure dependence of the liquid "loading", L, i.e. total moles of reversibly absorbed CO_2 per mole of amine or amino acid (which is included in figures 4.2.1.1-4). At CO_2 partial pressures typical of post-combustion flue gas, absorber bottoms loadings are unlikely to exceed 50%. Note that loading increases as temperature decreases; it varies slightly with amine concentration at lower CO_2 partial pressures and more markedly at higher partial pressures. Lower PG concentrations promote loading mainly because the CO_2 solubility increases with decreasing ionic strength.

Because physically dissolved gas is generally negligible compared with the total

CO_2 absorbed (see figures 4.2.1.1-4), equation 3.6.3 may be rewritten as:

$$E^{eq} \cong \beta\left(\frac{[PG]_{total}}{\alpha}\right)\frac{\Delta L}{\Delta p_{A,G}} \qquad (4.2.1.3)$$

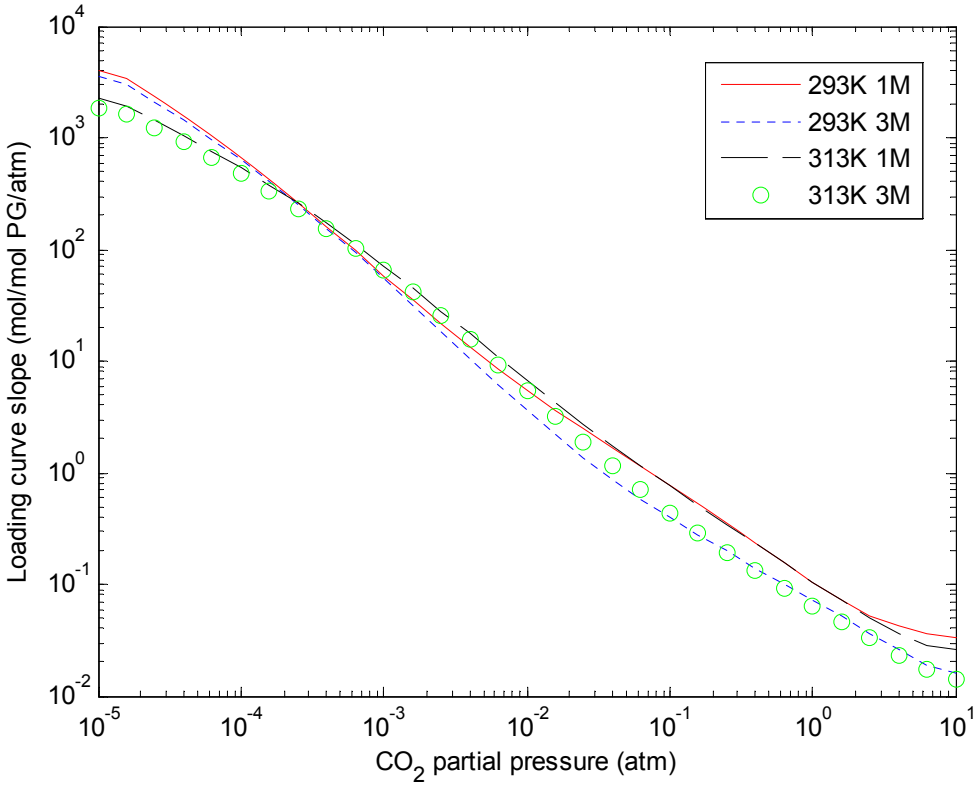

Figure 4.2.1.7 Loading curve slope *vs*. CO_2 partial pressure.

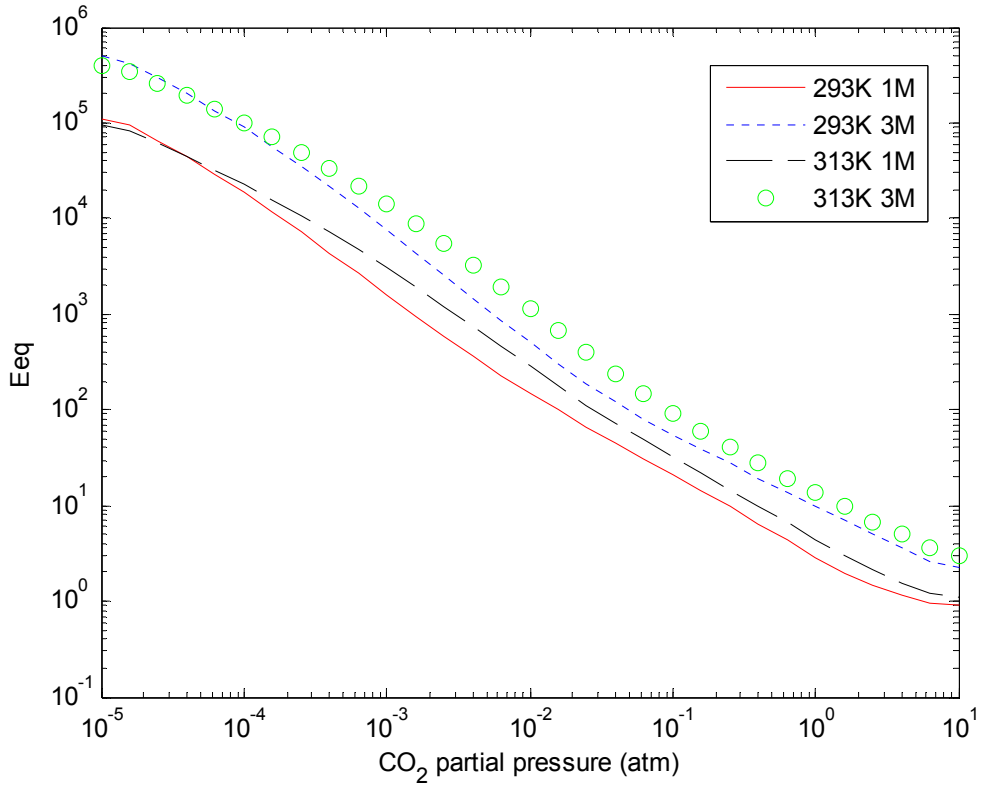

Figure 4.2.1.8 Equilibrium enhancement factor *vs*. CO_2 partial pressure.

Figure 4.2.1.7 depicts the CO_2 partial pressure dependence of $dL/dp_{A,G}$ (i.e., $\lim_{\Delta p_{A,G}\to 0} \Delta L/\Delta p_{A,G}$). Equilibrium enhancement factors, E^{eq}, calculated using equation 4.2.1.3, are shown in figure 4.2.1.8. Extremely high E^{eq} values are possible at very low partial pressures, suggesting PG solutions as candidate sorbents for capturing the CO_2 in ambient air. For operating conditions more typical of flue gas capture, E^{eq} values are in the 10 to 10^2 range. Larger E^{eq} values are attained at higher amino acid concentrations, because of both the increased contributions of carbamate and bicarbonate to CO_2 transport, and the lower CO_2 solubility at higher ionic strengths.

4.2.2 Validation of perturbation analysis

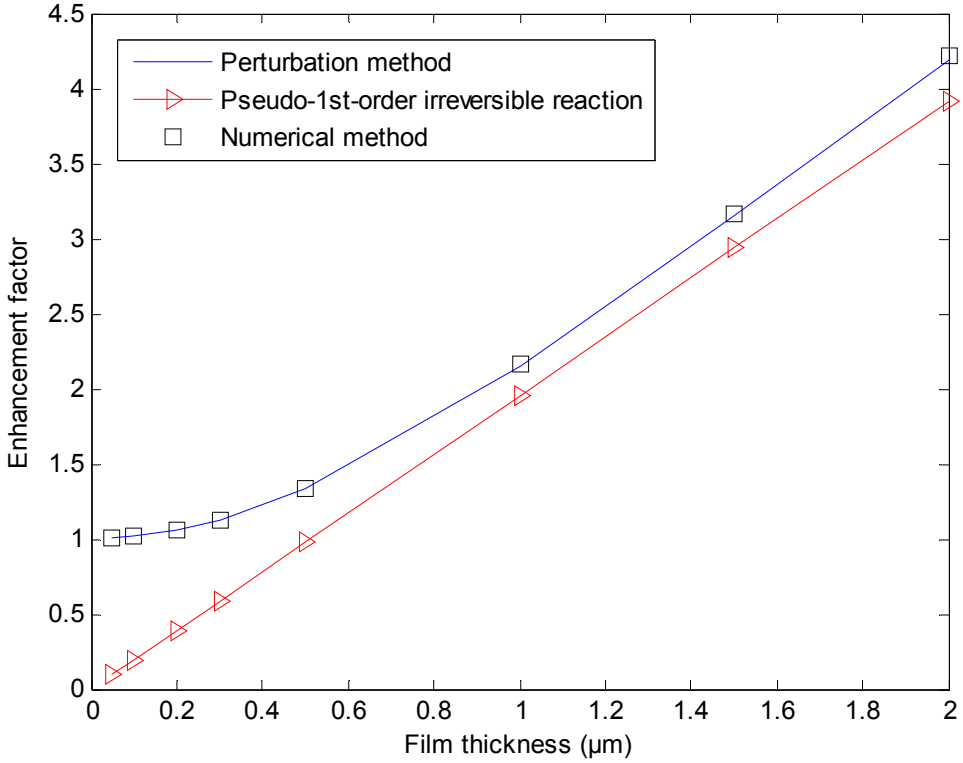

Figure 4.2.2 Absorption enhancement factor *vs*. liquid film thickness. (3 M PG, 293 K, bulk gas CO_2 partial pressure = 0.15 atm, bulk liquid loading = 40%)

Figure 4.2.2 compares enhancement factors (with liquid film thickness ranging from zero to 2 μm) calculated on the basis of Thick Film theory, with those obtained via: the numerical method; and from the closed-form expression for pseudo-first-order-irreversible reaction, E^+.

The pseudo-first-order-irreversible assumption retains only the forward reactions and assigns all concentrations other than that of dissolved CO_2 to their bulk liquid values (see equation 4.2.2.1).

$$D_A \frac{d^2[A]}{dx^2} = \left(\frac{k_{1a}[R^-]\left(k_{R^-}[R^-] + k_W[W]\right)}{k_{-1a} + k_{R^-}[R^-] + k_W[W]} + k_2 + \frac{k_3 K_2 [R^-]}{K_3 K_6 [R]} \right)[A] \equiv k_+ [A] \qquad (4.2.2.1)$$

where $k_+ = \left(\frac{k_{1a}[R^-]\left(k_{R^-}[R^-] + k_W[W]\right)}{k_{-1a} + k_{R^-}[R^-] + k_W[W]} + k_2 + \frac{k_3 K_2 [R^-]}{K_3 K_6 [R]} \right)_{x=\delta}$

Equation 4.2.2.1 can be rearranged as $\frac{d^2[A]}{dx^2} = \frac{k_+}{D_A}[A]$ (4.2.2.1')

A general solution to equation 4.2.2.1' should be: $[A] = ae^{\sqrt{\frac{k_+}{D_A}}x} + be^{-\sqrt{\frac{k_+}{D_A}}x}$

However, as film thickness $x \to +\infty$, the term, $e^{\sqrt{\frac{k_+}{D_A}}x}$, gives a possitive infinite value, which violates the physical model that [A] must be finite.

Therefore, a reasonable solution should be: $[A] = [A]_{x=0} e^{-\sqrt{\frac{k_+}{D_A}}x}$ (4.2.2.2)

where $[A]_{x=0}$ (= b) is the concentration of CO_2 at the gas-liquid interphase.

Thus, reaction-enhanced flux $= -D_A \left(\frac{d[A]}{dx} \right)_{x=0} = D_A [A]_{x=0} \sqrt{\frac{k_+}{D_A}}$ (4.2.2.3)

while purely mass transfer flux $= D_A \frac{[A]_{x=0}}{\delta}$ (4.2.2.4)

Therefore, $E^+ = \frac{\text{reaction-enhanced flux}}{\text{purely mass transfer flux}} = \frac{D_A [A]_{x=0} \sqrt{\frac{k_+}{D_A}}}{D_A \frac{[A]_{x=0}}{\delta}} = \delta \sqrt{\frac{k_+}{D_A}} = Ha$ (4.2.2.5)

(Ha is the Hatta number).

Figure 4.2.2 shows that thick film theory enhancement factors match those based on numerical analysis and are in close agreement with E^+ values calculated from equation 4.2.2.5.

With liquid film thickness in the range from 0.1 to 0.3 μm, E values are not much

greater than 1 and di-carbamate formation is effectively a "slow" reaction. The pseudo-first-order irreversible reaction assumption is roughly valid from thickness 1 μm to 10 μm, although by 10 μm the combined negative effects of glycinate anion depletion and reaction reversibility are apparent in Figure 4.2.3.1's 1 M PG curve and Figure 4.2.3.2's 50% loading curve.

4.2.3 Results of perturbation analysis

4.2.3.1 Effect of concentration

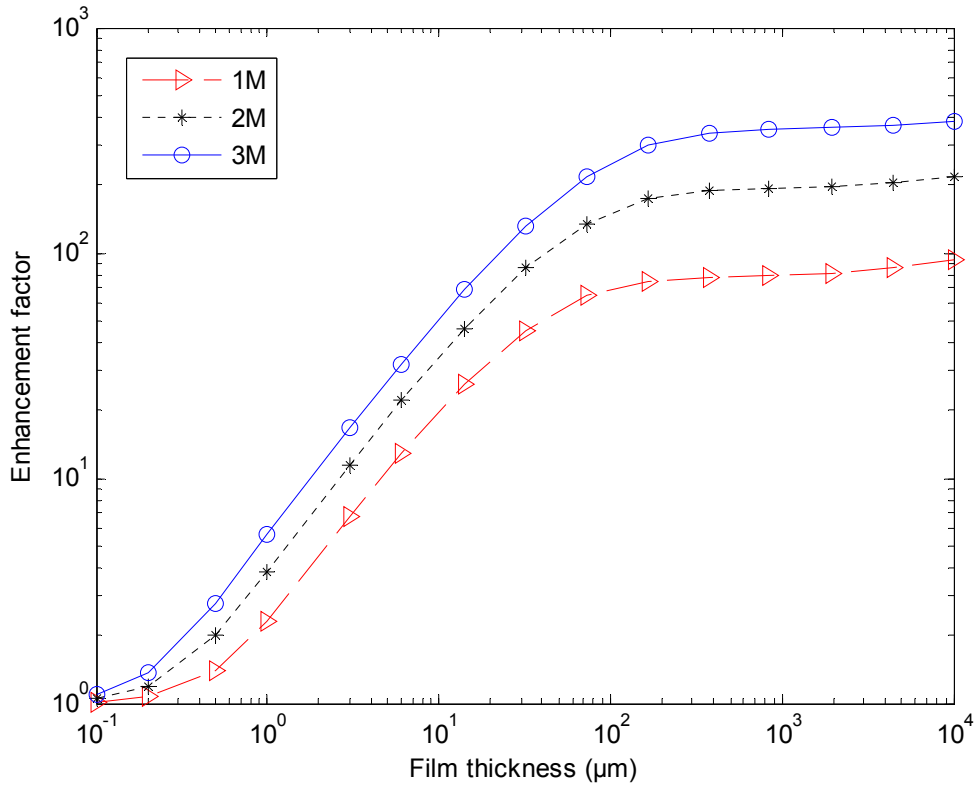

Figure 4.2.3.1 Absorption enhancement factor *vs*. liquid film thickness. (Bulk liquid loading = 10%, 293 K, bulk gas CO_2 partial pressure = 0.15 atm)

Figure 4.2.3.1 reflects the fact that at higher salt concentration there is less glycinate anion depletion at the interphase. At large film thicknesses, absorption of CO_2 becomes limited by the diffusion of the glycinate anions to the reaction zone, especially at low PG concentrations, and E values plateaus, and then approaches a maximum value reflecting the effect of the CO_2 hydration reaction.

4.2.3.2 Effect of bulk liquid loading

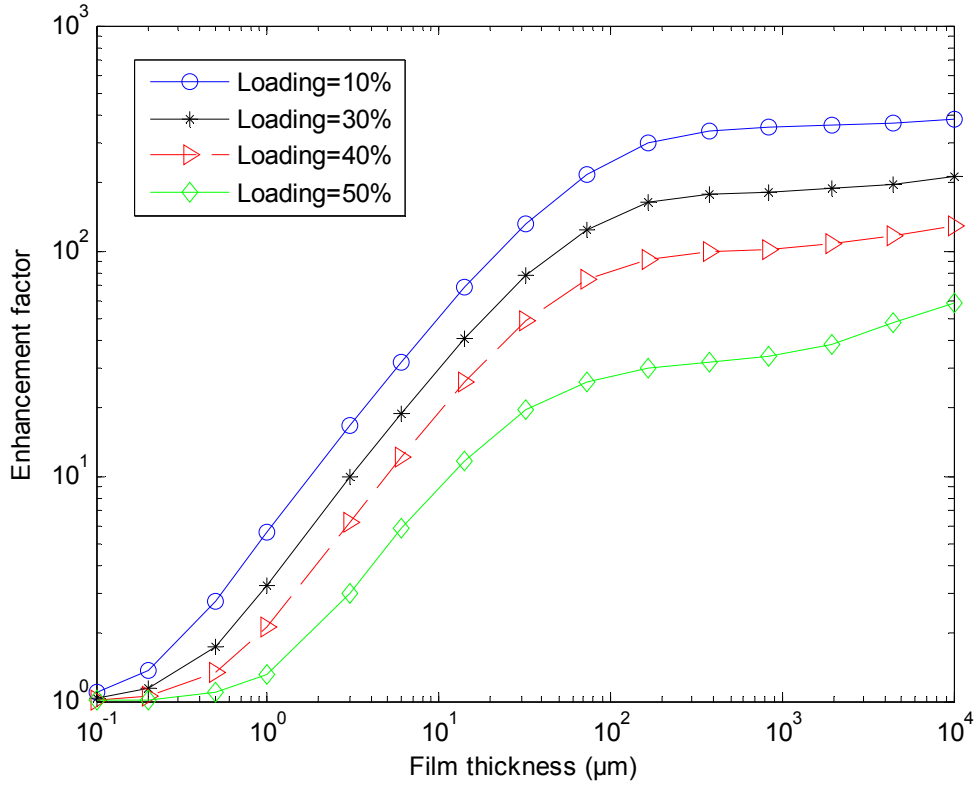

Figure 4.2.3.2 Absorption enhancement factor *vs*. liquid film thickness. (3 M PG, 293 K, bulk gas CO_2 partial pressure = 0.15 atm)

Figure 4.2.3.2 shows that lower bulk liquid loading promote consumption of absorbed CO_2 and therefore yield higher absorption rates (E values). At still higher film thicknesses, curves appear to plateau, which suggests local equilibrium of reaction 3.1.1. However, the plateaus are only temporary, because as thickness increases from 100 μm to 1000 μm, CO_2 diffusion becomes so slow that even intrinsically slow reactions, such as CO_2 hydration, proceeds significantly within the liquid film. The E values ultimately approach the E^{eq} values in Figure 4.2.1.8 as bicarbonate ions finally facilitate CO_2 transport from the gas-liquid interface to bulk liquid. This phenomenon is more obvious

in Figure 4.2.3.2's 50% loading curve. Although CO_2 reacts much faster with hydroxyl ion, its effects are suppressed by hydroxyl ion depletion at the interface.

4.2.3.3 Concentration profiles within a film

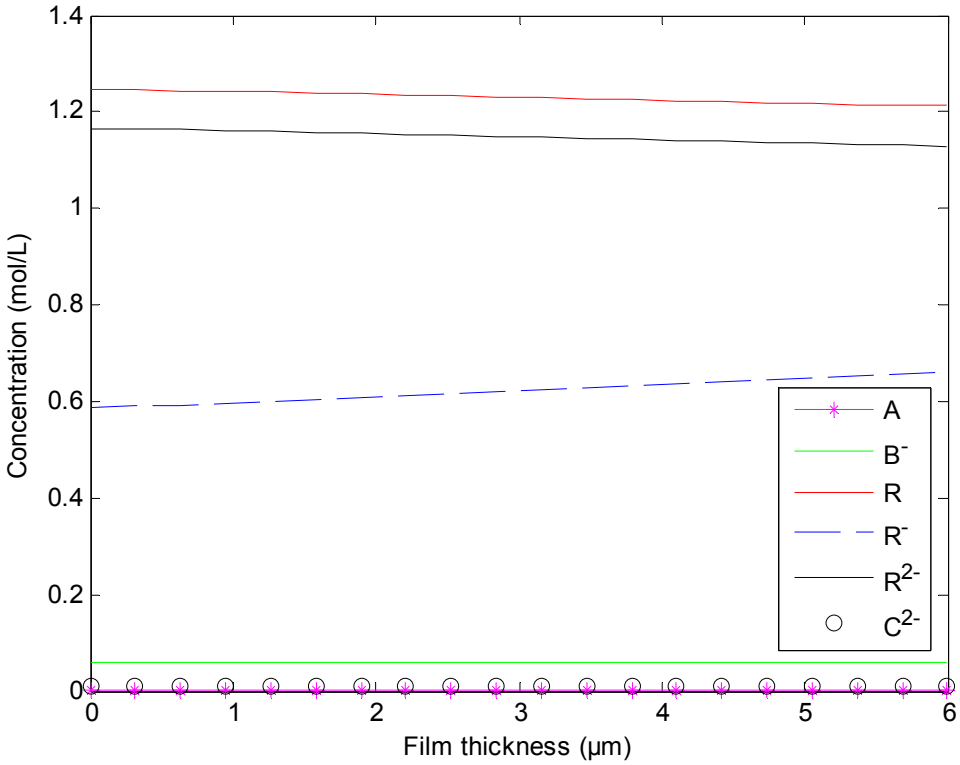

Figure 4.2.3.3.1 Concentration profiles within a 6 μm liquid film. (3 M PG, 293 K, bulk liquid loading = 40%, bulk gas CO_2 partial pressure = 0.15 atm)

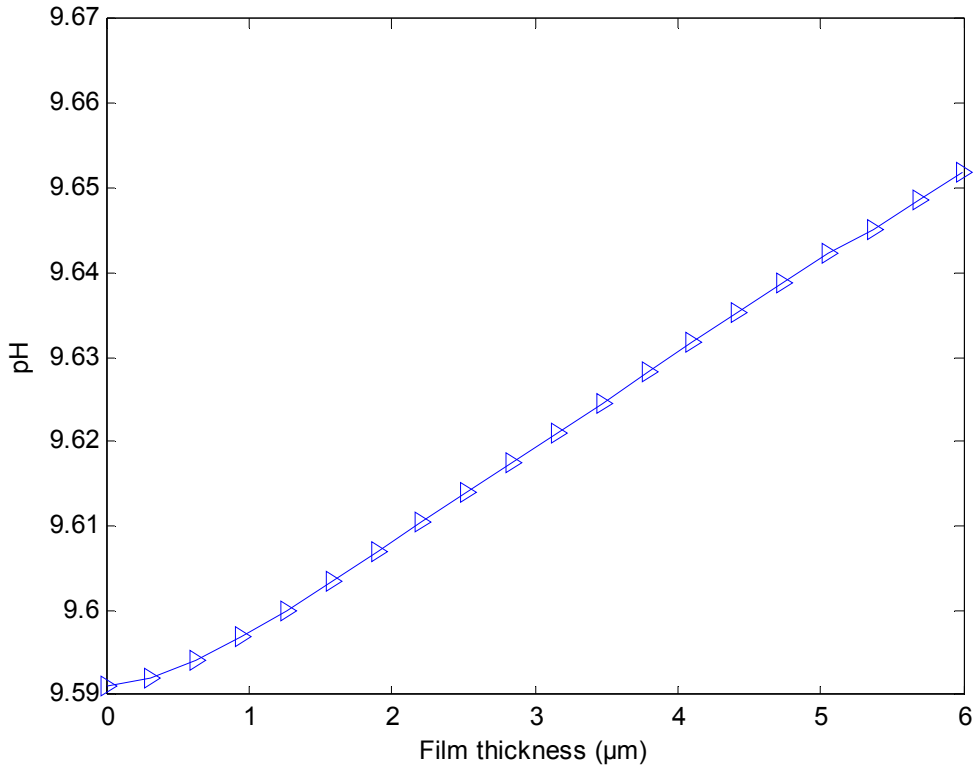

Figure 4.2.3.3.2 pH change within a 6 μm liquid film. (3 M PG, 293 K, bulk liquid loading = 40%, bulk gas CO_2 partial pressure = 0.15 atm)

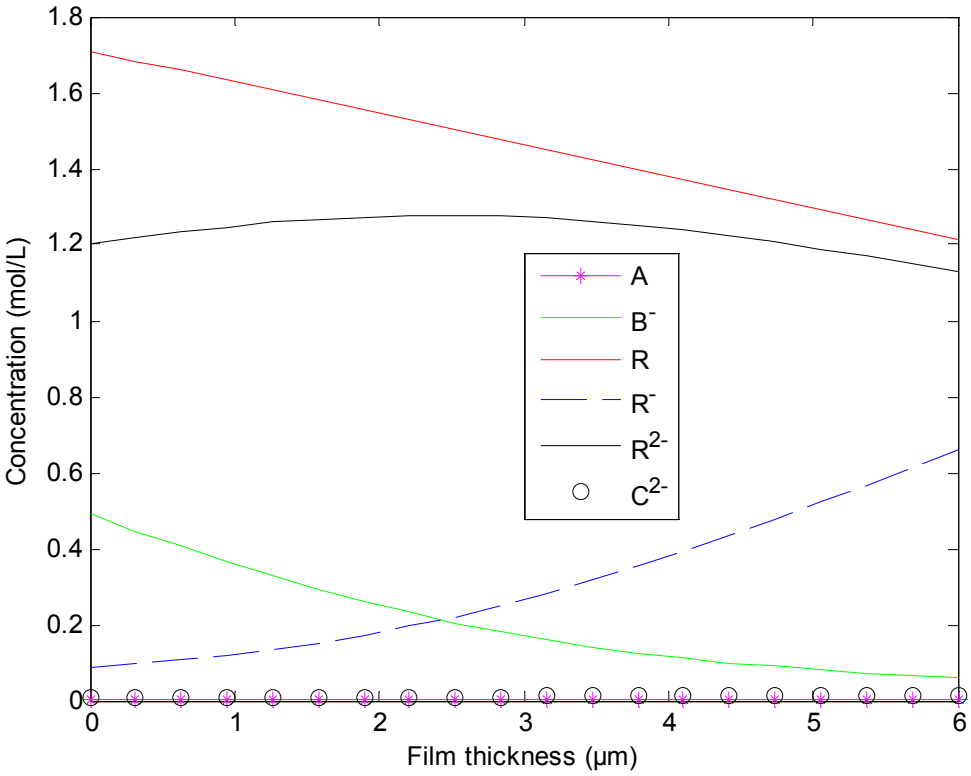

Figure 4.2.3.3.3 Equilibrium concentration profiles within a 6 μm liquid film. (3 M PG, 293 K, bulk liquid loading = 40%, bulk gas CO_2 partial pressure = 0.15 atm)

Figure 4.2.3.3.1 and 4.2.3.3.2 show concentration and pH profiles within a 6 μm liquid film. The film is relatively acidic near the gas-liquid interface; still, the pH is close to 10 throughout the film. As compared with the equilibrium concentration profiles (Figure 4.2.3.3.3), reaction effects are small because chemical reaction is effectively "slow" within a 6 μm liquid film (through which diffusion is rapid).

4.2.3.4 CO_2 consumption rate within a film

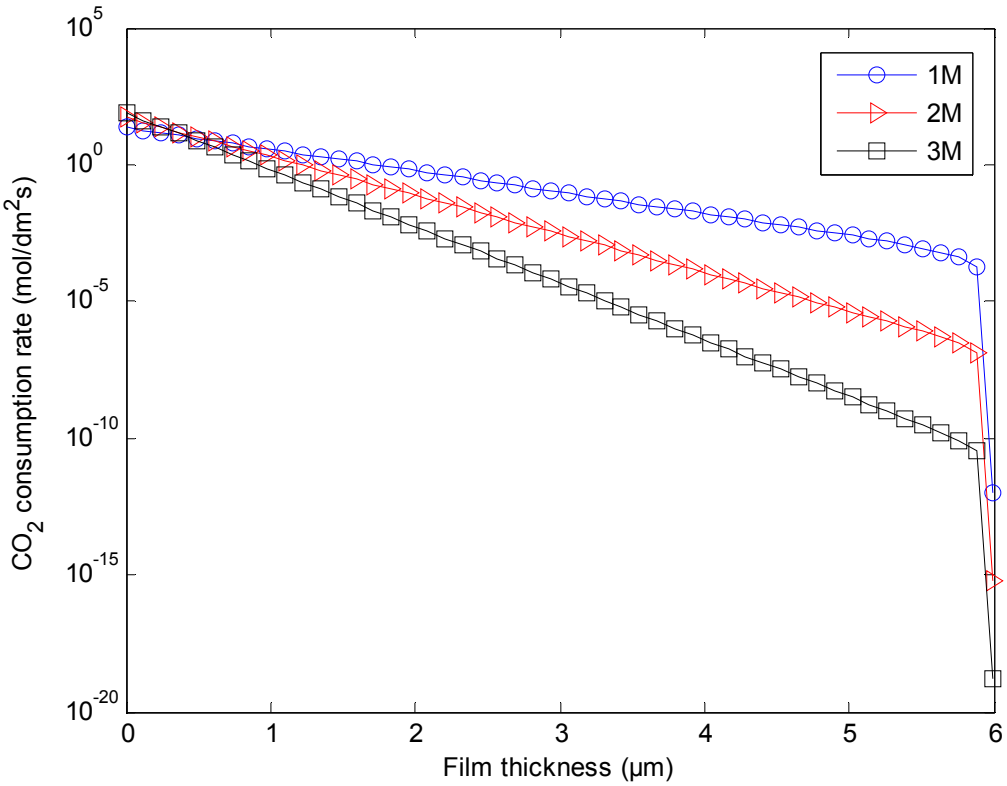

Figure 4.2.3.4.1 CO_2 consumption rate within a 6 μm liquid film. (Bulk liquid loading = 10%, 293 K, bulk gas CO_2 partial pressure = 0.15 atm)

Figure 4.2.3.4.1 compares CO_2 consumption rates within a 6 μm liquid film at three PG concentrations. The CO_2 reaction rate is fastest at the gas-liquid interface in the most concentrated film, and drops precipitously further into the film, because of the equilibrium condition in bulk liquid.

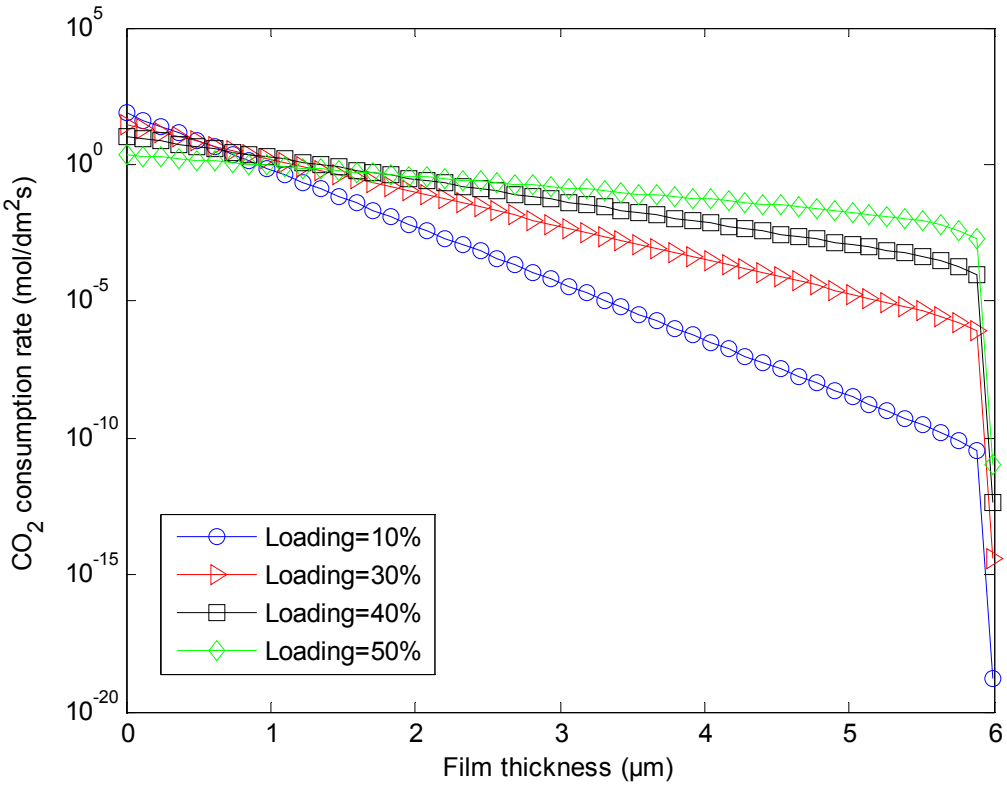

Figure 4.2.3.4.2 CO_2 consumption rate within a 6 μm liquid film. (3 M PG, 293 K, bulk gas CO_2 partial pressure = 0.15 atm)

Figure 4.2.3.4.2 shows CO_2 consumption rates within a 6 μm liquid film at 3 M PG concentration, with different bulk liquid loadings. CO_2 is consumed most rapidly at the lowest bulk liquid loading because the correspondingly suppressed reverse reaction.

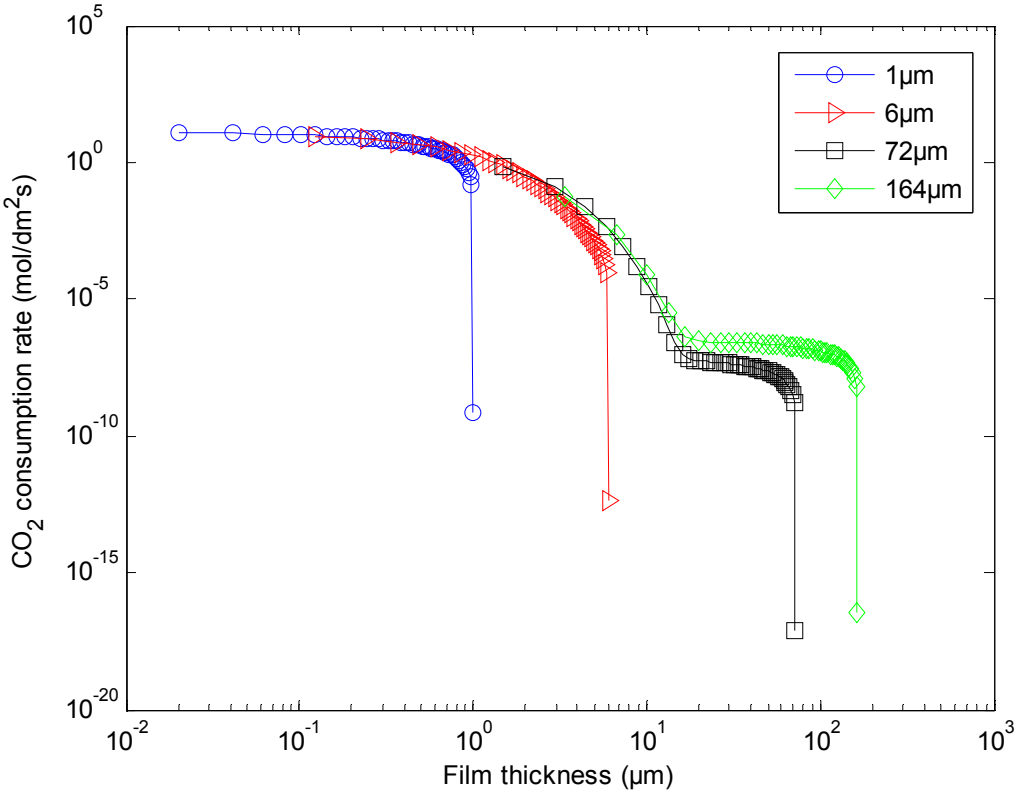

Figure 4.2.3.4.3 CO_2 consumption rate within liquid film. (3 M PG, 293 K, Bulk liquid loading = 40%, bulk gas CO_2 partial pressure = 0.15 atm)

Figure 4.2.3.4.3 shows CO_2 consumption rate in films of different thicknesses. In the two thinner films (1 and 6 μm), diffusion is fast relative to reaction, so CO_2 is consumed throughout the liquid film until its reaction equilibrium prevails at the entrance to the bulk liquid zone. In thicker films (72 and 164 μm), CO_2 consumption is relatively fast compared to diffusion, and local equilibrium prevails before the CO_2 reaches the bulk liquid. Given the reaction kinetics and operating conditions considered here, films thicker than 10 μm may be regarded as "thick".

4.2.3.5 Fluxes of CO_2-containing species

In this section, it is shown that the fluxes of CO_2 into and out of the liquid film are equal, consistent with the steady-state assumption.

The calculation is in two steps – a first calculation is conducted at x = 0 to solve all the constants.

We start with the following equations, which are calculated by fixing the underbarred constants at x = 0, as is the case for standard perturbation method:

$$\frac{d\Delta[R^{2-}]}{dx} = \sum_{j=1}^{4} \varepsilon_j m_j b_j e^{m_j x} \tag{3.7.22d}$$

$$\frac{d\Delta[A]}{dx} = \sum_{j=1}^{4} m_j b_j e^{m_j x} \tag{3.7.23d}$$

$$\Delta[B^-] = \omega_1 \Delta[R^{2-}] + \omega_2 \Delta[A] \tag{3.7.16}$$

$$\Delta[R] = \omega_3 \Delta[R^{2-}] + \omega_4 \Delta[A] \tag{3.7.17}$$

$$\Delta[R^-] = \omega_5 \Delta[R^{2-}] + \omega_6 \Delta[A] \tag{3.7.18}$$

(ω's are fixed at x = 0)

$$\Delta[C^{2-}] = \left(\frac{K_4 \underline{[B^-]}}{K_6 \underline{[R]}}\right)_{x=0} \Delta[R^-] + \left(\frac{K_4 \underline{[R^-]}}{K_6 \underline{[R]}}\right)_{x=0} \Delta[B^-] - \left(\frac{K_4 \underline{[R^-]}\underline{[B^-]}}{K_6 \underline{[R]}^2}\right)_{x=0} \Delta[R] \tag{3.7.15}$$

Once the other constants are solved (i.e., b's, E's, m's etc.), we then continue on to obtain $\frac{d\Delta[R^{2-}]}{dx}$ and $\frac{d\Delta[A]}{dx}$ values at x = δ:

$$\left(\frac{d\Delta[R^{2-}]}{dx}\right)_{x=\delta} = \sum_{j=1}^{4} \varepsilon_j m_j b_j e^{m_j \delta} \tag{4.2.3.5.1}$$

$$\left(\frac{d\Delta[A]}{dx}\right)_{x=\delta} = \sum_{j=1}^{4} m_j b_j e^{m_j \delta} \tag{4.2.3.5.2}$$

And the other delta derivatives are obtained at x = δ:

$$\left(\frac{d\Delta[B^-]}{dx}\right)_{x=\delta} = \omega_1\left(\frac{d\Delta[R^{2-}]}{dx}\right)_{x=\delta} + \omega_2\left(\frac{d\Delta[A]}{dx}\right)_{x=\delta} \quad (4.2.3.5.3)$$

$$\left(\frac{d\Delta[R]}{dx}\right)_{x=\delta} = \omega_3\left(\frac{d\Delta[R^{2-}]}{dx}\right)_{x=\delta} + \omega_4\left(\frac{d\Delta[A]}{dx}\right)_{x=\delta} \quad (4.2.3.5.4)$$

$$\left(\frac{d\Delta[R^-]}{dx}\right)_{x=\delta} = \omega_5\left(\frac{d\Delta[R^{2-}]}{dx}\right)_{x=\delta} + \omega_6\left(\frac{d\Delta[A]}{dx}\right)_{x=\delta} \quad (4.2.3.5.5)$$

(ω's are again constants at x = 0)

$$\left(\frac{d\Delta[C^{2-}]}{dx}\right)_{x=\delta} = \left(\frac{K_4\underline{[B^-]}}{K_6\underline{[R]}}\right)_{x=0}\left(\frac{d\Delta[R^-]}{dx}\right)_{x=\delta} + \left(\frac{K_4\underline{[R^-]}}{K_6\underline{[R]}}\right)_{x=0}\left(\frac{d\Delta[B^-]}{dx}\right)_{x=\delta}$$

$$-\left(\frac{K_4\underline{[R^-]}\underline{[B^-]}}{K_6\underline{[R]}^2}\right)_{x=0}\left(\frac{d\Delta[R]}{dx}\right)_{x=\delta} \quad (4.2.3.5.6)$$

Note that we fix the θ's at x = 0 for solving the constants; but for calculating the underbarred derivatives at x = δ, we re-calculate the θ's at x = δ (while Φ_1 remains to be its value at x = 0) following equations 3.7.47 and 3.7.48:

$$\left(\frac{d\underline{[A]}}{dx}\right)_{x=\delta} = -\left(\frac{\theta_1}{\theta_1 D_A + D^*(\theta_2+\theta_4+\theta_5)}\right)_{x=\delta}(\Phi_1)_{x=0} \quad (4.2.3.5.7)$$

$$\left(\frac{d\underline{[R^{2-}]}}{dx}\right)_{x=\delta} = -\left(\frac{\theta_4}{\theta_1 D_A + D^*(\theta_2+\theta_4+\theta_5)}\right)_{x=\delta}(\Phi_1)_{x=0} \quad (4.2.3.5.8)$$

$$\left(\frac{d\underline{[B^-]}}{dx}\right)_{x=\delta} = -\left(\frac{\theta_2}{\theta_1 D_A + D^*(\theta_2+\theta_4+\theta_5)}\right)_{x=\delta}(\Phi_1)_{x=0} \quad (4.2.3.5.9)$$

$$\left(\frac{d\underline{[C^{2-}]}}{dx}\right)_{x=\delta} = -\left(\frac{\theta_5}{\theta_1 D_A + D^*(\theta_2+\theta_4+\theta_5)}\right)_{x=\delta}(\Phi_1)_{x=0} \quad (4.2.3.5.10)$$

Finally, the fluxes of CO_2-containing species (i.e. physically dissolved CO_2,

di-carbamate, carbonate, and bicarbonate) are calculated as follows:

$$-D_A\left(\frac{d[A]}{dx}\right)_{x=\delta} = -D_A\left[\left(\frac{d[\underline{A}]}{dx}\right)_{x=\delta} + \left(\frac{d\Delta[A]}{dx}\right)_{x=\delta}\right] \quad (4.2.3.5.11)$$

$$-D^*\left(\frac{d[R^{2-}]}{dx}\right)_{x=\delta} = -D^*\left[\left(\frac{d[\underline{R^{2-}}]}{dx}\right)_{x=\delta} + \left(\frac{d\Delta[R^{2-}]}{dx}\right)_{x=\delta}\right] \quad (4.2.3.5.12)$$

$$-D^*\left(\frac{d[B^-]}{dx}\right)_{x=\delta} = -D^*\left[\left(\frac{d[\underline{B^-}]}{dx}\right)_{x=\delta} + \left(\frac{d\Delta[B^-]}{dx}\right)_{x=\delta}\right] \quad (4.2.3.5.13)$$

$$-D^*\left(\frac{d[C^{2-}]}{dx}\right)_{x=\delta} = -D^*\left[\left(\frac{d[\underline{C^{2-}}]}{dx}\right)_{x=\delta} + \left(\frac{d\Delta[C^{2-}]}{dx}\right)_{x=\delta}\right] \quad (4.2.3.5.14)$$

Table 4.2.3.5 shows that the sum of the fluxes of CO_2-containing species (i.e. physically dissolved CO_2, di-carbamate, carbonate, and bicarbonate) into bulk liquid (i.e. at $x = \delta$) equals the CO_2 absorption flux at the gas-liquid interface (i.e. $x = 0$). This is consistent with the steady-state assumption, which requires that there be no accumulation or depletion of CO_2 within the film.

Under actual operating conditions, the slow CO_2 hydration reaction is likely to be unequilibrated in bulk liquid, to an extent that varies within a given contactor – whereas that reaction, like all others, is simply assumed in the foregoing analysis to be at equilibrium. Whether carbonate and bicarbonate will diffuse to (attain a positive value) or from (attain a negative value) the bulk liquid interface will depend on operating conditions.

In general, the dicarbamate fluxes dominates CO_2 transport away from the

interface, although their magnitude approaches zero as the film thickness approaches zero or bulk liquid approaches equilibrium with the feed gas.

Table 4.2.3.5 Summary of fluxes of CO_2-containing species at boundaries

Conditions: T = 293 K, [PG] = 3 M, CO_2 partial pressure = 0.15 atm			
Flux [=] mol dm^{-2} s^{-1}	CO_2 bulk loading = 10%		
	1 μm	6 μm	164 μm
Total fluxes of CO_2-containing species at x = 0	1.7293×10^{-4}	1.6298×10^{-4}	5.5402×10^{-5}
Total fluxes of CO_2-containing species at x = δ	1.7293×10^{-4}	1.6298×10^{-4}	5.5402×10^{-5}
Flux percentage of A at x = δ	1.2659 %	1.7288×10^{-4} %	0.0088 %
Flux percentage of R^{2-} at x = δ	98.7764 %	100.2533 %	127.6770 %
Flux percentage of B^- at x = δ	1.1625 %	0.9660 %	-23.7942 %
Flux percentage of C^{2-} at x = δ	-1.2047 %	-1.2195 %	-3.8916 %
	CO_2 bulk loading = 30%		
	1 μm	6 μm	164 μm
Total fluxes of CO_2-containing species at x = 0	1.0305×10^{-4}	9.6250×10^{-5}	2.9918×10^{-5}
Total fluxes of CO_2-containing species at x = δ	1.0305×10^{-4}	9.6250×10^{-5}	2.9918×10^{-5}
Flux percentage of A at x = δ	9.8560 %	0.0039 %	0.1313 %
Flux percentage of R^{2-} at x = δ	90.3781 %	101.4173 %	161.8368 %
Flux percentage of B^- at x = δ	1.7038 %	0.8744 %	-55.3794 %
Flux percentage of C^{2-} at x = δ	-1.9379 %	-2.2956 %	-6.5887 %

Table 4.2.3.5 Summary of fluxes of CO_2-containing species at boundaries (continued)

	CO_2 bulk loading = 40%		
	1 μm	6 μm	164 μm
Total fluxes of CO_2-containing species at x = 0	6.8064×10^{-5}	6.1141×10^{-5}	1.6663×10^{-5}
Total fluxes of CO_2-containing species at x = δ	6.8064×10^{-5}	6.1141×10^{-5}	1.6663×10^{-5}
Flux percentage of A at x = δ	28.3461 %	0.0381 %	0.4833 %
Flux percentage of R^{2-} at x = δ	72.3880 %	104.3154 %	174.3202 %
Flux percentage of B^{-} at x = δ	1.8752 %	-0.4386 %	-66.3413 %
Flux percentage of C^{2-} at x = δ	-2.6093 %	-3.9149 %	-8.4622 %
	CO_2 bulk loading = 50%		
	1 μm	6 μm	164 μm
Total fluxes of CO_2-containing species at x = 0	3.6999×10^{-5}	2.5190×10^{-5}	4.6833×10^{-6}
Total fluxes of CO_2-containing species at x = δ	3.6999×10^{-5}	2.5190×10^{-5}	4.6833×10^{-6}
Flux percentage of A at x = δ	67.3343 %	2.0324 %	2.7094 %
Flux percentage of R^{2-} at x = δ	34.3089 %	104.7317 %	128.6508 %
Flux percentage of B^{-} at x = δ	1.4385 %	2.8951 %	-19.4862 %
Flux percentage of C^{2-} at x = δ	-3.0817 %	-9.6592 %	-11.8740 %

5. RESULTS FOR CO_2-PS SYSTEM

5.1 Physiochemical parameters

The solubility, density, diffusivity, equilibrium and kinetic parameters as functions of temperature and concentration are presented below.

5.1.1 Solubility data

CO_2 vapor-liquid equilibrium is described by the Henry law:

$$p_{A,G} \equiv \frac{1}{\alpha}[A] = H_{CO_2}[A] \qquad (5.1.1)$$

where $p_{A,G}$ is the CO_2 partial pressure and H_{CO_2} is the Henry coefficient of CO_2 in the PS solution given by U. E. Aronu [53] and is derived by interpolation for the following temperatures:

Table 5.1.1 Henry coefficients of PS [48]

[PS] (M)	$H/10^6$ (Pa dm^3 mol^{-1})	
	313.15 (K)	333.15 (K)
1	6.20	8.37
2	8.20	10.69
3	10.02	12.81

5.1.2 Density data

Densities of PS solutions were studied by Jacco van Holst et al. [83] as:

$$\rho = -0.4862T + 50.00[PS] + 1146 \quad (\rho\ [=]\ g/L, C\ [=]\ mol/L, T\ [=]\ K) \qquad (5.1.2)$$

5.1.3 Diffusivity data

The diffusivity of CO_2 in the aqueous sarcosine salt solution is estimated using the relation as follows [47, 48]:

$$D_{CO_2,PS} = D_{CO_2,W}(\mu_W / \mu_{PS})^{0.8} \quad (5.1.3.1)$$

where $D_{CO_2,W}$ is the diffusivity of CO_2 in water, given by J. Haubrock [84] as:

$$\log D_{CO_2,W} = -8.176 + 712.5/T - 2.591\times10^5/T^2 \quad \left(D_{CO2,W}[=]m^2/s\right) \quad (5.1.3.2)$$

μ_W is the viscosity of water, given by Kampmeyer [85] as:

$$\log \mu_W = -5.485471 + 5.041873\times10^3/T - 1.551439\times10^6/T^2 + 0.1849577\times10^9/T^3$$

$$\left(\mu_W[=]\text{poise}\times10^{-3}[=]0.1\ \text{mPa}\cdot\text{s}\right) \quad (5.1.3.3)$$

μ_{PS} is the viscosity of PS solution, given by Jacco van Holst [83] as:

$$\mu_{PS} = 2.950\times10^{-3}\exp\left[\frac{14150\exp(0.1047[PS])}{R_gT}\right]\exp(-0.3124[PS])\ \ (\text{mPa}\cdot\text{s}) \quad (5.1.3.4)$$

$$\left(R_g = 8.314\ \text{J/mol}\cdot\text{K}\right)$$

Diffusion coefficients of PS is tabulated in Table 5.1.3 [79].

Table 5.1.3 Diffusion coefficients of PS [79]

T (K)	D_{PS} /10^{-7} ($dm^2\ s^{-1}$)			
[PS] (M)	293.15	298.15	313.15	333.15
0.971 ± 0.001	0.945	1.04	1.50	2.27
1.99	0.893	0.993	1.45	2.18
2.91	0.865	0.982	1.39	2.08

5.1.4 Equilibrium data

Equilibrium constants -K_2, K_4, K_5- in the aqueous CO_2-PS system are the same as those in CO_2-PG system.

For carbamate zwitterion deprotonation, equation 3.1.6, K_6 is given by U. E. Aronu [53] as:

$$K_6 = \frac{[R^-][H^+]}{[R]} = \exp(-5.9752 - 5185.10/T) \quad (\text{mol dm}^{-3}) \tag{5.1.4.1}$$

The di-carbamate hydrolysis reaction is regarded as a dependent reaction in the analysis. It is a linear combination of di-carbamate formation and carbonate formation reactions and its equilibrium constant is given by Aronu [53] as follows (valid in temperature range 40-120 ^oC):

$$K_{carbhydrolysis} = \left(\frac{[R^-][B^-]}{[R^{2-}]}\right)_{eq} = \exp(-7.4569 + 0.9753/T) \quad (\text{mol dm}^{-3}) \tag{5.1.4.2}$$

From the definition of $K_{Acid_j} \equiv \left(\frac{[B_jH^+]}{[B_j][H^+]}\right)^{eq}$, it follows that:

$$K_{Acid,R^-} = \frac{1}{K_6} \tag{5.1.4.3}$$

and that:

$$K_{Acid,W} = \frac{1}{[W]} \tag{5.1.4.4}$$

From the definition of $K_{Carb} \equiv \left(\frac{[R^{2-}][H^+]}{[A][R^-]}\right)^{eq}$, it is easily shown that:

$$K_{Carb} = \frac{K_2}{K_{carbhydrolysis}} \tag{5.1.4.5}$$

5.1.5 Kinetic data

The zwitterion mechanism constants are given by Aronu [48], and the nonidealities of the salt solution are lumped into a salt effect expressed by:

$$k_{ion} = \exp(bI) \qquad (5.1.5.1)$$

where the ionic strength is defined by:

$$I = \frac{1}{2}\Sigma c_i z_i^{\,2}$$

and b is a constant that depends on the nature of the salt. In this thesis, an average value of b = 0.45 is adopted from a rigorous model used to interpret the effect of the ionic strength that was developed by Cullinane and Rochelle [86]. From equation 5.1.5.1, it is clear that for the limiting case where ionic strength is zero, k_{ion} is one, which then reduces to the nonionic case, as with an alkanolamine. As a first approximation, the ionic strength used in the calculations is that in bulk liquid, i.e.:

$$I = \frac{1}{2}\left([K^+]_{x=\delta} + [B^-]_{x=\delta} + [R^-]_{x=\delta} + 4[R^{2-}]_{x=\delta} + 4[C^{2-}]_{x=\delta}\right) \qquad (5.1.5.2)$$

Note that the ionic strength contribution by the zwitterion, R, is considered to be zero [87].

In addition:

$$k_{1a} = 2.6198\times10^{9}\exp(-915.8/T) \quad (dm^3\ mol^{-1}\ s^{-1}) \qquad (5.1.5.3)$$

$$k_W / k_{-1a} = \frac{3.9805\times10^{8}\exp(-3924.4/T)}{k_{1a}} \quad (dm^3\ mol^{-1}) \qquad (5.1.5.4)$$

$$k_{R^-} / k_{-1a} = \frac{6.3494\times10^{6}\exp(-1589.6/T)}{k_{1a}} \quad (dm^3\ mol^{-1}) \qquad (5.1.5.5)$$

The large value of k_{1a} indicates that deprotonation of the zwitterion is the

rate-determining step. The deprotonation rate constants for water and sarcosinate anion are such that water has a more significant effect in deprotonation of the zwitterion of AAS compared to alkanolamines.

The forward reaction rate of carbonic acid formation (k_2), and the forward reaction rate of bicarbonate formation (k_3) are assumed to be the same as those in the CO_2-PG system, which themselves do not account for ionic strength effects consideration [20].

Incorporation of ionic strength effects modifies the key differential mass balance (3.7.1) to become:

$$D^* \frac{d^2[R^{2-}]}{dx^2} = -\frac{k_{ion} k_{1a} [A][R^-]\left(k_{R^-}[R^-] + k_W[W]\right)\left(1 - \frac{K_6[R^{2-}][R]}{K_{Carb}[A][R^-]^2}\right)}{k_{-1a} + k_{R^-}[R^-] + k_W[W]} \qquad (3.7.1')$$

In the same fashion, terms in all other differential mass balances in the linearized analysis, i.e. η_1, η_2, λ_1, and λ_2, are multiplied by k_{ion}.

5.2 Results and discussion

5.2.1 Speciation profiles

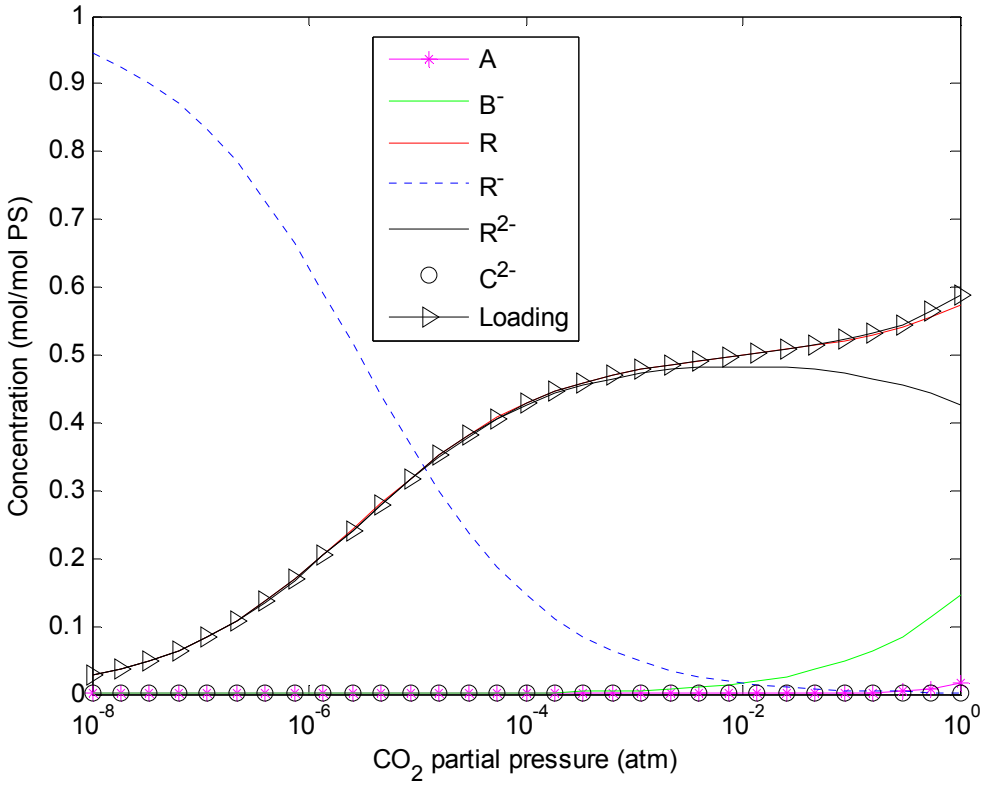

Figure 5.2.1.1 Speciation and CO_2 loading *vs*. CO_2 partial pressure (1 M PS, 313 K).

Figure 5.2.1.1-4 depict the speciation profiles for 1 M and 3 M PS solutions at 313 K and 333 K, respectively. It is striking that the di-carbamate forms in the presence of even trace amounts of CO_2, i.e. at CO_2 partial pressures as low as 10^{-8} atm. At partial pressure up to 10^{-2} atm, dissolved CO_2 combines primarily with R^- to form equal proportions of R and R^{2-}. In PS solutions, bicarbonate formation is vanishingly low under the operating conditions typical of post-combustion CO_2 capture at power plants.

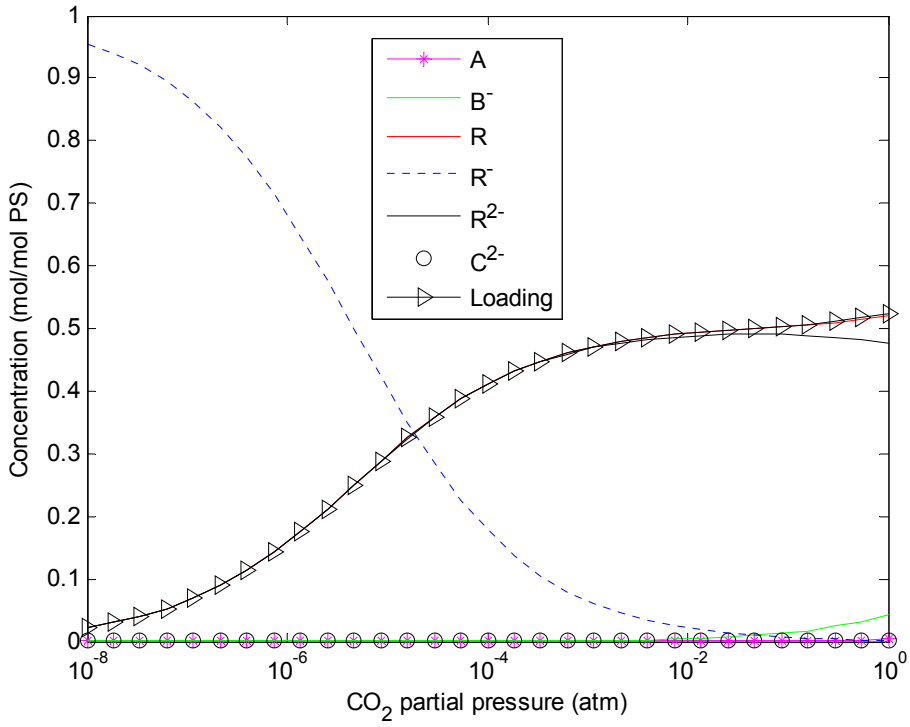

Figure 5.2.1.2 Speciation and CO_2 loading *vs*. CO_2 partial pressure (3 M PS, 313 K).

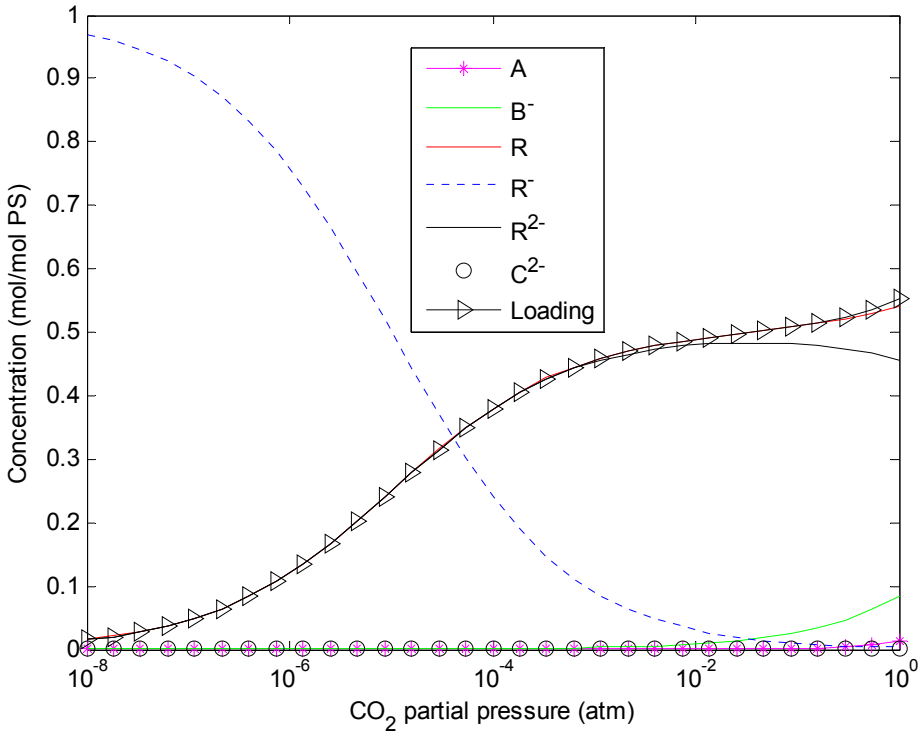

Figure 5.2.1.3 Speciation and CO_2 loading *vs*. CO_2 partial pressure (1 M PS, 333 K).

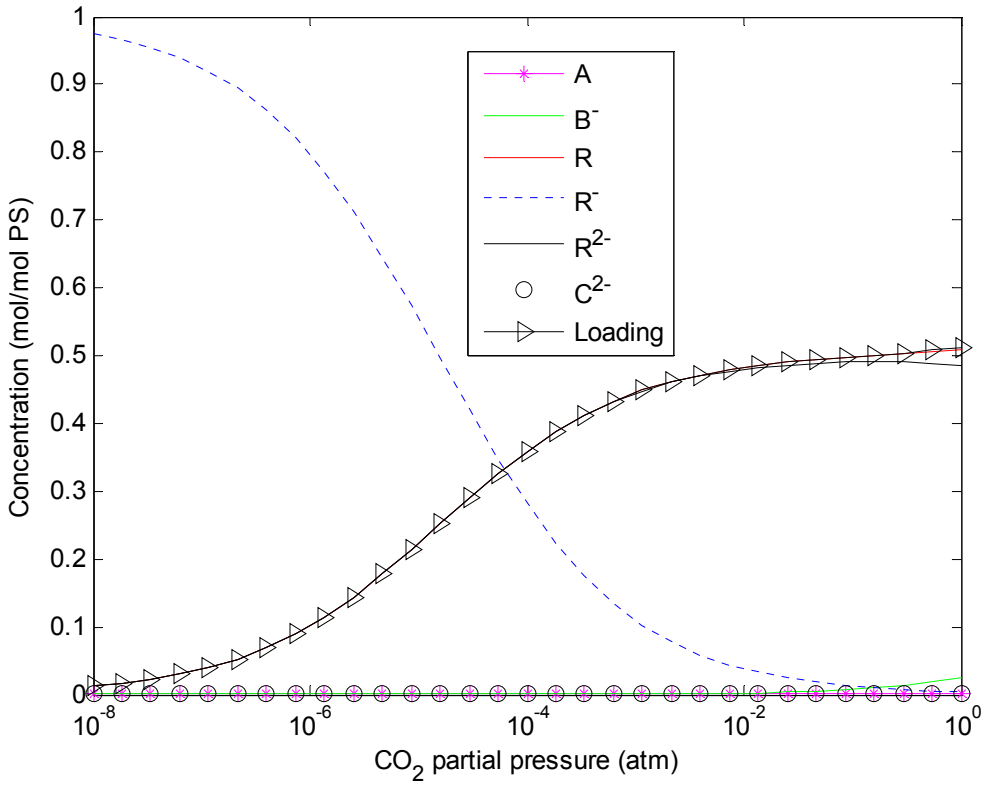

Figure 5.2.1.4 Speciation and CO_2 loading *vs*. CO_2 partial pressure (3 M PS, 333 K).

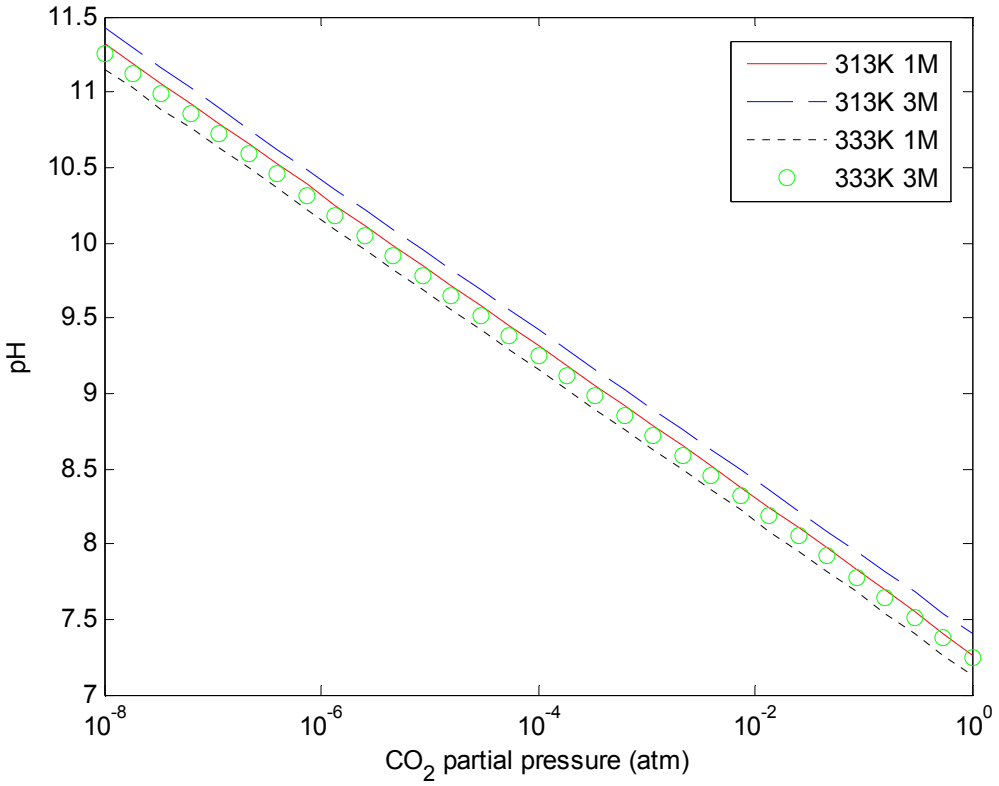

Figure 5.2.1.5 pH *vs*. CO_2 partial pressure.

Figure 5.2.1.5 shows that the pH in the bulk liquid at overall equilibrium decreases from *ca*. 11.5 at 10^{-8} atm CO_2 partial pressure to around 7.25 at 1 atm; the same trend is followed at all four assumed temperatures.

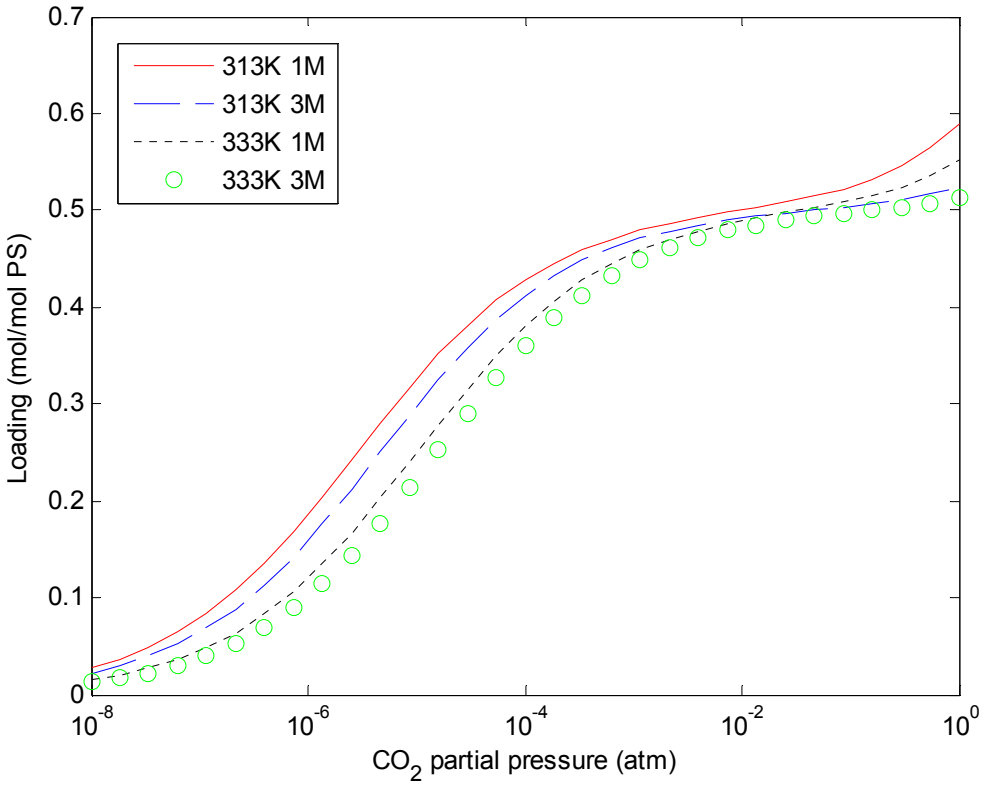

Figure 5.2.1.6 Loading *vs*. CO_2 partial pressure.

Figure 5.2.1.6 shows CO_2 loadings at the same temperatures. Lower temperatures favor CO_2 loading, which varies only slightly with amine concentration.

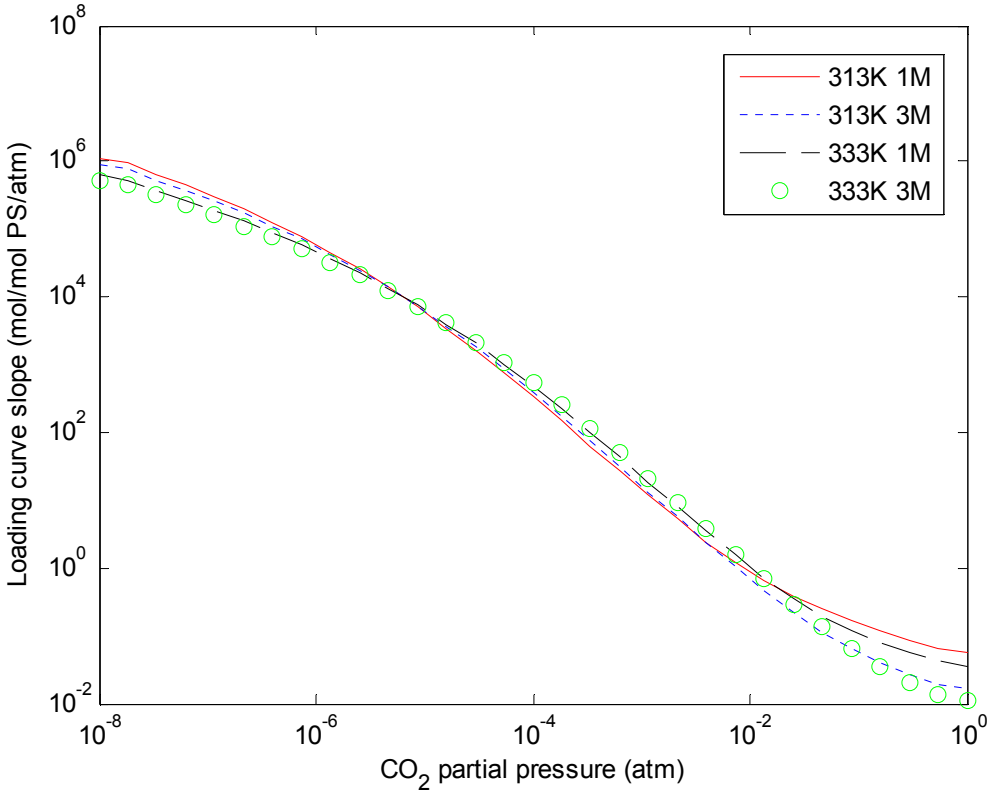

Figure 5.2.1.7 Loading curve slope *vs*. CO_2 partial pressure.

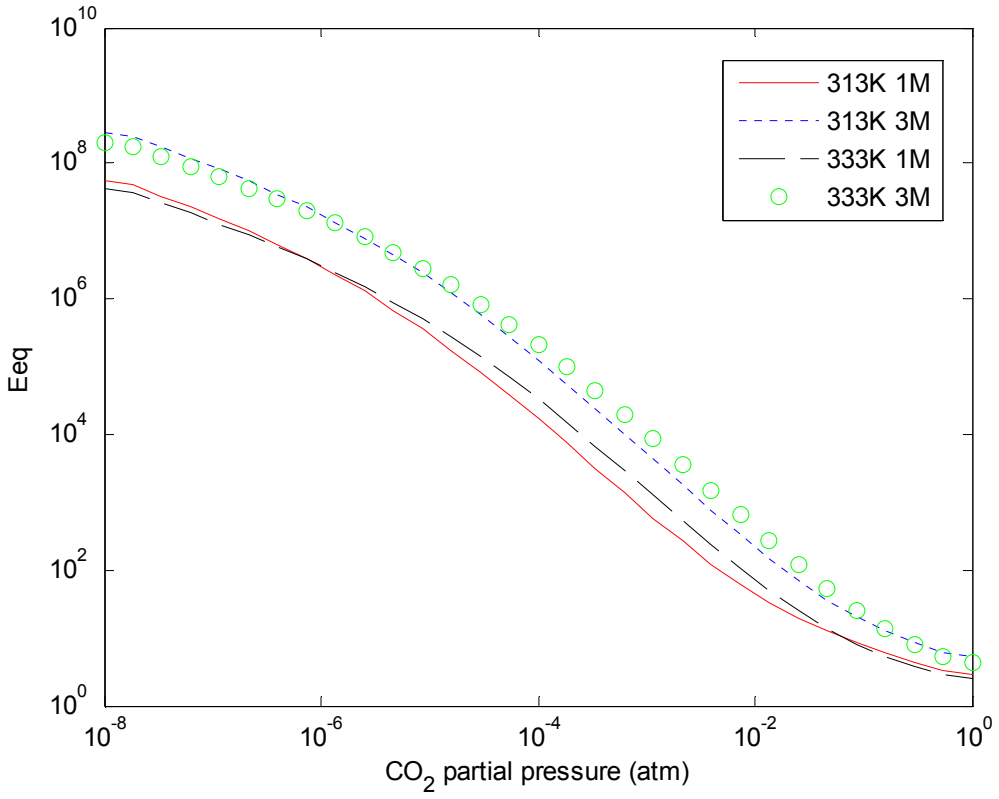

Figure 5.2.1.8 Equilibrium enhancement factor *vs*. CO_2 partial pressure

Figure 5.2.1.8 again indicates very large enhancement factors at very low CO_2 partial pressure, which even exceed those calculated for PG solutions. Furthermore, E is apparently more sensitive to PS concentration than temperature change.

5.2.2 Validation of perturbation analysis

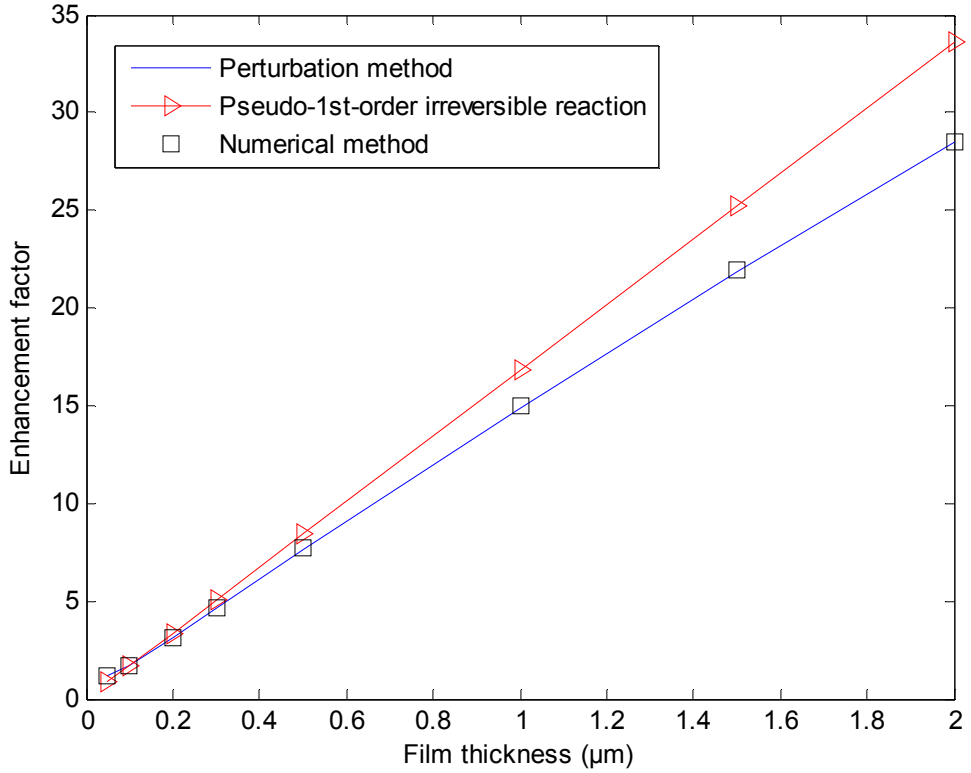

Figure 5.2.2 Absorption enhancement factor *vs*. liquid film thickness. (3 M PS, 313 K, bulk gas CO_2 partial pressure = 0.15 atm, bulk liquid loading = 40%)

Calculated enhancement factors are again in line with those obtained from numerical analysis. The rapid increase of E with film thickness reflects the very rapid reaction of PS with CO_2.

5.2.3 Results from perturbation analysis

5.2.3.1 Effect of concentration

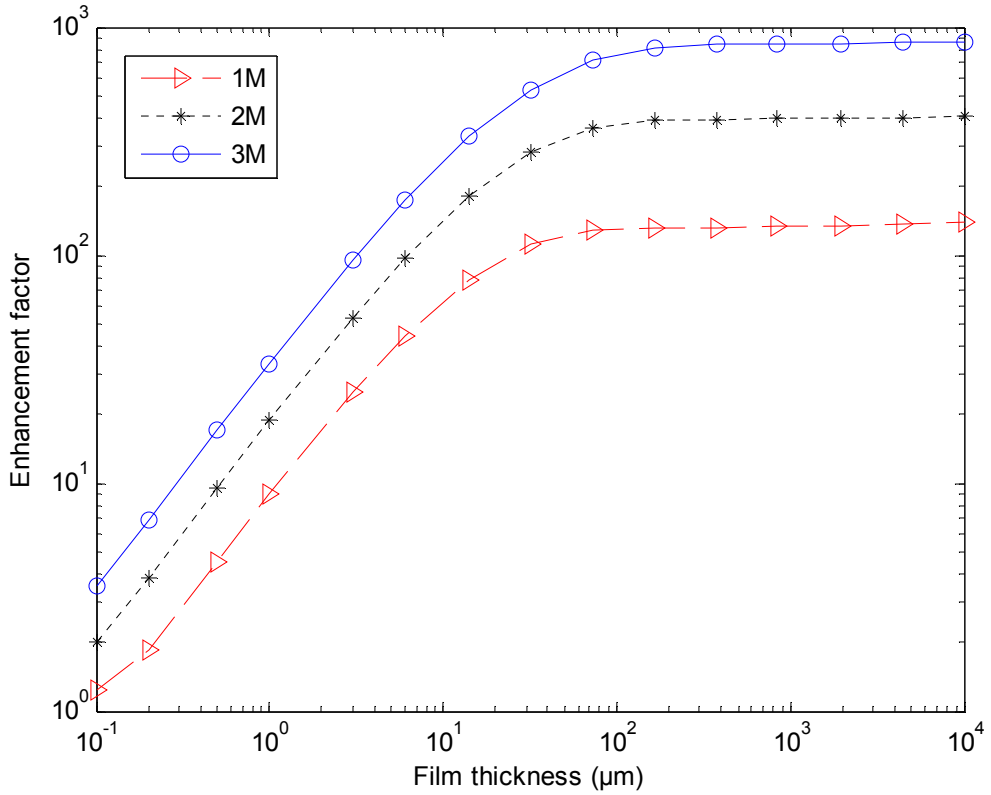

Figure 5.2.3.1 Absorption enhancement factor *vs*. liquid film thickness. (Bulk liquid loading = 10%, 313 K, bulk gas CO_2 partial pressure = 0.15 atm)

Figure 5.2.3.1 compares E values at three concentrations - 1, 2 and 3 M PS. The results are qualitatively similar to those obtained for PG solutions, although the E values are roughly double those for the latter; notably, E exceeds 1 even in very thin films.

5.2.3.2 Effect of bulk liquid loading

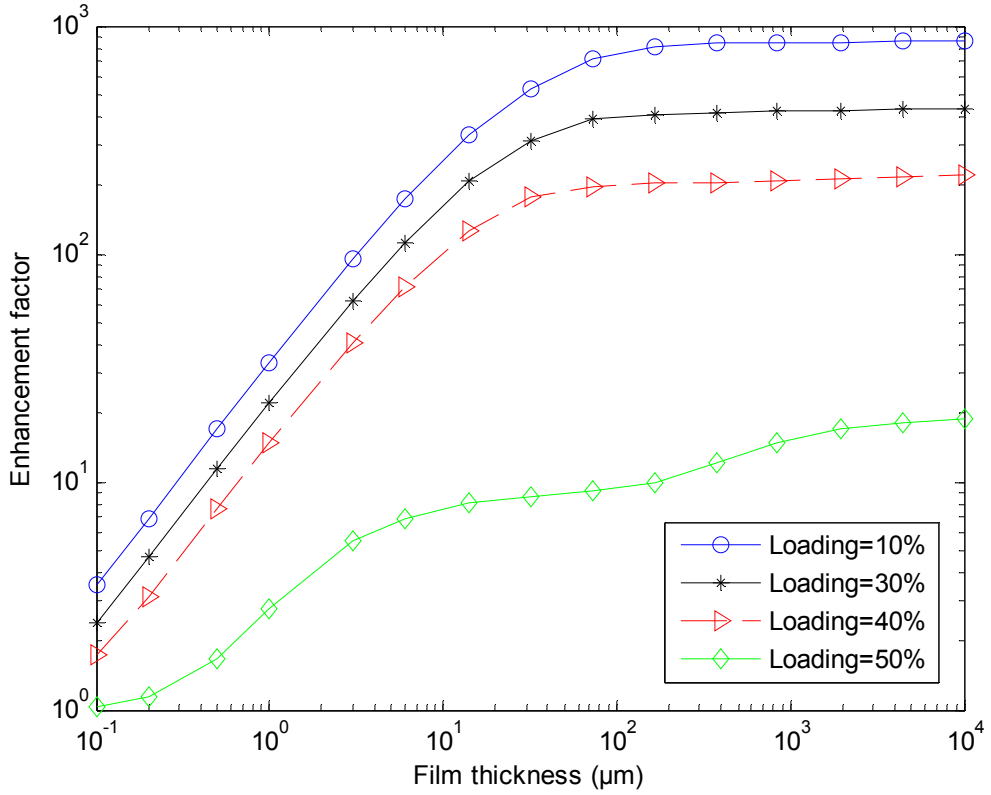

Figure 5.2.3.2 Absorption enhancement factor *vs*. liquid film thickness. (3 M PS, 313 K, bulk gas CO_2 partial pressure = 0.15 atm)

Calculated enhancement factors with various bulk liquid CO_2 loadings are shown in Figure 5.2.3.2, and the behavior is again similar to that observed for PG solutions. Notably, the results for 50% loading reflect the fact that the gas-phase CO_2 partial pressure only slightly exceeds that in equilibrium with bulk liquid (which is 0.05 atm). Thus, the reverse reaction markedly inhibits the absorption of CO_2.

6. CONCLUSION

The perturbation method efficiently models CO_2 absorption in PG and PS solutions. This bodes well for its general applicability to diffusion with multiple reversible reactions, including CO_2 absorption in solutions of mixed amines and amino acids; and its potential utility as an adjunct to scoping calculations for the design of coupled absorber-stripper systems.

NOMENCLATURE

$A = CO_2$

AAS = amino acid salt

b = salt-dependent constant

$b_1 – b_4$ = constants defined by equations 3.7.26, 3.7.30 and 3.7.31

B_j = base species

$B^- = HCO_3^-$

c_1, c_2 = constants defined by equations 3.7.28-29

C_i, [i] = concentration for species i

$C^{2-} = CO_3^{2-}$

D_A = diffusivity of CO_2 into aqueous amino acid salt solution, $m^2\ s^{-1}$

D* = diffusivity of amino acid salt into aqueous solution, $m^2\ s^{-1}$

E = enhancement factor defined by equation 3.5.11

G = defined by equation 3.8.5

$H = 1/\alpha$, Henry constant, atm $m^3\ mol^{-1}$

Ha = Hatta number

i = component i

$\underline{[i]}$ = pseudo local equilibrium concentration for component i

$\Delta\underline{[i]}$ = concentration departure from pseudo local equilibrium

I = ionic strength

J = defined by 3.8.5

k_1, k_{-1} = forward and reverse reaction rate constants of equation 2.2.4

k_{1a}, k_{-1a} = forward and reverse reaction rate constants of equation 3.1.1a

k_2, k_{-2} = forward and reverse reaction rate constants of equation 3.1.2

k_3, k_{-3} = forward and reverse reaction rate constants of equation 3.1.3

k_4, k_{-4} = forward and reverse reaction rate constants of equation 3.1.4

k_5, k_{-5} = forward and reverse reaction rate constants of equation 3.1.5

k_6, k_{-6} = forward and reverse reaction rate constants of equation 3.1.6

k_{Bj} = rate constant of protonated di-carbamate deprotonation by base

(B_j = W, OH^-, R^-)

k_{ion} = ionic strength correction factor

k_L^o = CO_2 liquid phase mass transfer coefficient

K_{1a} = equilibrium constant for reaction 3.1.1a

K_{1j} = equilibrium constant for reaction 3.1.1

$K_{Acid,j}$ = reciprocal of acid dissociation constants

K_{Carb} = di-carbamate formation constant

K_2 = equilibrium constant for reaction 3.1.2

K_3 = equilibrium constant for reaction 3.1.3

K_4 = equilibrium constant for reaction 3.1.4

K_5 = equilibrium constant for reaction 3.1.5

K_6 = equilibrium constant for reaction 3.1.6

$K_{carbhydrolysis}$ = equilibrium constant defined by equations 4.1.4.5 and 5.1.4.2

$L = CO_2$ bulk liquid loading

$m_1 – m_4$ = constants defined by equations 3.7.22-23

MEA = monoethanolamine

ODE = ordinary differential equation

$P_{A,G}$ = CO_2 partial pressure in gas phase

PG = potassium glycinate

PS = potassium sarcosinate

Q = defined by 3.8.1

r = reaction rate, mol dm^{-3} s^{-1}

R = shorthand notation for protonated amino acid anion (a zwitterion)

R_g = gas constant, 8.314 J mol^{-1} K^{-1}

R^- = shorthand notation for amino acid anion

R^{2-} = shorthand notation for di-carbamate anion

R^z = shorthand notation for protonated di-carbamate anion

R', R'' = alkyl group

T = temperature, K

u_1, u_2 = constants defined by 3.7.22-23

W = water

x = position, defined in Figure 3.2, μm

$x_1 – x_4$ = defined by equations 3.8.7-10

y = dimensionless position

z = ion charge

GREEK LETTERS

β = square root of D* over D_A defined by equation 3.5.11

δ = liquid film thickness, μm

Φ_1 = CO_2 absorption rate expressed as a flux defined by equation 3.5.7

Φ_2 = constant defined by equation 3.5.9

ε_1, ε_2, E_1, E_2 = constants defined by equations 3.7.22-23

$\eta_1 - \eta_4$ = constants defined by equations 3.7.19 and 3.7.21

$\theta_1 - \theta_5$ = constants defined by equations 3.7.42-46

λ_1, λ_2 = constants defined by equation 3.7.20

μ = viscosity, kg m^{-1} s^{-1}

ξ = defined by equation 3.8.1

ρ = density, kg m^{-3}

ρ_i = consumption rate for component i, mol dm^{-3} s^{-1}

$\omega_1 - \omega_6$ = constants defined by equations 3.7.16-18

SUPERSCRIPTS

eq = equilibrium

+ = pseudo-first-order irreversible reaction

SUBSCRIPTS

j = index

o = initial condition

∞ = infinite

REFERENCES

1. Smith, K.A., Meldon, J.H. and Colton, C.K., *Analysis of carrier-facilitated transport.* AIChE Journal, 1973, **19**(1), 102-111.

2. Meldon, J.H., Smith, K.A. and Colton, C.K., *Effect of weak acids upon transport of carbon-dioxide in alkaline-solutions.* Chemical Engineering Science, 1977, **32**(8), 939-950.

3. Yoshitake, H., Yokoi, T. and Tatsumi, T., *Adsorption of chromate and arsenate by amino-functionalized MCM-41 and SBA-1.* Chemistry of Materials, 2002, **14**(11), 4603-4610.

4. Song, C.S., *Global challenges and strategies for control, conversion and utilization of CO_2 for sustainable development involving energy, catalysis, adsorption and chemical processing.* Catalysis Today, 2006, **115**(1-4), 2-32.

5. Yang, H.Q., Xu, Z.H., Fan, M.H., Gupta, R., Slimane, R.B., Bland, A.E., and Wright, I., *Progress in carbon dioxide separation and capture: A review.* Journal of Environmental Sciences-China, 2008, **20**(1), 14-27.

6. Blomen, E., Hendriks, C. and Neele, F., *Capture technologies: Improvements and promising developments*, in *Greenhouse Gas Control Technologies 9*. 2009. 1505-1512.

7. Mendes, D., Mendes, A., Madeira, L.M., Iulianelli, A., Sousa, J.M. and Basile, A., *The water-gas shift reaction: from conventional catalytic systems to Pd-based membrane reactors - A review.* Asia-Pacific Journal of Chemical Engineering, 2010, **5**(1), 111-137.

8. Zanganeh, K.E., Shafeen, A. and Salvador, C., *CO_2 capture and development of an advanced pilot-scale cryogenic separation and compression unit*, in *Greenhouse Gas Control Technologies 9*. 2009. 247-252.

9. Olajire, A.A., *CO_2 capture and separation technologies for end-of-pipe applications - A review.* Energy, 2010, **35**(6), 2610-2628.

10. Feron, P.H.M. and Hendriks, C.A., *CO_2 capture process principles and costs.* Oil & Gas Science and Technology-Revue De L Institut Francais Du Petrole, 2005, **60**(3), 451-459.

11. Kather, A. and Scheffknecht, G., *The oxycoal process with cryogenic oxygen supply.*

Naturwissenschaften, 2009, **96**(9), 993-1010.

12. Ryden, M. and Lyngfelt, A., *Using steam reforming to produce hydrogen with carbon dioxide capture by chemical-looping combustion.* International Journal of Hydrogen Energy, 2006, **31**(10), 1271-1283.

13. Kittel, J., Idem, R., Gelowitz, D., Tontiwachwuthikul, P., Parrain, G. and Bonneau, A., *Corrosion in MEA units for CO_2 capture: pilot plant studies*, in *Greenhouse Gas Control Technologies 9*. 2009. 791-797.

14. Stewart, C. and Hessami, M.A., *A study of methods of carbon dioxide capture and sequestration - the sustainability of a photosynthetic bioreactor approach.* Energy Conversion and Management, 2005, **46**(3), 403-420.

15. Fauth, D.J., Frommell, E.A., Hoffman, J.S., Reasbeck, R.P. and Pennline, H.W., *Eutectic salt promoted lithium zirconate: Novel high temperature sorbent for CO_2 capture.* Fuel Processing Technology, 2005, **86**(14-15), 1503-1521.

16. Resnik, K.P., T., Y.J. and W., P.H., *Aqua ammonia process for simultaneous removal of CO_2, SO_2 and NO_x.* International Journal of Environmental Technology and Managment, 2004, **4**(1-2), 89-104.

17. Yeh, J.T., Resnik, K.P., Rygle, K. and Pennline, H.W., *Semi-batch absorption and regeneration studies for CO_2 capture by aqueous ammonia.* Fuel Processing Technology, 2005, **86**(14-15), 1533-1546.

18. Idem, R., Wilson, M., Tontiwachwuthikul, P., Chakma, A., Veawab, A., Aroonwilas, A., and Gelowitz, D., *Pilot plant studies of the CO_2 capture performance of aqueous MEA and mixed MEA/MDEA solvents at the University of Regina CO_2 capture technology development plant and the Boundary Dam CO_2 capture demonstration.* Industrial & Engineering Chemistry Research, 2006, **45**(8), 2414-2420.

19. Gray, M.L., Soong, Y., Champagne, K.J., Pennline, H., Baltrus, J.P., Stevens, R.W., Khatri, R., Chuang, S.S.C., and Filburn, T., *Improved immobilized carbon dioxide capture sorbents.* Fuel Processing Technology, 2005, **86**(14-15), 1449-1455.

20. Danckwerts, P.V. and Sharma, M.M., *Absorption of carbon dioxide into solutions of alkalis and amines (with some notes on hydrogen sulphide and carbonyl sulphide).* Transactions of the Institution of Chemical Engineers and the Chemical Engineer, 1966, **44**(8), CE244.

21. Donaldson, T.L. and Nguyen, Y.N., *Carbon-dioxide reaction-kinetics and transport in aqueous amine membranes.* Industrial & Engineering Chemistry Fundamentals, 1980,

19(3), 260-266.

22. Chakravarty, T., Phukan, U.K. and Weiland, R.H., *Reaction of acid gases with mixtures of amines.* Chemical Engineering Progress, 1985, **81**(4), 32-36.

23. Sartori, G. and Savage, D.W., *Sterically hindered amines for CO_2 removal from gases.* Industrial & Engineering Chemistry Fundamentals, 1983, **22**(2), 239-249.

24. Danckwerts, P.V., *Reaction of CO_2 with ethanolamines.* Chemical Engineering Science, 1979, **34**(4), 443-446.

25. Sharma, M.M., *PhD Thesis.* Cambridge University, 1964.

26. Sharma, M.M., *Kinetics of reactions of carbonyl sulphide and carbon dioxide with amines and catalysis by Bronsted bases of hydrolysis of COS.* Transactions of the Faraday Society, 1965, **61**(508P), 681.

27. Hook, R.J., *An investigation of some sterically hindered amines as potential carbon dioxide scrubbing compounds.* Industrial & Engineering Chemistry Research, 1997, **36**(5), 1779-1790.

28. Majchrowicz, M.E., Brilman, D.W.F. and Groeneveld, M.J., *Precipitation regime for selected amino acid salts for CO_2 capture from flue gases*, in *Greenhouse Gas Control Technologies 9*. 2009. 979-984.

29. Penny, D.E. and Ritter, T.J., *Kinetic-study of the reaction between carbon-dioxide and primary amines.* Journal of the Chemical Society-Faraday Transactions I, 1983, **79**, 2103-2109.

30. Aronu, U.E., Svendsen, H.F. and Hoff, K.A., *Investigation of amine amino acid salts for carbon dioxide absorption.* International Journal of Greenhouse Gas Control, 2010, **4**(5), 771-775.

31. Darde, V., Thomsen, K., van Well, W.J.M. and Stenby, E.H., *Chilled ammonia process for CO_2 capture.* International Journal of Greenhouse Gas Control, 2010, **4**(2), 131-136.

32. Huang, H.P., Shi, Y., Li, W. and Chang, S.G., *Dual alkali approaches for the capture and separation of CO_2.* Energy & Fuels, 2001, **15**(2), 263-268.

33. Li, Z.S., Cai, N.S. and Croiset, E., *Process analysis of CO_2 capture from flue gas using carbonation/calcination cycles.* AIChE Journal, 2008, **54**(7), 1912-1925.

34. Fang, F., Li, Z.S. and Cai, N.S., *CO_2 capture from flue gases using a fluidized bed*

reactor with limestone. Korean Journal of Chemical Engineering, 2009, **26**(5), 1414-1421.

35. Manovic, V., Charland, J.P., Blamey, J., Fennell, P.S., Lu, D.Y. and Anthony, E.J., *Influence of calcination conditions on carrying capacity of CaO-based sorbent in CO_2 looping cycles.* Fuel, 2009, **88**(10), 1893-1900.

36. Blamey, J., Anthony, E.J., Wang, J. and Fennell, P.S., *The calcium looping cycle for large-scale CO_2 capture.* Progress in Energy and Combustion Science, 2010, **36**(2), 260-279.

37. Bara, J.E., Camper, D.E., Gin, D.L. and Noble, R.D., *Room-temperature ionic liquids and composite materials: Platform technologies for CO_2 capture.* Accounts of Chemical Research, 2010, **43**(1), 152-159.

38. Davis, J.H., *Green industrial applications of ionic liquids.* NATO Science Series, Volume 92, Kluwer Academic Publishers, Dordrecht, 2000.

39. Camper, D., Bara, J.E., Gin, D.L. and Noble, R.D., *Room-temperature ionic liquid-amine solutions: tunable solvents for efficient and reversible capture of CO_2.* Industrial & Engineering Chemistry Research, 2008, **47**(21), 8496-8498.

40. Swatloski, R.P., Holbrey, J.D. and Rogers, R.D., *Ionic liquids are not always green: hydrolysis of 1-butyl-3-methylimidazolium hexafluorophosphate.* Green Chemistry, 2003, **5**(4), 361-363.

41. Garcia, M.T., Gathergood, N. and Scammells, P.J., *Biodegradable ionic liquids - Part II. Effect of the anion and toxicology.* Green Chemistry, 2005, **7**(1), 9-14.

42. Pretti, C., Chiappe, C., Pieraccini, D., Gregori, M., Abramo, F., Monni, G., and Intorre, L., *Acute toxicity of ionic liquids to the zebrafish (Danio rerio).* Green Chemistry, 2006, **8**(3), 238-240.

43. Kumar, P.S., Hogendoorn, J.A., Feron, P.H.M. and Versteeg, G.F., *New absorption liquids for the removal of CO_2 from dilute gas streams using membrane contactors.* Chemical Engineering Science, 2002, **57**(9), 1639-1651.

44. Pohorecki, R. and Moniuk, W., *Kinetics of reaction between carbon-dioxide and hydroxyl ions in aqueous-electrolyte solutions.* Chemical Engineering Science, 1988, **43**(7), 1677-1684.

45. Pinsent, B.R.W., Pearson, L. and Roughton, F.J.W., *The kinetics of combination of carbon dioxide with hydroxide ions.* Transactions of the Faraday Society, 1956, **52**(11), 1512-1520.

46. Edwards, T.J., Maurer, G., Newman, J. and Prausnitz, J.M., *Vapor-liquid-equilibria in multicomponent aqueous-solutions of volatile weak electrolytes.* AIChE Journal, 1978, **24**(6), 966-976.

47. Simons, K., Brilman, W., Mengers, H., Nijmeijer, K. and Wessling, M., *Kinetics of CO_2 absorption in aqueous sarcosine salt solutions: Influence of concentration, temperature, and CO_2 loading.* Industrial & Engineering Chemistry Research, 2010, **49**(20), 9693-9702.

48. Aronu, U.E., Hartono, A., Hoff, K.A. and Svendsen, H.F., *Kinetics of carbon dioxide absorption into aqueous amino acid salt: potassium salt of sarcosine solution.* Industrial & Engineering Chemistry Research, 2011, **50**(18), 10465-10475.

49. Caplow, M., *Kinetics of carbamate formation and breakdown.* Journal of the American Chemical Society, 1968, **90**(24), 6795-&.

50. Crooks, J.E. and Donnellan, J.P., *Kinetics and mechanism of the reaction between carbon-dioxide and amines in aqueous-solution.* Journal of the Chemical Society-Perkin Transactions 2, 1989, (4), 331-333.

51. da Silva, E.F. and Svendsen, H.F., *Ab initio study of the reaction of carbamate formation from CO_2 and alkanolamines.* Industrial & Engineering Chemistry Research, 2004, **43**(13), 3413-3418.

52. Blauwhoff, P.M.M., Versteeg, G.F. and Vanswaaij, W.P.M., *A study on the reaction between CO_2 and alkanolamines in aqueous-solutions.* Chemical Engineering Science, 1984, **39**(2), 207-225.

53. Aronu, U.E., Hessen, E.T., Haug-Warberg, T., Hoff, K.A. and Svendsen, H.F., *Vapor-liquid equilibrium in amino acid salt system: Experiments and modeling.* Chemical Engineering Science, 2011, **66**(10), 2191-2198.

54. Versteeg, G.F. and Oyevaar, M.H., *The reaction between CO_2 and diethanolamine at 298 K.* Chemical Engineering Science, 1989, **44**(5), 1264-1268.

55. Xu, S., Wang, Y.W., Otto, F.D. and Mather, A.E., *Kinetics of the reaction of carbon dioxide with 2-amino-2-methyl-1-propanol solutions.* Chemical Engineering Science, 1996, **51**(6), 841-850.

56. Kumar, P.S., Hogendoorn, J.A., Feron, P.H.M. and Versteeg, G.F., *Equilibrium solubility of CO_2 in aqueous potassium taurate solutions: Part 1. Crystallization in carbon dioxide loaded aqueous salt solutions of amino acids.* Industrial & Engineering Chemistry Research, 2003, **42**(12), 2832-2840.

57. Kumar, P.S., Hogendoorn, J.A., Versteeg, G.F. and Feron, P.H.M., *Kinetics of the reaction of CO_2 with aqueous potassium salt of taurine and glycine.* AIChE Journal, 2003, **49**(1), 203-213.

58. da Silva, E.F. and Svendsen, H.F., *Prediction of the pKa values of amines using ab initio methods and free-energy perturbations.* Industrial & Engineering Chemistry Research, 2003, **42**(19), 4414-4421.

59. Versteeg, G.F. and Vanswaaij, W.P.M., *On the Kinetics between CO_2 and alkanolamines both in aqueous and non-aqueous solutions .1. Primary and secondary-amines.* Chemical Engineering Science, 1988, **43**(3), 573-585.

60. Sada, E., Kumazawa, H., Han, Z.Q. and Matsuyama, H., *Chemical-kinetics of the reaction of carbon-dioxide with ethanolamines in nonaqueous solvents.* AIChE Journal, 1985, **31**(8), 1297-1303.

61. Littel, R.J., Versteeg, G.F. and Vanswaaij, W.P.M., *Kinetics of CO_2 with primary and secondary-amines in aqueous-solutions. 2. Influence of temperature on zwitterion formation and deprotonation rates.* Chemical Engineering Science, 1992, **47**(8), 2037-2045.

62. Versteeg, G.F., Kuipers, J.A.M., Vanbeckum, F.P.H. and Vanswaaij, W.P.M., *Mass-transfer with complex reversible chemical-reactions. 2. Parallel reversible chemical-reactions.* Chemical Engineering Science, 1990, **45**(1), 183-197.

63. Decoursey, W.J., *Enhancement factors for gas-absorption with reversible-reaction.* Chemical Engineering Science, 1982, **37**(10), 1483-1489.

64. Decoursey, W.J. and Thring, R.W., *Effects of unequal diffusivities on enhancement factors for reversible and irreversible reaction.* Chemical Engineering Science, 1989, **44**(8), 1715-1721.

65. Onda, K., Sada, E., Kobayash.T and Fujine, M., *Gas absorption accompanied by complex chemical reactions. 2. Consecutive chemical reactions.* Chemical Engineering Science, 1970, **25**(5), 761-768.

66. Onda, K., Sada, E., Kobayash.T and Fujine, M., *Gas absorption accompanied by complex chemical reactions. 3. Parallel chemical reactions.* Chemical Engineering Science, 1970, **25**(6), 1023-1031.

67. Lewis, W.K. and Whitman, W.G., *Principles of gas absorption.* Industrial & Engineering Chemistry, 1924, **16**, 1215-1220.

68. Hatta, S., *On the absorption velocity of gases by liquids.* Tech. Rep. Tohoku Imp.

Univ., 1932, **10**, 119.

69. Meldon, J.H., Olawoyin, O.O. and Bonanno, D., *Analysis of mass transfer with reversible chemical reaction.* Industrial & Engineering Chemistry Research, 2007, **46**(19), 6140-6146.

70. van Krevelen, D.W. and Hoftijzer, P.J., *Kinetics of gas-liquid reactions.1. General theory.* Recueil Des Travaux Chimiques Des Pays-Bas-Journal of the Royal Netherlands Chemical Society, 1948, **67**(9-10), 563-586.

71. Meldon, J.H. and Morales-Cabrera, M.A., *Analysis of carbon dioxide absorption in and stripping from aqueous monoethanolamine.* Chemical Engineering Journal, 2011, **171**(3), 753-759.

72. Higbie, R., *The rate of absorption of a pure gas into a still liquid during short periods of exposure.* Transactions of the American Institute of Chemical Engineers, 1935, **31**, 365-389.

73. Danckwerts, P.V., *Significance of liquid-film coefficients in gas absorption.* Industrial and Engineering Chemistry, 1951, **43**(6), 1460-1467.

74. Chang, C.S. and Rochelle, G.T., *Mass-transfer enhanced by equilibrium reactions.* Industrial & Engineering Chemistry Fundamentals, 1982, **21**(4), 379-385.

75. Glasscock, D.A. and Rochelle, G.T., *Numerical-simulation of theories for gas-absorption with chemical-reaction.* AIChE Journal, 1989, **35**(8), 1271-1281.

76. Jonsson, P.G. and Kvick, A., *Precision neutron-diffraction structure determination of protein and nucleic-acid components. 3. Crystal and molecular structure of amino-acid alpha-glycine.* Acta Crystallographica Section B-Structural Crystallography and Crystal Chemistry, 1972, **B 28**(6), 1827-1833.

77. Portugal, A.F., Derks, P.W.J., Versteeg, G.E., Magalhaes, F.D. and Mendes, A., *Characterization of potassium glycinate for carbon dioxide absorption purposes.* Chemical Engineering Science, 2007, **62**(23), 6534-6547.

78. Versteeg, G.F. and Vanswaaij, W.P.M., *Solubility and diffusivity of acid gases (CO_2, N_2O) in aqueous alkanolamine solutions.* Journal of Chemical and Engineering Data, 1988, **33**(1), 29-34.

79. Hamborg, E.S., van Swaaij, W.P.M. and Versteeg, G.F., *Diffusivities in aqueous solutions of the potassium salt of amino acids.* Journal of Chemical and Engineering Data, 2008, **53**(5), 1141-1145.

80. Benamor, A. and Aroua, M.K., *Modeling of CO_2 solubility and carbamate concentration in DEA, MDEA and their mixtures using the Deshmukh-Mather model.* Fluid Phase Equilibria, 2005, **231**(2), 150-162.

81. Perrin, D., *Dissociation constants of organic bases in aqueous solutions.* Butterworth, London, 1965.

82. Jensen, A., Jensen, J.B. and Faurholt, C., *Studies on carbamates. 6. the carbamate of glycine.* Acta Chemica Scandinavica, 1952, **6**(3), 395-397.

83. van Holst, J., Kersten, S.R.A. and Hogendoorn, K.J.A., *Physiochemical properties of several aqueous potassium amino acid salts.* Journal of Chemical and Engineering Data, 2008, **53**(6), 1286-1291.

84. Haubrock, J., Hogendoorn, J.A. and Versteeg, G.F., *The applicability of activities in kinetic expressions: A more fundamental approach to represent the kinetics of the system CO_2-OH-salt in terms of activities.* Chemical Engineering Science, 2007, **62**(21), 5753-5769.

85. Kampmeyer, P.M., *The temperature dependence of viscosity for water and mercury.* Journal of Applied Physics, 1952, **23**(1), 99-102.

86. Cullinane, J.T. and Rochelle, G.T., *Kinetics of carbon dioxide absorption into aqueous potassium carbonate and piperazine.* Industrial & Engineering Chemistry Research, 2006, **45**(8), 2531-2545.

87. Stellwagen, E., Prantner, J.D. and Stellwagen, N.C., *Do zwitterions contribute to the ionic strength of a solution?* Analytical Biochemistry, 2008, **373**(2), 407-409.

MAIN MATLAB CODE

The computer program shown below indicates potassium glycinate. For potassium sarcosinate, change the physiochemical parameters accordingly.

```
%%-------------------------------------------------------------------------------------------------------------
Speciation Calculation:
%%-------------------------------------------------------------------------------------------------------------
function F=speciation(x,A)
T=313;
C=3;% [PG] M
K=62.183098/T-0.111175;
Hco2w=exp(-2044/T)/(3.54*10^-7);
H=Hco2w*10^(C*K)*(1000/101325); % atm mol-1 dm3
K2=exp(-12092.1/T-36.7816*log(T)+235.482);
K4=exp(-12431.7/T-35.4819*log(T)+220.067);
K6=exp(-0.000237956*(T^2)+0.202203*T-61.6499);
Kcarb=K2/exp(-2767.18/T+6.10312);
% B=x(1)
% R=x(2)
% Rn=x(3)
% Rnn=x(4)
% C=x(5)
F=[x(2)+x(3)+x(4)-C;% [PG]
    x(1)+x(3)+2*x(4)+2*x(5)-C;% [PG]
    x(4).*x(2)-(Kcarb/K6).*A.*(x(3)^2);
    x(1).*x(2)-(K2/K6).*A.*x(3);
    x(5).*x(2)-(K4/K6).*x(3).*x(1)];

% Command window:
T=313;
C=3; % M [PG]
K=62.183098/T-0.111175;
Hco2w=exp(-2044/T)/(3.54*10^-7);
H=Hco2w*10^(C*K)*(1000/101325); %atm

x0=[0.02*C;0.4*C;0.3*C;0.3*C;0.04*C];
A=(1/H)*logspace(-5,1,31);
for i=1:1:length(A)
    AA=A(i);
    x=fsolve(@(x)speciation(x,AA),x0);
```

```
    x1(i)=x(1);
    x2(i)=x(2);
    x3(i)=x(3);
    x4(i)=x(4);
    x5(i)=x(5);
end

atm=logspace(-5,1,31);
Ad=A./C;
x1d=x1./C;
x2d=x2./C;
x3d=x3./C;
x4d=x4./C;
x5d=x5./C;
Loading=Ad+x1d+x4d+x5d;
semilogx(atm,Ad,'-*m',atm,x1d,'-g',atm,x2d,'-r',atm,x3d,':b',atm,x4d,'-
k',atm,x5d,'ok',atm,Loading,'->k');
xlabel('CO_{2} partial pressure (atm)');
ylabel('Concentration (mol/mol PG)');
legend('A','B^{-}','R','R^{-}','R^{2-}','C^{2-}','Loading');

%%-------------------------------------------------------------------------------------------------------
Perturbation method:
%%-------------------------------------------------------------------------------------------------------
function F=speciationtry(x,A)
T=293;
C=1;% [PG] M
K2=exp(-12092.1/T-36.7816*log(T)+235.482);
K4=exp(-12431.7/T-35.4819*log(T)+220.067);
K6=exp(-0.000237956*(T^2)+0.202203*T-61.6499);
Kcarb=K2/exp(-2767.18/T+6.10312);
% B=x(1)
% R=x(2)
% Rn=x(3)
% Rnn=x(4)
% C=x(5)
F=[x(2)+x(3)+x(4)-C;% [PG]
    x(1)+x(3)+2*x(4)+2*x(5)-C;% [PG]
    x(4).*x(2)-(Kcarb/K6).*A.*(x(3)^2);
    x(1).*x(2)-(K2/K6).*A.*x(3);
    x(5).*x(2)-(K4/K6).*x(3).*x(1)];
```

```
function f=check(z)
% parameters
global delta
T=293;
C=1;
pA=0.15;
density=1056.57;
K=62.183098/T-0.111175;
Hco2w=exp(-2044/T)/(3.54*10^-7);
H=Hco2w*10^(C*K)*(1000/101325);
K2=exp(-12092.1/T-36.7816*log(T)+235.482);
K4=exp(-12431.7/T-35.4819*log(T)+220.067);
K6=exp(-0.000237956*(T^2)+0.202203*T-61.6499);
Kcarb=K2/exp(-2767.18/T+6.10312);

DA=2.35*100*(10^-6)*exp(-2119/T)*(1+0.2109*C+0.05124*C^2)^-0.48;
Dionic=(-2.412-9.403*(10^-3)*T+7.11*(10^-5)*(T^2)-0.2177*C-5.447*(10^-2
)*(C^2)+1.296*(10^-3)*T*C)*(10^-9)*100;
MW=113;
W=(density-C*MW)/18;
K5=exp(-13445.9/T-22.4773*log(T)+140.932);
K3=K2/K5;
k1a=2.81*(10^10)*exp(-5800/T)*1000;
kw=1.05*(10^-4)*exp(-1265/T)*1000;
kRn=4.89*(10^3)*exp(-5307/T)*1000;
k2=10^(329.850-110.541*log10(T)-17265.4/T);
k3=10^(13.635-2895/T);
AL=1.5480*10^-7;
BL=0.0038;
% RL=0.1096;
% RnL=0.8038;
RnnL=0.0866;
CL=0.0096;

global Bobar Robar Rnobar Rnnobar Cobar
% Bobar=x(1);
% Robar=x(2);
% Rnobar=x(3);
% Rnnobar=x(4);
% Cobar=x(5);
```

```
% one expression for phi_1
phiex1=(DA*(z-AL)+Dionic*(Bobar-BL+Rnnobar-RnnL+Cobar-CL))/delta;
% solve for constants
theta1matrix=zeros(3,3);
theta1matrix(1,1)=1+2*K4*Rnobar/(K6*Robar);
theta1matrix(1,2)=1+2*K4*Bobar/(K6*Robar)+2*K4*Rnobar*Bobar/(K6*Robar^2
);
theta1matrix(1,3)=2+2*K4*Rnobar*Bobar/(K6*Robar^2);
theta1matrix(2,2)=Rnnobar+2*Kcarb*z*Rnobar/K6;
theta1matrix(2,3)=Rnnobar-Robar;
theta1matrix(3,1)=-Robar;
theta1matrix(3,2)=Bobar+K2*z/K6;
theta1matrix(3,3)=Bobar;
theta1=det(theta1matrix);

theta2matrix=zeros(3,3);
theta2matrix(1,2)=1+2*K4*Bobar/(K6*Robar)+2*K4*Rnobar*Bobar/(K6*Robar^2
);
theta2matrix(1,3)=2+2*K4*Rnobar*Bobar/(K6*Robar^2);
theta2matrix(2,1)=-Kcarb*Rnobar^2/K6;
theta2matrix(2,2)=Rnnobar+2*Kcarb*z*Rnobar/K6;
theta2matrix(2,3)=Rnnobar-Robar;
theta2matrix(3,1)=-K2*Rnobar/K6;
theta2matrix(3,2)=Bobar+K2*z/K6;
theta2matrix(3,3)=Bobar;
theta2=det(theta2matrix);

theta3matrix=zeros(3,3);
theta3matrix(1,1)=1+2*K4*Rnobar/(K6*Robar);
theta3matrix(1,3)=2+2*K4*Rnobar*Bobar/(K6*Robar^2);
theta3matrix(2,2)=-Kcarb*Rnobar^2/K6;
theta3matrix(2,3)=Rnnobar-Robar;
theta3matrix(3,1)=-Robar;
theta3matrix(3,2)=-K2*Rnobar/K6;
theta3matrix(3,3)=Bobar;
theta3=det(theta3matrix);

theta4matrix=zeros(3,3);
theta4matrix(1,1)=1+2*K4*Rnobar/(K6*Robar);
theta4matrix(1,2)=1+2*K4*Bobar/(K6*Robar)+2*K4*Rnobar*Bobar/(K6*Robar^2
```

```
);
theta4matrix(2,2)=Rnnobar+2*Kcarb*z*Rnobar/K6;
theta4matrix(2,3)=-Kcarb*Rnobar^2/K6;
theta4matrix(3,1)=-Robar;
theta4matrix(3,2)=Bobar+K2*z/K6;
theta4matrix(3,3)=-K2*Rnobar/K6;
theta4=det(theta4matrix);

theta5=K4*Bobar*theta3/(K6*Robar)+K4*Rnobar*theta2/(K6*Robar)+K4*Rnobar
*Bobar*(theta3+theta4)/(K6*Robar^2);

MTA=zeros(3,3); % matrix template for deltas
MTA(1,2)=1;
MTA(1,3)=1;
MTA(2,1)=1+2*K4*Rnobar/(K6*Robar);
MTA(2,2)=-2*K4*Rnobar*Bobar/(K6*Robar^2);
MTA(2,3)=1+2*K4*Bobar/(K6*Robar);
MTA(3,1)=1+K4*Rnobar/(K6*Robar);
MTA(3,2)=-K4*Rnobar*Bobar/(K6*Robar^2);
MTA(3,3)=K4*Bobar/(K6*Robar);

MTB=zeros(3,2); % matrix template for deltas
MTB(1,1)=-1;
MTB(2,1)=-2;
MTB(3,1)=-1;
MTB(3,2)=-DA/Dionic;

DeltaMatrix=MTA\MTB;

omega1=DeltaMatrix(1,1);
omega2=DeltaMatrix(1,2);
omega3=DeltaMatrix(2,1);
omega4=DeltaMatrix(2,2);
omega5=DeltaMatrix(3,1);
omega6=DeltaMatrix(3,2);

lenda1=k2*omega5*z/Rnobar-k2*omega3*z/Robar+k3*K5*omega5*z/(K6*Robar)-k
3*omega3*Bobar/(K3*Robar)-k3*omega1/K3-k2*omega1*z/Bobar;
lenda2=k2-k3*omega2/K3-k2*omega2*z/Bobar-k2*omega4*z/Robar+k2*omega6*z/
Rnobar+k3*K5*Rnobar/(K6*Robar)+k3*K5*omega6*z/(K6*Robar)-k3*omega4*Boba
r/(K3*Robar);
```

```
eta1=(k1a/Dionic)*((kRn*z*Rnobar^2+kw*W*z*Rnobar)/(1+kRn*Rnobar+kw*W))*
(1/Rnnobar+omega3/Robar-2*omega5/Rnobar);
eta2=(k1a/Dionic)*((kRn*z*Rnobar^2+kw*W*z*Rnobar)/(1+kRn*Rnobar+kw*W))*
(omega4/Robar-1/z-2*omega6/Rnobar);
eta3=(lenda1/DA)-(Dionic*eta1/DA);
eta4=(lenda2/DA)-(Dionic*eta2/DA);

u1=(eta1+eta4+sqrt((eta1+eta4)^2-4*(eta1*eta4-eta2*eta3)))/2;
u2=(eta1+eta4-sqrt((eta1+eta4)^2-4*(eta1*eta4-eta2*eta3)))/2;

m1=sqrt(u1);
% m2=-m1;
m3=sqrt(u2);
% m4=-m3;

E1=eta2/(u1-eta1);
E2=eta2/(u2-eta1);

c1=pA/H-z;

diffAobar=-theta1*phiex1/(theta1*DA+Dionic*(theta2+theta4+theta5));
c2=-theta4*phiex1/(theta1*DA+Dionic*(theta2+theta4+theta5));
%=diffRnnobar
diffdeltaAo=-(m1*(E2*m3*c1-c2*tanh(m3*delta))+m3*(c2*tanh(m1*delta)-E1*
m1*c1))/(E2*m3*tanh(m1*delta)-E1*m1*tanh(m3*delta));

% second expression of phi_1
% phiex2=-DA*(diffAobar+diffdeltaAo);

% check if phiex1=phiex2
f=phiex1+(diffAobar+diffdeltaAo)*DA;

% Command window:
clear all
clc
global delta
delta=10000*10^-5; % dm
C=1;x0=[0.02*C;0.4*C;0.3*C;0.3*C;0.04*C];
A=linspace(0.0005122,0.0005136,100);
for i=1:length(A)
```

```
    AA=A(i);
    x=fsolve(@(x)speciationtry(x,AA),x0);
    x1(i)=x(1);
    x2(i)=x(2);
    x3(i)=x(3);
    x4(i)=x(4);
    x5(i)=x(5);
end

for k=1:length(A)
global Bobar Robar Rnobar Rnnobar Cobar
Bobar=x1(k);
Robar=x2(k);
Rnobar=x3(k);
Rnnobar=x4(k);
Cobar=x5(k);
z(k)=feval(@check,A(k));
end

ID=37; % find z(ID)==0, and change the index accordingly
z=A(ID);
Bobar=x1(ID);
Robar=x2(ID);
Rnobar=x3(ID);
Rnnobar=x4(ID);
Cobar=x5(ID);

% Follow the equations shown below to calculate the enhancement factor
b2=(E2*m3*c1*(1+exp(-2*m3*delta))-(1-exp(-2*m3*delta))*c2)/(E2*m3*(1+ex
p(-2*m3*delta))*(1-exp(-2*m1*delta))-E1*m1*(1+exp(-2*m1*delta))*(1-exp(
-2*m3*delta)));
b4=((1-exp(-2*m1*delta))*c2-E1*m1*c1*(1+exp(-2*m1*delta)))/(E2*m3*(1+ex
p(-2*m3*delta))*(1-exp(-2*m1*delta))-E1*m1*(1+exp(-2*m1*delta))*(1-exp(
-2*m3*delta)));

deltaA=((E2*m3*c1-c2*tanh(m3*delta))*tanh(m1*delta)+(c2*tanh(m1*delta)-
E1*m1*c1)*tanh(m3*delta))/(E2*m3*tanh(m1*delta)-E1*m1*tanh(m3*delta));
deltaRnn=E1*b2*(1-exp(-2*m1*delta))+E2*b4*(1-exp(-2*m3*delta));

deltaB=omega1*deltaRnn+omega2*deltaA;
deltaR=omega3*deltaRnn+omega4*deltaA;
```

```
deltaRn=omega5*deltaRnn+omega6*deltaA;
deltaC=K4*Bobar*deltaRn/(K6*Robar)+K4*Rnobar*deltaB/(K6*Robar)-K4*Rnoba
r*Bobar*deltaR/(K6*Robar^2);

FA=z+deltaA;
FB=Bobar+deltaB;
FR=Robar+deltaR;
FRn=Rnobar+deltaRn;
FRnn=Rnnobar+deltaRnn;
FC=Cobar+deltaC;

EnhanceFactor=1+sqrt(Dionic/DA)*(FB-BL+FRnn-RnnL+FC-CL)/(pA/H-AL)

% Follow the equations shown below to calculate the concentration profiles
within the liquid film
function F=barsearch(x,y)
T=293;
C=3;% [PG] M
delta=6*10^-5;
phi1=6.1141*10^-5; % 293K 3M L40 delta=6um
K2=exp(-12092.1/T-36.7816*log(T)+235.482);
K4=exp(-12431.7/T-35.4819*log(T)+220.067);
K6=exp(-0.000237956*(T^2)+0.202203*T-61.6499);
Kcarb=K2/exp(-2767.18/T+6.10312);
DA=2.35*100*(10^-6)*exp(-2119/T)*(1+0.2109*C+0.05124*C^2)^-0.48;
Dionic=(-2.412-9.403*(10^-3)*T+7.11*(10^-5)*(T^2)-0.2177*C-5.447*(10^-2
)*(C^2)+1.296*(10^-3)*T*C)*(10^-9)*100;
AL=3.3037*10^-5;
BL=0.0605;
RnnL=1.1283;
CL=0.0113;
phi2=DA*AL+Dionic*(BL+RnnL+CL)+phi1*delta;
% Bbar=x(1)
% Rbar=x(2)
% Rnbar=x(3)
% Rnnbar=x(4)
% Cbar=x(5)
% Abar=x(6)
F=[x(2)+x(3)+x(4)-C;% [PG]
    x(1)+x(3)+2*x(4)+2*x(5)-C;% [PG]
    x(4).*x(2)-(Kcarb/K6).*x(6).*(x(3)^2);
```

```
    x(1).*x(2)-(K2/K6).*x(6)*x(3);
    x(5).*x(2)-(K4/K6).*x(3).*x(1)
    DA*x(6)+Dionic*(x(1)+x(4)+x(5))+phi1*y-phi2];

% Command Window:
x0=[0.0694;1.2503;0.5913;1.1585;0.0112;4.3679*10^-5];
y=linspace(0,delta,20);
for i=1:length(y)
    x=fsolve(@(x)barsearch(x,y(i)),x0);
    x1(i)=x(1);
    x2(i)=x(2);
    x3(i)=x(3);
    x4(i)=x(4);
    x5(i)=x(5);
    x6(i)=x(6);
end

for k=1:length(y)
b2=(E2*m3*c1*(1+exp(-2*m3*delta))-(1-exp(-2*m3*delta))*c2)/(E2*m3*(1+ex
p(-2*m3*delta))*(1-exp(-2*m1*delta))-E1*m1*(1+exp(-2*m1*delta))*(1-exp(
-2*m3*delta)));
b4=((1-exp(-2*m1*delta))*c2-E1*m1*c1*(1+exp(-2*m1*delta)))/(E2*m3*(1+ex
p(-2*m3*delta))*(1-exp(-2*m1*delta))-E1*m1*(1+exp(-2*m1*delta))*(1-exp(
-2*m3*delta)));

deltaA(k)=(E2*m3*c1-c2*tanh(m3*delta))*sinh(m1*(delta-y(k)))/(E2*m3*sin
h(m1*delta)-E1*m1*tanh(m3*delta)*cosh(m1*delta))+(c2*tanh(m1*delta)-E1*
m1*c1)*sinh(m3*(delta-y(k)))/(E2*m3*tanh(m1*delta)*cosh(m3*delta)-E1*m1
*sinh(m3*delta));
deltaRnn(k)=E1*b2*(exp(-m1*y(k))-exp(-2*m1*delta+m1*y(k)))+E2*b4*(exp(-
m3*y(k))-exp(-2*m3*delta+m3*y(k)));

deltaB(k)=omega1*deltaRnn(k)+omega2*deltaA(k);
deltaR(k)=omega3*deltaRnn(k)+omega4*deltaA(k);
deltaRn(k)=omega5*deltaRnn(k)+omega6*deltaA(k);
deltaC(k)=K4*Bobar*deltaRn(k)/(K6*Robar)+K4*Rnobar*deltaB(k)/(K6*Robar)
-K4*Rnobar*Bobar*deltaR(k)/(K6*Robar^2);
end

FA=x6+deltaA;
FB=x1+deltaB;
```

```
FR=x2+deltaR;
FRn=x3+deltaRn;
FRnn=x4+deltaRnn;
FC=x5+deltaC;
pH=-log10(K6*FR./FRn);

Y=y*10^5;
plot(Y,FA,'-*m',Y,FB,'-g',Y,FR,'-r',Y,FRn,'--b',Y,FRnn,'-k',Y,FC,'ok');
xlabel('Film thickness (μm)');
ylabel('Concentration (mol/L)');
legend('A','B^{-}','R','R^{-}','R^{2-}','C^{2-}');

plot(Y,pH,'->b');
xlabel('Film thickness (μm)');
ylabel('pH');

%%-------------------------------------------------------------------------
Pseudo-1st-order irreversible reaction:
%%-------------------------------------------------------------------------
kforward=k1a*RnL*(kRn*RnL+kw*W)/(1+kRn*RnL+kw*W)+k2+k3*K2*RnL/(K3*K6*RL
);
Enforward=(delta*10^-5)*sqrt(kforward/DA);


%%-------------------------------------------------------------------------
Numerical method:
%%-------------------------------------------------------------------------
function dx=PGodefull(y,x,phi)
% parameters
delta=2*10^-5; % um
T=293;
C=3;
pA=0.15;
density=1163.85;
K=62.183098/T-0.111175;
Hco2w=exp(-2044/T)/(3.54*10^-7);
H=Hco2w*10^(C*K)*(1000/101325);
K2=exp(-12092.1/T-36.7816*log(T)+235.482);
K4=exp(-12431.7/T-35.4819*log(T)+220.067);
K6=exp(-0.000237956*(T^2)+0.202203*T-61.6499);
Kcarb=K2/exp(-2767.18/T+6.10312);
```

```
DA=2.35*100*(10^-6)*exp(-2119/T)*(1+0.2109*C+0.05124*C^2)^-0.48;
Dionic=(-2.412-9.403*(10^-3)*T+7.11*(10^-5)*(T^2)-0.2177*C-5.447*(10^-2
)*(C^2)+1.296*(10^-3)*T*C)*(10^-9)*100;
MW=113;
W=(density-C*MW)/18;
K5=exp(-13445.9/T-22.4773*log(T)+140.932);
K3=K2/K5;
k1a=2.81*(10^10)*exp(-5800/T)*1000;
kw=1.05*(10^-4)*exp(-1265/T)*1000;
kRn=4.89*(10^3)*exp(-5307/T)*1000;
k2=10^(329.850-110.541*log10(T)-17265.4/T);
k3=10^(13.635-2895/T);
AL=3.3037*10^-5;
BL=0.0605;
RL=1.2113;
RnL=0.6604;
RnnL=1.1283;
CL=0.0113;
kesi=DA*AL+Dionic*(BL+RnnL+CL);

Q=(phi.*delta.*(1-y)+kesi-DA.*x(1))./Dionic;
G=2.*x(3)-3.*Q-K4.*(C-2.*Q)./K6;
J=2.*Q.^2-3.*Q.*x(3)+(x(3).^2);

Bn=(-G-sqrt(G.^2-4*(1-K4/K6).*J))/(2.*(1-K4/K6));
Cnn=Q-x(3)-Bn;
Rn=C-2*Q+Bn;
R=2*Q-Bn-x(3);

% numerical method ODEs
dx=[x(2)

    delta.^2.*k1a.*x(1).*Rn.*(kRn*Rn+kw*W).*(1-K6*x(3).*R./(Kcarb.*x(1).
    *Rn.^2))./(DA*(1+kRn*Rn+kw*W))+delta.^2*k2.*x(1)./DA-delta.^2*k2*K6.
    *Bn.*R./(DA*K2.*Rn)+delta.^2*k3*K5.*x(1).*Rn./(DA*K6.*R)-delta^2*k3.
    *Bn./(DA*K3)

    x(4)

    -delta.^2.*k1a.*x(1).*Rn.*(kRn*Rn+kw*W).*(1-K6*x(3).*R./(Kcarb.*x(1)
    .*Rn.^2))./(Dionic*(1+kRn*Rn+kw*W))];
```

```
function res=PGbc(xa,xb,phi)
% parameters
delta=2e-5;
T=293;
C=3;
pA=0.15;
K=62.183098/T-0.111175;
Hco2w=exp(-2044/T)/(3.54*10^-7);
H=Hco2w*10^(C*K)*(1000/101325);
AL=3.3037*10^-5;
RnnL=1.1283;
DA=2.35*100*(10^-6)*exp(-2119/T)*(1+0.2109*C+0.05124*C^2)^-0.48;

% numerical method BCs
res=[xa(1)-pA/H;
    xa(2)+phi*delta/DA;
    xa(4);
    xb(1)-AL;
    xb(3)-RnnL];

% Command window:
phi=6.4498e-5; % initial guess of phi1
solinit=bvpinit(linspace(0,1,10000),[pA/H;-phi*delta/DA;1.1392;0],phi);
sol=bvp5c(@PGodefull,@PGbc,solinit);
y=linspace(0,1,10000);
x=deval(sol,y);

phires=-x(2,1)*DA/delta;

% calculate conc profiles
Q=(phires*delta*(1-y)+kesi-DA*x(1))/Dionic;
G=2*x(3)-3*Q-K4*(C-2*Q)/K6;
J=2*Q.^2-3*Q.*x(3)+(x(3).^2);

Bn=(-G-sqrt(G.^2-4*(1-K4/K6)*J))/(2*(1-K4/K6));
Cnn=Q-x(3)-Bn;
Rn=C-2*Q+Bn;
R=2*Q-Bn-x(3);
EnNum=1+sqrt(Dionic/DA)*(Bn(1)-BL+x(3,1)-RnnL+Cnn(1)-CL)/(pA/H-AL);
```

```
plot(delta,EnThickFilm,'-b',delta,Enforward,'-r>',delta,EnNum,'sk');
xlabel('Film thickness (μm)');
ylabel('Enhancement factor');
legend('Perturbation method','Pseudo-1st-order irreversible
reaction','Numerical method');
```